Abstract N°: 2

Clinical Diagnostic Accuracy of Pilomatricoma: A Clinicopathological Analysis of 55 Lesions

Yu Matsui*[1], Shohei Kitayama[1], Teruhiko Makino[1], Tadamichi Shimizu[1]

[1] University of Toyama, Toyama, Japan

Introduction
Pilomatricoma is a benign adnexal tumor originating from hair matrix cells and is frequently encountered in pediatric and young adult populations. Although its histopathological features are well characterized, accurate preoperative clinical diagnosis remains challenging because of its heterogeneous clinical presentation. This study aimed to evaluate the diagnostic accuracy and associated clinicopathological characteristics of pilomatricoma.

Materials and Methods
We retrospectively analyzed patients with histopathologically confirmed pilomatricoma treated at a single university hospital between 2006 and 2024. A total of 55 lesions from 51 patients were included. Clinical information, including patient demographics, lesion location, size, mobility, color characteristics, and the duration from lesion awareness to initial consultation and surgical excision, was extracted from medical records. Diagnostic accuracy was defined as concordance between the initial clinical diagnosis made by board-certified dermatologists and the final pathological diagnosis. Histopathological evaluation included the presence of calcification and quantitative assessment of basophilic and shadow cell components, expressed as the basophilic-to-shadow cell (B/S) ratio.

Results
The overall preoperative diagnostic accuracy was 38.2%. Patients correctly diagnosed at the initial visit were significantly younger than those who were misdiagnosed and had a longer interval between lesion awareness and the first clinical consultation. Bluish coloration was significantly associated with correct diagnosis, whereas reddish coloration was more frequently observed in misdiagnosed cases. Other clinical features, including lesion size, mobility, and anatomical location, were not significantly associated with diagnostic accuracy. Multivariate analysis did not identify independent predictors of correct diagnosis. Histopathological analysis demonstrated a moderate negative correlation between the B/S ratio and the duration from lesion awareness to surgical excision, consistent with temporal histological maturation from basophilic cells to shadow cells.

Conclusions
Preoperative diagnosis of pilomatricoma remains difficult in routine clinical practice, with fewer than half of cases correctly identified at the initial presentation. While younger age, longer lesion duration, and bluish coloration may facilitate recognition, atypical clinical features frequently lead to misdiagnosis. Greater awareness of the diverse clinical spectrum of pilomatricoma may help improve diagnostic accuracy in dermatological practice.

EA DV CONGRESS
VIENNA
30 SEP - 3 OCT 2026

Abstract N°: 30

Primary cutaneous cryptococcosis in an immunocompetent host: first case report with multimodal diagnosis and treatment from the Philippines

Marividez Nina Domingo*[1], Andrea Marie Bernales-Mendoza[1], Ma. Cricelda Rescober-Valencia[1, 2], Matilde Krisha Montenegro[1]

[1] Jose R. Reyes Memorial Medical Center, Manila, Philippines
[2] Dr. Jose N. Rodriguez Memorial Hospital, Caloocan, Philippines

Introduction

Cutaneous cryptococcosis arises as a manifestation of disseminated fungal infection in immunocompromised individuals. Its presentation as a primary cutaneous infection in an otherwise healthy, immunocompetent host is rare and diagnostically challenging, often mimicking more common dermatologic conditions

Case Presentation

We report the case of a 59-year-old immunocompetent Filipino male, with chronic sun exposure and environmental exposure to pigeon excreta, who developed a non-healing erythematous plaque on the right ear. The lesion initially appeared as gradually enlarging asymptomatic papule with spontaneous rupturing. One year later, a similar lesion recurred at the same site, evolving into a tender, ulcerated plaque. The patient underwent multiple misdiagnoses with no improvement despite multiple therapies. Histopathology from biopsies revealed yeast-like organisms with confirmatory staining on PAS,GMS, Alcian Blue, and mucicarmine. PCR and gene sequencing on FFPE tissue later identified Cryptococcus neoformans var grubii. The treatment plan was to give oral itraconazole 200 mg daily for at least 6 months, however, the patient observed dramatic clinical improvement and was lost to follow-up. Upon repeat biopsy after recurrence, fungal culture, and MALDI-TOF analysis confirmed Cryptococcus neoformans. This integration of these diagnostic methods strengthens diagnosis and treatment confidence. Upon resuming antifungal therapy, the patient achieved complete clinical clearance.



Figure 1: Right auricle with erythematous, crusted ulcerated nodules at baseline (Day 0), showing near-complete resolution with mild scarring after 2 months of itraconazole re-initiation.

Conclusion

This case underscores the polymorphic and indolent nature of primary cutaneous cryptococcosis and highlights its capacity to mimic other dermatologic conditions in immunocompetent hosts. Clinicians must maintain a high index of suspicion for fungal infections in chronic, non-healing skin lesions, particularly endemic regions or in

patients with relevant environmental exposures.

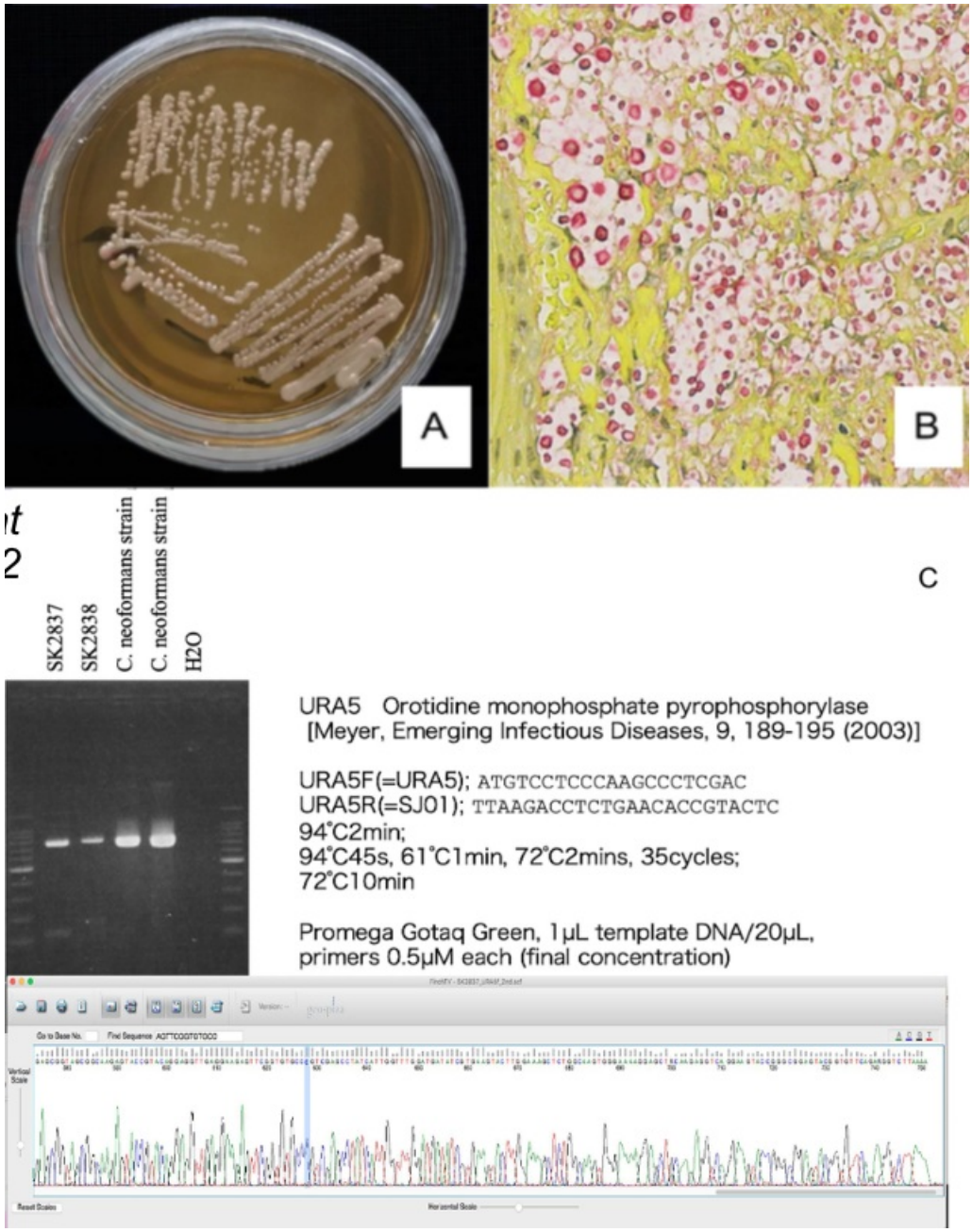

Figure 2: (A) Fungal culture on Sabouraud Dextrose Agar (B) Histologic findings on Mucicarmine Stain (C) Molecular confirmation of Cryptococcus species; representative sequencing chromatograms of the URA5 gene showing distinct base calls used for species identification

EA DV CONGRESS
VIENNA
30 SEP - 3 OCT 2026

Abstract N°: 113

Toward Standardized Diagnostic Criteria in Darier Disease: A Scoping Review by the Darier Disease International Task Force

Itzhak Shabat*[1], grace Xiong[2], sofia labbouz[3], Tal Kaminski Rosenberg[1], michael ziv[4], Khaled Ezzedine[5], RONI gad[1]

[1] The Ruth and Bruce Rappaport Faculty of Medicine, Technion – Israel Institute of Technology, Haifa, Israel., HAIFA, Israel

[2] Michael G. DeGroote School of Medicine, McMaster University, Hamilton, Ontario, Canada, ontario, Canada

[3] Department, Ramon y Cajal University Hospital, Madrid, Spain. My current affiliation is: Chesterfield Royal Hospital, Chesterfield, United Kingdom, Chesterfield, United Kingdom

[4] department, Emek medical center, afula, Israel

[5] Department of Dermatology, Hôpital Henri Mondor and Université Paris-Est Créteil, EpiDermE (Epidemiology in Dermatology and Evaluation of therapeutics, Institut Mondor de Recherche Biomédicale, Inserm U955, Université Paris Est Créteil (UPEC), paris, France

Introduction

Introduction: Darier Disease (DD), or keratosis follicularis, is a rare autosomal-dominant genodermatosis often characterized by scaly, yellow-to-brown papules and plaques most commonly in seborrheic areas.The clinical characterization and diagnostic criteria of DD remains heterogenous.Objective: This scoping review aims to evaluate the range of diagnostic criteria used for *DD and assess the consistency of their application across prior literature, with the broader goal of supporting the development of an international diagnostic consensus.

Materials and Methods

Methods: A scoping review was reported following PRISMA-ScR guidelines. Comprehensive searches were performed in Embase (Elsevier), Medline(OVID), CENTRAL (Cochrane), and Web of Science (Clarivate) through 4-10.6.2025 Two independent researchers conducted the screening and extracted data on study characteristics, clinical, histopathological, genetic features, and family history of DD. Quality assessment was conducted using the Joanna Briggs Institute checklists.

Results

Results: From 258 initial records, sixteen studies were identified. Amongst the included articles, 50% (8/16) had explicitly defined diagnostic criteria. Clinical features were consistently reported across all studies, with histopathology described in 87.5% (14/16), genetic testing in 18.8% (3/16), and family history in 25% (4/16) of studies. Case reports and case series were more likely to specify diagnostic criteria than cohort or cross-sectional studies. Temporal analysis demonstrated that older studies relied more heavily on clinical and histopathological findings, whereas recent studies increasingly incorporated genetic testing as part of diagnostic criteria. Geographic variability was observed, with European studies frequently integrating both histopathological and genetic assessments, studies from the United States and United Kingdom predominantly emphasizing clinical and histopathological criteria, and Asian studies more often prioritizing genetic testing.

Conclusions

Conclusion: Currently, there is no standardized diagnostic framework for Darier Disease. Clinical and histopathological features are the most consistently used criteria, while genetic and familial information are applied inconsistently. Temporal trends indicate increased integration of molecular diagnostics in recent studies. However, a unified international consensus remains lacking.

EADV CONGRESS
VIENNA
30 SEP - 3 OCT 2026

Abstract N°: 265

Multimodal optical coherence tomography assessment of the neck skin in Wilson's Diseasepatients exposed to D-Penicillamine

Carmen Cantisani*[1], Michele Blasco[2], Giorgia Carnevale[2], Manuela Merli[3]

[1] UOC of Dermatology Department of internal and cardiovascular science. University Sapienza of Rome, Rome, Italy

[2] Orphalan, Rome, Italy

[3] Department of Gastroenterology, Sapienza University of Rome, Rome, Italy

Introduction

Cutaneous laxity has been described following treatment of Wilson's disease (WD) with D-penicillamine and its indicative of drug-induced dermopathy. Invasive skin biopsy remains the gold standard for confirmatory diagnosis. Objective, non invasive assessment distinguishing drug-induced changes from chronological or sun exposure (photoaging) remain insufficiently defined. This study aims to quantitatively characterize dermal architectural and microvascular alterations using Dynamic Optical coherence tomography (D-OCT) and Line-Field confocal optical Coherence tomography (LC-OCT) in DPA exposed subjects.

Case Presentation

Methods: Three WD patients under long-term DPA therapy with clinical cutis laxa were compared with two younger healthy controls, two age- and sex-matched healthy controls, and one 85-year-old subject with advanced photoaging. Standardized imaging was performed at the same anatomical site. LC-OCT provided quasi-histological vertical and horizontal scans enabling semi-quantitative assessment of dermal fibre morphology. D-OCT was used to measure epidermal thickness, dermal reflectivity indices, vessel density, and vascular morphology.

Results: DPA patients showed[OK1] [CC2] increased elastic fibre fragmentation scores (mean 2.7 ± 0.3) compared with age-matched controls (1.1 ± 0.4) and the photoaged subject (1.9) (effect size >1.5). Epidermal thickness was markedly reduced in the DPA group (0.06–0.10 mm) versus healthy controls (0.13–0.27 mm), corresponding to a mean reduction of approximately 45–55%. Superficial vessel density was lower in DPA patients (8–11%) compared to age-matched controls (14–18%) and the photoaged subject (16%), representing a relative decrease of ~35–40%. This study identifies in vivo evidence of microvascular remodeling associated with chronic DPA therapy.indicating extracellular matrix rarefaction and architectural disorganization. Lysil oxidase inhibition may weaken perivascular matrix support, leading to capillary instability and regressionImportantly, D-OCT was able to differentiate DPA-related changes (hypovascularity) from photoaging (vascular ectasia and preserved or increased vessel density) have removed significantly unless you have performed statistical comparison with p values.

Conclusion

Conclusions: Multimodal OCT identifies quantitative imaging characteristics of DPA-induced elastolysis. These preliminary data indicate potential utility of OCT-based technologies for early detection and longitudinal non-invasive monitoring of drug-related dermal damage.Conclusions: Multimodal OCT identifies quantitative imaging characteristics of DPA-induced elastolysis. These preliminary data indicate potential utility of OCT-based technologies for early detection and longitudinal non-invasive monitoring of drug-related dermal damage.

POWERED BY M-ANAGE.COM

EA DV CONGRESS
VIENNA
30 SEP - 3 OCT 2026

Abstract N°: 277

Automatic Fluorescence Microscopic Image Analyzer: A Novel AI-Based Tool for Early Diagnosing Superficial Fungal Infections

Chunjiao Zheng*[1], Lianjuan Yang[1]

[1] Shanghai Skin Disease Hospital, Shanghai, China

Introduction

Superficial fungal infections (SFIs) are highly prevalent globally, affecting approximately 20–25% of the population. Traditional diagnostic methods such as potassium hydroxide (KOH) microscopy and fluorescence staining are limited by operator dependency, variable sensitivity, and time-consuming procedures. To improve diagnostic accuracy and efficiency, we evaluated a novel artificial intelligence (AI)-powered fluorescence microscopic image analyzer (FMIA) for early detection of SFIs.

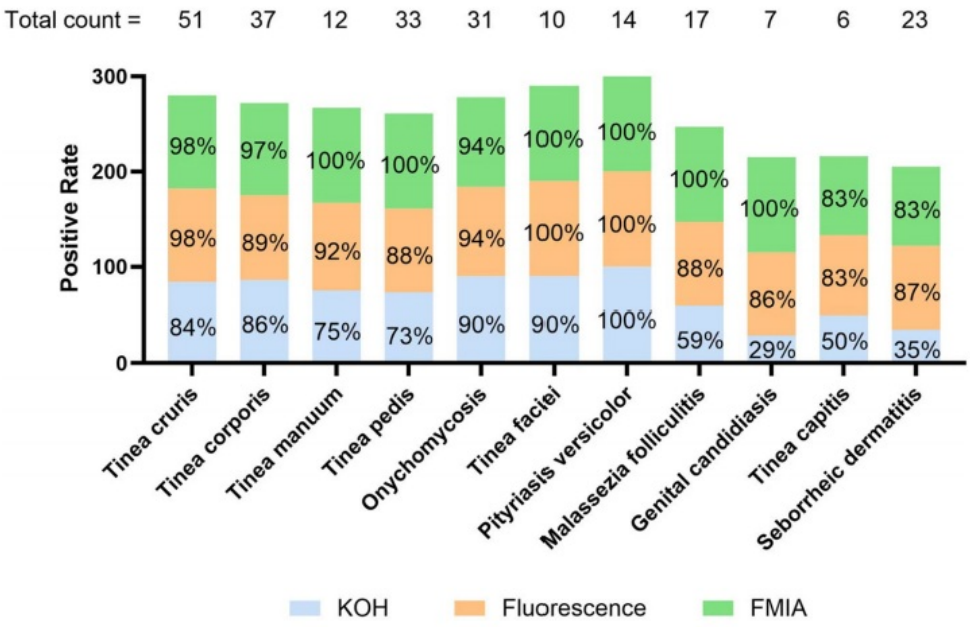

Fig. 3 Comparison of positive detection rates of KOH microscopy, fluorescent staining, and FMIA in diagnosing superficial fungal diseases FMIA, fluorescence microscopic image analyzer; KOH, potassium hydroxide

Materials and Methods

A total of 300 patients with suspected SFIs were enrolled. Each specimen was examined using KOH microscopy, fluorescence staining, and FMIA. A composite gold standard based on clinical presentation, mycological findings, and expert consensus was used for reference. Diagnostic performance was compared across methods using sensitivity, specificity, predictive values, and area under the ROC curve (AUC).

Results

Among 241 confirmed SFI cases, FMIA achieved the highest sensitivity (96.27%), outperforming fluorescence staining (92.95%) and KOH microscopy (75.52%), while maintaining high specificity (94.92%). FMIA demonstrated

an AUC of 0.96. In spore-dominant infections such as Malassezia folliculitis, genital candidiasis, tinea capitis, and seborrheic dermatitis, where KOH microscopy showed low detection rates (29–59%), FMIA achieved significantly higher sensitivities (83–100%). FMIA provided results within 3–5 minutes at low per-test cost, with automated focusing and frame validation minimizing false positives.

Conclusions

The FMIA system offers a highly accurate, rapid, and cost-effective tool for diagnosing SFIs. By addressing the limitations of traditional microscopy and current AI-based image analysis methods, FMIA improves diagnostic precision and efficiency, supporting its implementation in both high-throughput laboratories and resource-limited healthcare settings.

EADV CONGRESS
VIENNA
30 SEP - 3 OCT 2026

Abstract N°: 284

Optical Super-High Magnification Dermoscopy: a Complementary Means in the Diagnosis of Trombiculosis

Giulio Cortonesi*[1], Corinne Orsini[1], Pietro Rubegni[1], Elisa Cinotti[1], Vittoria Cioppa[1]

[1] Dermatology department - AOUS - Siena University, Siena, Italy

Introduction

Trombiculosis is a common but underreported ectoparasitosis caused in Europe by the larval stage of Neotrombicula Autumnalis. Diagnosis of trombiculosis can be difficult: clinical presentation is extremely vague, mainly asymptomatic, occasionally consists of multiple pruritic papules due to parasite biting. Futhermore, larvae show tiny dimensions (200-400 µm) and can easily be missed at conventional 10 x dermoscopy, so high-magnification dermoscopy could represent an useful means in the diagnosis of trombiculosis.

Case Presentation

In October 2021, a 27-year-old man working in the countryside of Tuscany (Italy) presented with a 3-day history of diffuse intense pruritus. Dermatological examination revealed multiple, erythematous macules localized on his right side of the trunk, the genitals, and the right popliteal fossa. A 10x dermoscopy examination revealed in the center of each macula the presence of a tiny bright yellow mite, hard to recognize due to its small size. Videodermoscopy at 40x and 400x magnification (Medicam 1000, Fotofinder System(R)) allowed to observe six-legged golden colored parasites, strongly attached to the skin, and thus to identify an infestation of the larval stage of Neotrombicula Autumnalis, a mite involved in the underestimated and misdiagnosed trombiculosis.

Conclusion

Only one case of Neotrombicula Autumnalis described by using high-magnification videodermoscopy was found in literature. In particular, under optical 400 x magnification, the color, the entire contour of the body and the details of the legs of the parasite are better visible, allowing a precise diagnosis.

EADV CONGRESS
VIENNA
30 SEP - 3 OCT 2026

Abstract N°: 304

Line-field confocal optical coherence tomography (LC-OCT) as a second-line tool after dermoscopy: Three practical cases

Piotr Sobolewski*[1, 2], Mateusz Koper[1], Irena Walecka[1, 2]

[1] Dermatology Clinic, National Institute of Medicine of the Ministry of Interior and Administration, Woloska 137, 02-507 Warsaw, Poland, Warsaw, Poland

[2] Chair and Clinic of Dermatology and Pediatric Dermatology, Centre of Postgraduate Medical Education, Woloska 137, 02-507 Warsaw, Poland, Warsaw, Poland

Introduction

Dermoscopy is the primary non-invasive diagnostic tool in dermatology, significantly improving diagnostic accuracy compared to eye examination. Despite these, diagnostic uncertainty persists in certain clinical cases, particularly for lesions on anatomically challenging sites. Benign lesions often mimic malignancies in though locations: for example, follicular tumors like trichoblastoma or trichoepithelioma imitate basal cell carcinoma (BCC) through shared dermoscopic features such as arborizing telangiectasias and peripheral pearly borders. Line-field confocal optical coherence tomography (LC-OCT) serves as an advanced second-line imaging technique, providing an "optical biopsy" with near-cellular resolution in real-time horizontal (en face) and vertical cross-sectional planes. LC-OCT visualizes detailed microstructural features—including epidermal keratinocyte atypia, tumor architecture, stromal changes, and invasion patterns — bridging the gap between dermoscopy's surface-level morphology and histopathology's cellular detail. This case series demonstrates LC-OCT's practical value through three representative cases, evaluated sequentially by clinical examination, dermoscopy, LC-OCT imaging, and management decisions confirmed by histopathology when indicated.

Case Presentation

Case 1: A 16-year-old female patient presented with a firm, skin-colored nodule with peripheral pearliness on the forehead, persisting for approximately one year without improvement. Dermoscopic examination showed telangiectasias on yellowish-brown background, suggesting BCC. LC-OCT revealed well-circumscribed lobules in superficial to mid-dermis with uniform aggregates, peripheral palisading and horn cysts. However, there were no BCC features like clefting, mucoid edema or irregular lobules. This indicated benign follicular tumor, prompting narrow-margin excision; histopathology confirmed trichoblastoma.

Case 2: A 58-year-old male patient presented with a slowly enlarging, scaly brownish pigmented patch on the photoaged skin of the left lower eyelid, which had been present for approximately three years and raised significant concern for lentigo maligna melanoma. Dermoscopic examination revealed heterogeneous brown/gray pigmentation, a pseudonetwork of structureless areas – features that precluded definitive distinction AK from early melanocytic neoplasia. LC-OCT provided critical insights, demonstrating epidermal thickening with prominent hyperkeratosis and parakeratosis Dermoepidermal junction (DEJ) was without nesting, pagetoid spread, or papillary deformation. These characteristics strongly supported a diagnosis of in situ keratinocytic dysplasia rather than melanoma, guiding a targeted biopsy from the areas of maximal atypia. Histopathology confirmed pigmented AK, enabling conservative eyelid-sparing management with cryotherapy instead of extensive surgical excision.

Case 3: A 44-year-old female presented with a well-demarcated verrucous pigmented plaque on the right breast beneath the areola, enlarging over four years; clinical features suggested seborrheic keratosis (SK), but dermoscopy showed disrupted pigment network and dark blotches without classic SK signs (comedo-like openings, milia-like cysts, cerebriform ridges), raising concern for melanoma or pigmented basal cell carcinoma.

LC-OCT revealed acanthotic epidermis with exophytic/endophytic proliferation, undulating invaginations, papillomatous hyperplasia, horn pseudocysts, and intact DEJ without invasion—confirming benign SK. Elective shave removal was performed; histopathology verified the diagnosis, avoiding wide excision.

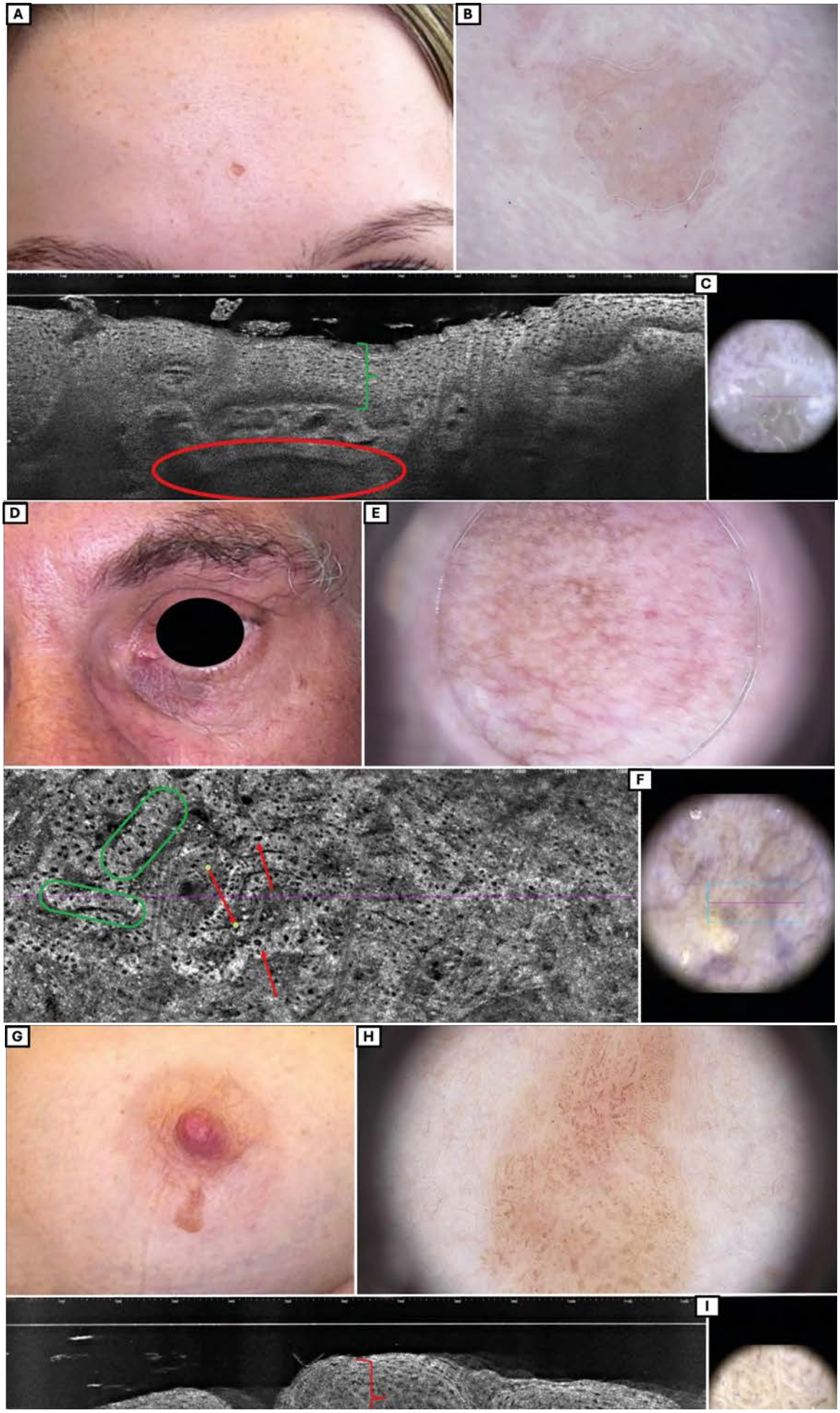

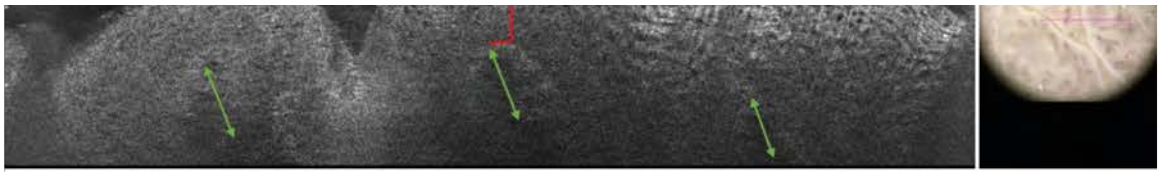

Figure 1. Case 1 — a skin-colored, pearly in periphery plaque on the forehead of a 16-year-old female patient, present for ~1 year; (A) clinical view; (B) dermoscopy showed a pearly peripheral plaque with short, fine teleangectasias on a yelowish-brownish background, suggestive of pigmented BCC; (C) LC-OCT (vertical mode) revealed small, well-demarcated round lobule without peripheral “palisading” (red circle) and normal epithelium without atypia (green bracket), consistent with a adnexal benign tumor rather than an invasive skin carcinoma; Case 2 — a brown macule on the left lower eyelid of a 58-year-old male patient, present for ~3 years; (D) clinical view; (E) dermoscopy revealed heterogeneous brown/gray pigmentation, a pseudonetwork of structureless areas interrupted by follicular openings, and gray dots — raising suspicion of lentigo maligna; (F) LC-OCT (vertical mode) revealed thickened, disorganized epidermis with hyperkeratosis/parakeratosis; atypical keratinocytes (irregular bright cells) clustered with epidermal pattern disruption (red arrows); DEJ was intact with elongated epithelial cords (green circles), without nesting or deformation — favoring in situ AK over invasive carcinoma or melanoma; Case 3 — a pigmented plaque on the right breast under the areola of a 44-year-old female patient, present for ~4 years; (G) clinical view; (H) dermoscopy showed a disrupted pigment network and dark blotches, which were atypical and did not fully exclude melanoma; comedo-like openings, milia-like cysts, cerebriform ridges were absent; (I) LC-OCT (vertical mode) revealed a markedly acanthotic epidermis with exophytic/endophytic proliferation and undulating invaginations. The DEJ was intact, with no dermal invasion or atypical breaching; features — acanthosis (red brackets), papillomatous hyperplasia (green arrows), no invasion and cellular atypia — confirmed benign SK. BCC — basal cell carcinoma; LC-OCT— line-field confocal optical coherence tomography; AK — actinic keratosis; DEJ — dermoepidermal junction; SK — seborrheic keratosis.

Conclusion

LC-OCT resolves dermoscopic uncertainty in facial, pigmented, sun-damaged lesions by providing quasi-histological details that guide precise, conservative management and reduce unnecessary procedures. Limitations include ~500 μm depth, training needs, standardized criteria, and cost.

EADV CONGRESS
VIENNA
30 SEP - 3 OCT 2026

Abstract N°: 792

Multispectral and Dynamic Thermal Imaging for Differentiation of Melanoma from Dysplastic and Benign Nevi: A Pilot Clinical Study

Maria Oniga*[1], Alina Sultana[1], Daniel Costache[2, 3], Olguta Anca Orzan[2, 4], Anton Mihai Tilea[3], Horia Blejan[2, 3], Andrei Marin[5]

[1] National University of Science and Technology POLITEHNICA Bucharest, Bucharest, Romania

[2] Carol Davila University of Medicine and Pharmacy, Central Military Emergency University Hospital Dr. Carol Davila, Bucharest, Romania

[3] Central Military Universitary Emergency Hospital "Carol Davila", Bucharest, Romania

[4] Elias Emergency University Hospital, Bucharest, Romania

[5] Plastic Surgery Department, St John's Clinical Emergency Hospital, Bucharest, Romania

Introduction

Accurate non-invasive differentiation between melanoma (MM), dysplastic nevi (DN), and benign nevi (NV) remains a diagnostic challenge in dermatology. Current approaches are primarily based on morphological criteria and may not fully capture underlying physiological and functional differences between lesions. This limitation can contribute to diagnostic uncertainty, particularly in borderline cases.

In this context, we propose a multimodal imaging approach that integrates multispectral imaging with dynamic thermal analysis, aiming to provide complementary structural and functional information. The objective of this study is to evaluate whether features derived from visible (VIS), near-infrared (NIR), and thermal (TH) imaging enable differentiation between MM, DN, and NV.

Materials and Methods

A total of 182 clinically evaluated lesions (37 MM, 74 DN, 72 NV) were analyzed. Imaging was performed using the MelanoDet system (Figure 1), which integrates three cameras within a unified optical setup. The VIS camera employs a 2 MP sensor for high-resolution assessment of lesion morphology and surface pigmentation. The NIR camera uses a 5 MP sensor with multi-wavelength illumination (805-940 nm) to analyze subsurface pigment distribution. TH imaging is performed using an infrared camera (8-14 µm), enabling both static temperature mapping and dynamic thermoregulation analysis following controlled cooling. In this case, quantitative parameters were extracted, including temperature difference relative to surrounding skin (ΔT), TH recovery time (τ), and slope of the TH recovery curve (TRC).

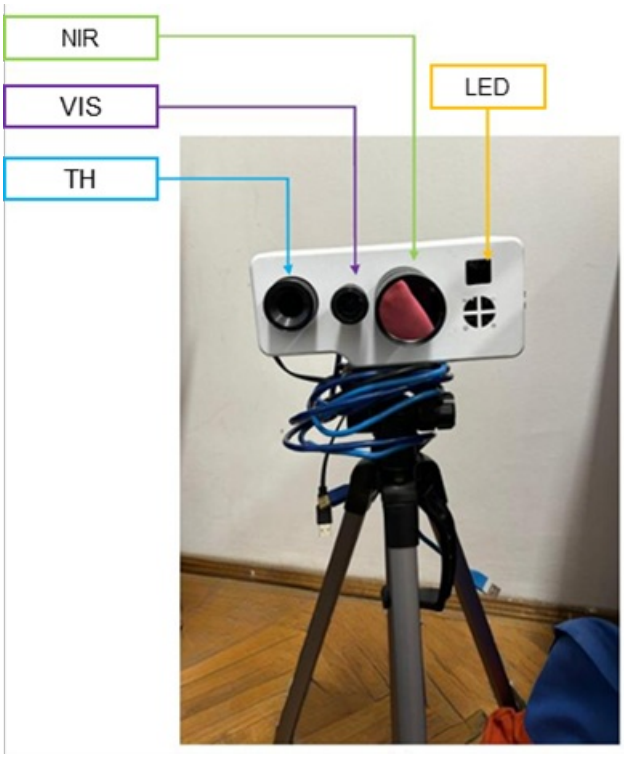

Figure 1. The MelanoDet imaging system with the three cameras and LED illumination module

Results

Multimodal imaging revealed consistent differences between lesion classes across all spectra (Figure 2). In the VIS modality, NV and DN preserved lesion structure, with NV showing regular, symmetric morphology and homogeneous pigmentation, while DN introduced increasing asymmetry and pigment heterogeneity. In contrast, MM displayed irregular borders, asymmetry, and marked heterogeneity in pigmentation, consistent with established criteria.

NIR imaging provided additional information on subsurface organization. While NV exhibited low contrast and uniformity, DN showed increased contrast and moderate heterogeneity, suggesting more complex pigment architecture. This trend was further accentuated in MM, where higher contrast and spatially heterogeneous patterns reflected irregular, depth-dependent pigment distribution.

TH imaging revealed clear quantitative differences between lesion classes. In the static phase, MM exhibited elevated ΔT, while DN showed only slight TH contrast, and NV remained comparable to adjacent healthy tissue. In contrast, dynamic TH analysis provided the strongest separation, as reflected by τ and TRC (Table 1). Following controlled cooling, MM displayed rapid reheating (within 10 seconds) and steep recovery dynamics. DN exhibited intermediate behavior, whereas NV showed minimal variation, closely tracking the TH profile of surrounding skin without full recovery.

Table 1. Quantitative TH parameters for lesion differentiation, showing increased ΔT, faster recovery, and steeper TRC in MM compared to DN and NV

Parameter	NV	DN	MM
ΔT (°C)	0-0.2	0-0.5	0.7-3.0

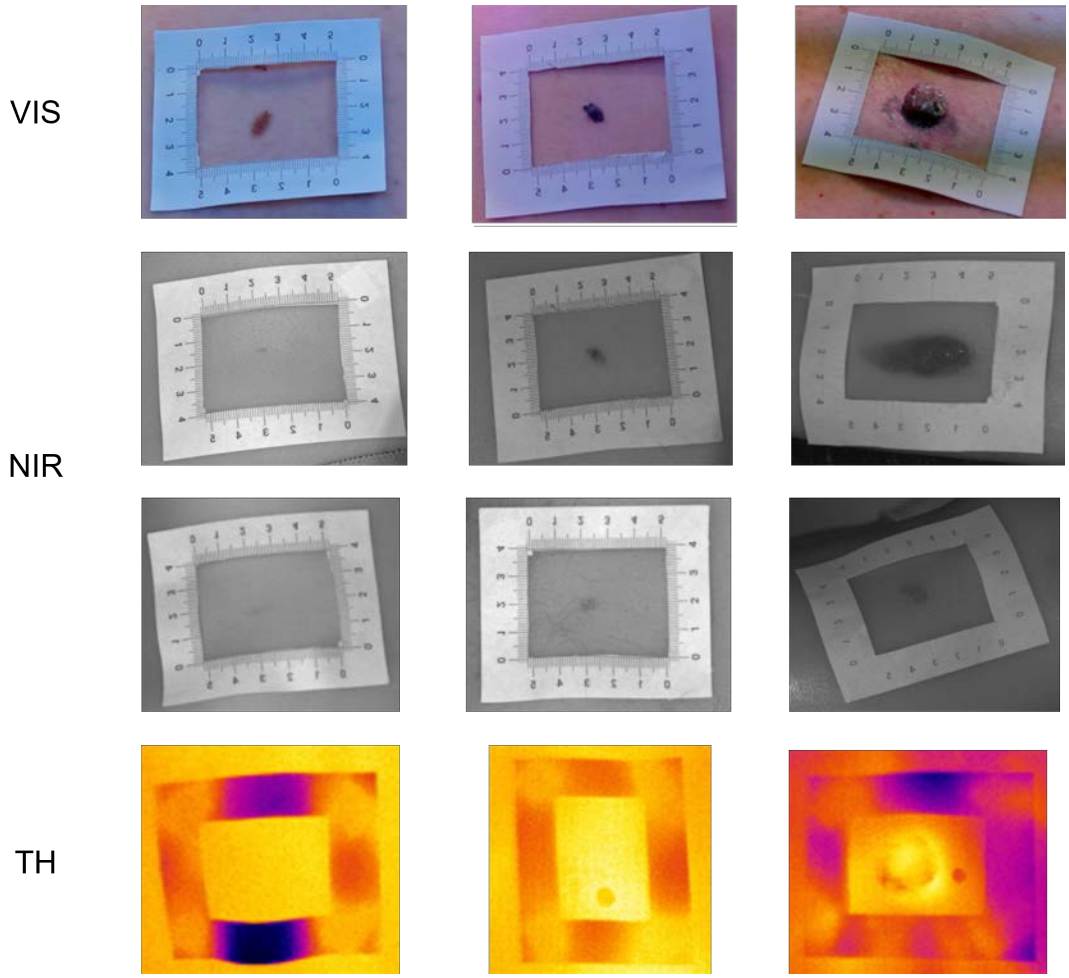

Figure 2. Examples of images obtained in the VIS spectrum (first row), NIR spectrum with the 940 nm wavelength (second and third row) and TH (fourth row) with the MelanoDet multimodal system

Conclusions

Accurate non-invasive differentiation between MM, DN, and NV remains challenging, particularly in lesions with overlapping morphological features. To address this, a multimodal approach combining VIS, NIR, and TH imaging was used to capture complementary structural and functional information. The analysis showed clear differences between lesion types, with MM exhibiting higher TH contrast and faster recovery (Figure 3), consistent with increased vascularization and metabolic activity and resulting in enhanced heat generation and faster TH equilibration. Separation between MM, DN, and NV was observed across all modalities, highlighting the value of integrating morphological and functional data in real time to support clinical decision-making and more selective biopsy indication.

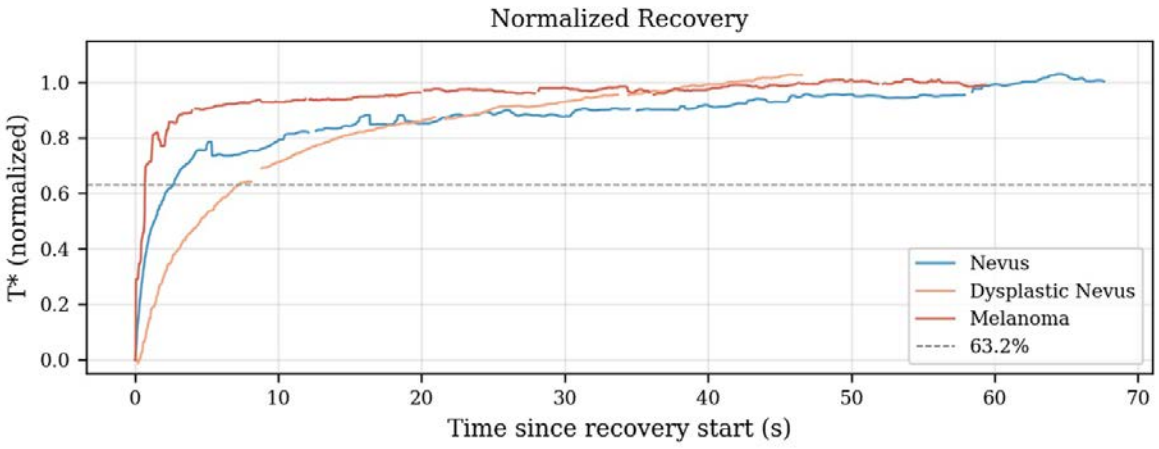

Figure 3. Normalized recovery curves further highlight differences in thermoregulation dynamics, with MM reaching the 63.2% recovery threshold earlier than the trends of recovery curves of DN and NV

EADV Congress 2026, VIENNA
30 SEPTEMBER - 03 OCTOBER 2026
POWERED BY M-ANAGE.COM

EADV CONGRESS
VIENNA
30 SEP - 3 OCT 2026

Abstract N°: 868

Comparison of subjective skin typing and objective skin pigmentation measurements in a skin colour diverse cohort from the Netherlands.

Lotte van den Oord*[1], Stijn Krul[1], Robert Rissman[2], Wouter ten Voorde[2], Deepak Balak[1]

[1] Leiden University Medical Center, Leiden, Netherlands

[2] Centre For Human Drug Research, Leiden, Netherlands

Introduction

Skin pigmentation plays an important role in dermatology. Clinical assessment of skin type is commonly based on subjective classification systems, including the Fitzpatrick Skin Phototype (FSP) scale. The FSP remains the most widely used system, despite having important limitations. The Monk Skin Tone (MST) scale was more recently developed to improve inclusivity and is increasingly being explored in dermatology. However, both systems rely on subjective assessment and may be influenced by observer perception and contextual factors. Objective methods, such as colorimetry and multispectral imaging, provide quantitative measures of skin pigmentation. This study aimed to assess inter-rater agreement between participants and investigators, and to evaluate the agreement between subjective skin type classifications and objective pigmentation measurements.

Materials and Methods

This is an ongoing observational, cross-sectional study in healthy volunteers and patients with skin disease conducted in the Netherlands. Subjective skin typing was assessed using both the FSP and MST scales by participants and an investigator. Participants completed a standardized Fitzpatrick questionnaire based on self-reported phenotypes and sun reactivity, while the investigator assigned FSP based on visual inspection, reflecting routine clinical practice. For the MST scale assessment, both participants and the investigator categorized skin tone using a standardized physical reference chart.

Objective skin pigmentation was measured using the DSM-4 colorimeter and Antera 3D multispectral camera at 14 anatomical skin sites. Agreements were assessed using Cohen's kappa, and associations were evaluated using Spearman's correlation coefficients.

Results

A total of 200 participants were included. According to investigator-assigned FSP, participants were distributed across the full spectrum, with 55% in type I–II and 17.5% in type V–VI. MST classifications were broadly distributed across the scale, with the highest frequencies in type 3 (28%) and type 2 (24%).

Inter-rater agreement between participants and investigator was poor for FSP ($\kappa = 0.038$, $p = 0.154$) and MST ($\kappa = 0.153$, $p < 0.001$). Agreement between investigator-assigned FSP and ITA-based objective categories was moderate ($\kappa = 0.404$, $p < 0.001$). Although both subjective scales correlated strongly with objective melanin measurements (FSP: $\rho = 0.745$; MST: $\rho = 0.783$; $p < 0.001$), categorical agreement was limited, as reflected by substantial overlap in objective pigmentation values between consecutive categories.

Conclusions

Subjective skin typing systems demonstrate limited agreement between observers and only moderate agreement with objective pigmentation measurements. Both FSP and MST show substantial overlap between categories, reflecting poor discriminatory accuracy. These findings highlight inherent limitations of current subjective classification systems.

Skin colorimetry and multispectral imaging provide more reproducible, accurate, and biologically relevant measures of skin pigmentation. Integration of objective pigmentation assessment into clinical and research settings could improve accuracy in skin type classification and support more individualized dermatological care.

EA DV CONGRESS
VIENNA
30 SEP - 3 OCT 2026

Abstract N°: 879

SuBScAN – Subclinical Basal Cell Carcinoma Screening by AI-Assisted Non-invasive Imaging: Diagnosis Before the Appearance of Lesions

Moritz Ronicke*[1], Laura Dürr[1], Michael Höner[1], Léonie Staats[1], Michael Erdmann[1], Carola Berking[1]

[1] Department of Dermatology, Uniklinikum Erlangen, Friedrich-Alexander University Erlangen-Nürnberg, Erlangen, Germany

Introduction

Basal cell carcinoma (BCC) is the most common cancer worldwide, with a lifetime risk of approximately 30% among Caucasians. On the face, its locally destructive growth leads to functional and aesthetic impairment. Early diagnosis enables less invasive treatment options and may reduce morbidity. Non-invasive imaging, particularly Line-field confocal optical coherence tomography (LC-OCT) diagnoses BCC with high sensitivity and specificity. However, these imaging methods are typically applied to pre-identified lesions, requiring a visible or clinically suspicious target to guide probe placement. Whether truly subclinical BCCs in inconspicuous skin can be identified using AI-assisted LC-OCT has not been investigated previously.

Materials and Methods

A prospective, cross-sectional, single-center feasibility study was conducted at the Department of Dermatology, Uniklinikum Erlangen, Germany (April–October 2025; DRKS00036702). Patients with at least two established BCC risk factors were consecutively enrolled. Following clinical exclusion of macroscopically suspicious lesions, inconspicuous facial skin was systematically screened using LC-OCT with an integrated, AI application providing a real-time, color-coded BCC probability score. AI-flagged regions were reviewed by a physician using established LC-OCT diagnostic criteria, independently of the AI score. Lesions diagnosed as BCC were biopsied for histological confirmation.

Results

A total of 150 patients were included (mean age 72.9 ± 10.3 years; 62.0% male). A total of 17 subclinical BCCs were identified in 14 patients (9.3%). All lesions were initially flagged by the AI application. Of 18 lesions diagnosed as BCC by AI-assisted LC-OCT, 15 were histologically confirmed, corresponding to a positive predictive value of 83.3% (95% CI 58.1%–96.4%). In a sensitivity analysis including two expert-confirmed non-biopsied cases, PPV was 94.4% (95% CI 72.7%–99.9%). The predominant subtype was superficial BCC (76.5%), followed by nodular (17.6%) and infiltrative BCC (5.9%). Subtype classification accuracy was 86.7% (13/15 histologically confirmed cases). Lesions were most frequently located on the forehead (35.3%), temples (29.4%), cheeks (11.8%), and nose (11.8%).

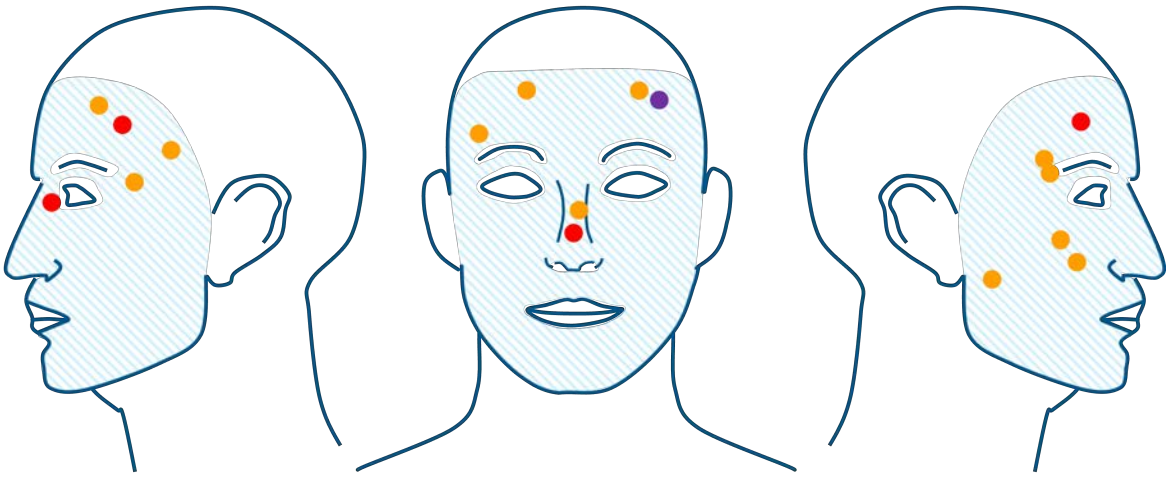

Location of subclinical BCCs. The shaded region represents the examined area. Each dot represents one BCC, displayed in the view from which it is best visible anatomically. Orange = superficial BCC (n=13); red = nodular BCC (n=3); purple = infiltrative BCC (n=1).

Conclusions

SuBScAN enables detection of subclinical BCC in clinically inconspicuous facial skin of high-risk patients with a high PPV and accurate subtype classification. The predominance of superficial BCC may reflect an early developmental stage preceding nodular transformation. AI-assisted LC-OCT allows trained non-physician examiners to perform the initial screening, with physician review limited to flagged areas, making large-area screening operationally feasible. Further prospective studies are needed to assess sensitivity, natural history of subclinical BCC, and cost-effectiveness before routine implementation can be recommended.

EA DV CONGRESS
VIENNA
30 SEP - 3 OCT 2026

Abstract N°: 1034

Circumscribed Lymphangioma: Diagnostic Innovation Using High-Frequency Ultrasonography

Ana Weber[1], Barbara Brunca*[1], Giulia Goedert[1], Leticia Nunes Tajra[1], Renan Doin[1], Enrico Dumbra Bonini[1], Paula Tavares Colpas[1, 1]

[1] Hospital PUC Campinas, Campinas, Brazil

Introduction

Lymphangiomas are rare lymphatic malformations, either congenital or acquired, representing approximately 4% of vascular tumors and 25% of benign pediatric vascular neoplasms. Circumscribed lymphangioma results from dilation of superficial lymphatic channels connected to deeper cisterns. Clinically, it is characterized by grouped translucent vesicles containing clear or serosanguineous fluid, frequently present at birth and often simulating angiokeratomas or hemangiomas. Owing to its broad clinical and dermoscopic spectrum, diagnosis may be challenging and may directly influence treatment planning. In this setting, high-frequency dermatologic ultrasonography (22 MHz), scarcely reported in the literature, has emerged as a valuable noninvasive diagnostic tool. This report describes a rare case of congenital circumscribed lymphangioma with recurrence after treatment, correlating clinical, dermoscopic, and high-frequency ultrasonographic findings to enhance diagnostic accuracy.

Case Presentation

A 12-year-old girl, initially followed by pediatric surgery, presented with a skin-colored dorsal nodule present since birth, with progressive local enlargement. Sclerotherapy with Picibanil (OK-432) was performed, with apparent lesion regression at 12 months of age. Ten years after the initial treatment, she was referred to Dermatology because of the progressive development of grouped erythematous papules at the site of the previous lesion in the right scapular area, clinically simulating angiokeratoma. Dermoscopy under polarized and ultraviolet light revealed reddish lacunae separated by whitish septa, as well as a dark-to-light color transition within some lacunae, corresponding to the “hypopyon sign” (two-tone lacunae). High-frequency dermatologic ultrasonography (12 and 22 MHz) demonstrated anechoic lesions involving the dermis and subcutaneous tissue, without continuous Doppler flow, in association with microcysts, supporting the diagnosis of cutaneous lymphangioma, as shown in figures 1 and 2. Based on the integrated clinical, dermoscopic, and ultrasonographic findings, and given the refractoriness to prior sclerotherapy, an incisional biopsy was performed. Histopathological examination revealed proliferation and dilation of thin-walled lymphatic vessels, confirming the diagnosis of circumscribed lymphangioma. The patient and her family elected clinical follow-up.

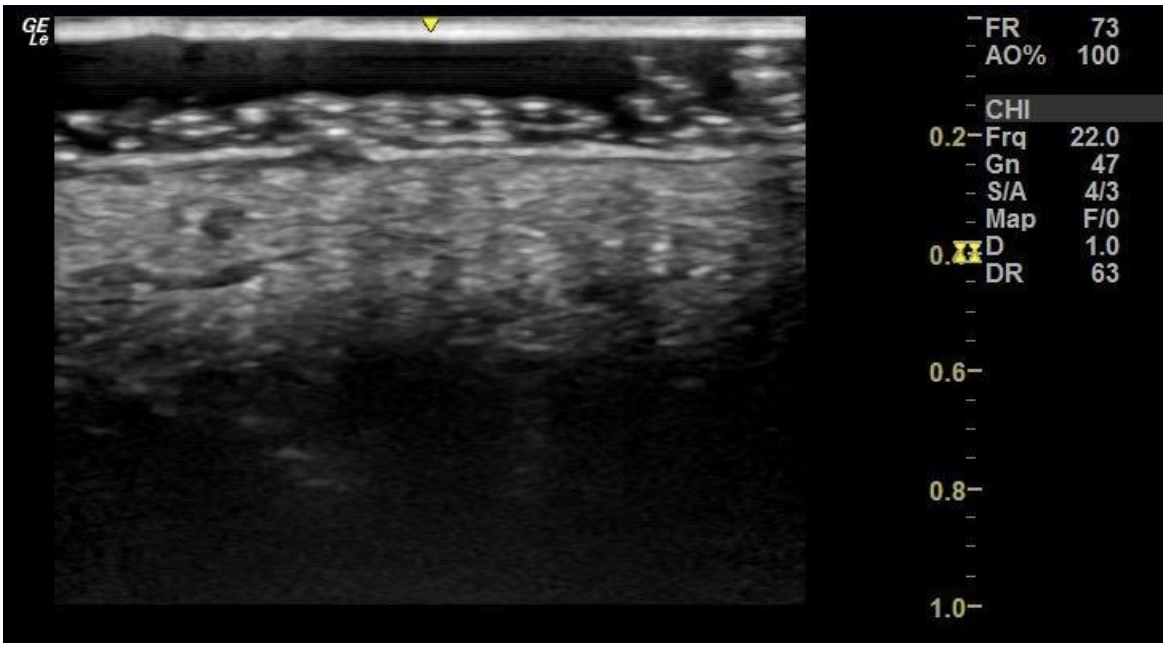

Figure 1 - High-frequency ultrasonography (22 MHz): presence of microcysts and absence of continuous Doppler flow.

Conclusion

Circumscribed lymphangioma is the most common form of lymphangioma, and approximately half of cases are present at birth. The clinical presentation in this case highlights the relevant differential diagnoses, as the translucent vesicles classically seen in lymphangioma may undergo intralesional hemorrhage and mimic angiokeratoma. In this context, the lacunae observed on dermoscopy, reported in 89% of lymphangioma cases in the literature, particularly the reddish lacunae (45%) and the classic hypopyon sign (47%), support the diagnosis of lymphangioma and are consistent with the present case. Given the diagnostic challenge, high-frequency dermatologic ultrasonography, considered a valuable noninvasive method, played an important role in the evaluation of the lymphatic malformation by allowing visualization of superficial structures. The examination typically demonstrates thin-walled cystic spaces with anechoic or hypoechoic content, presenting as macrocystic, microcystic, or mixed patterns, interspersed with septa and lacking continuous Doppler flow, thereby helping differentiate these lesions from vascular malformations. Histopathological examination confirmed the clinical suspicion. Available treatment options include surgical excision, ablative lasers, cryotherapy, and sclerotherapy; however, recurrence rates remain high. Therefore, reporting this rare case with combined clinical, dermoscopic, and ultrasonographic analysis—an approach still scarcely described in the literature—may contribute to earlier and noninvasive diagnostic recognition.

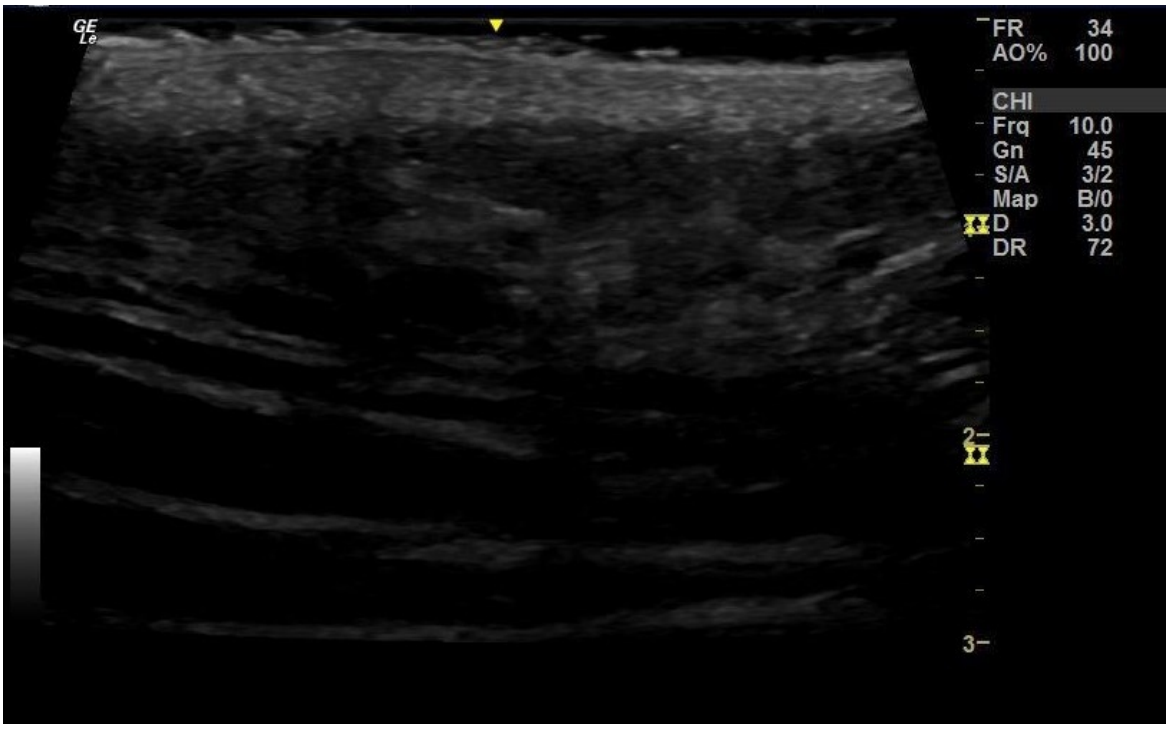

Figure 2 - High-frequency ultrasonography (12 MHz): anechoic lesions involving the dermis and subcutaneous tissue. References: 1. Kiran A, Komandla A. Cutaneous lymphangioma circumscriptum. Pan Afr Med J. 2023;45:46. doi:10.11604/pamj.2023.45.46.39047. 2. Miceli A, Stewart KM. Lymphangioma. In: StatPearls [Internet]. Treasure Island (FL): StatPearls Publishing; 2026 Jan– [updated 2023 Aug 8; cited 2026 Apr 12]. Available from: NCBI Bookshelf. 3. Zaballos P, del Pozo LJ, Argenziano G, Karaarslan IK, Landi C, Vera A, et al. Dermoscopy of lymphangioma circumscriptum: a morphological study of 45 cases. Australas J Dermatol. 2018;59(3):e189-e193. doi:10.1111/ajd.12668. 4. Levy J, Barrett DL, Harris N, Jeong JJ, Yang X, Chen SC. High-frequency ultrasound in clinical dermatology: a review. Ultrasound J. 2021;13(1):24. doi:10.1186/s13089-021-00222-w.

EADV CONGRESS
VIENNA
30 SEP - 3 OCT 2026

Abstract N°: 1270

Diagnostic performance of large language models in dermoscopic image classification: a pilot study on the HAM10000 dataset

Jakub Żółkiewicz*[1, 2]

[1] Department of Dermatology, Venereology and Allergology, Faculty of Medicine, Medical University of Gdańsk, Department and Clinic of Dermatology, Venerology and Allergology, University Clinical Center, Gdańsk, Poland
[2] Department and Clinic of Dermatology, Venerology and Allergology, University Clinical Center, Gdańsk, Poland

Introduction
Artificial intelligence models, including large language models (LLMs) with capability to evaluate images, are progressively employed for dermatological image classification. Before deploying LLMs in large-scale diagnostic studies, it is critical to verify their reliability in processing dermoscopic images. This study evaluated three commercially available LLMs on dermoscopic classification, reporting both respective instrument metrics (refusal rate, format compliance, visual grounding) and preliminary diagnostic performance.

Materials and Methods
This prospective pilot study assessed 60 dermoscopic images from the HAM10000 dataset, purposively sampled to include 30 malignant and 30 benign cases across three subgroups: melanoma (n = 30), benign melanocytic nevi (n = 20), and benign lichenoid keratoses (n = 10). Each image was independently classified by three LLMs (ChatGPT-5.4, Claude 4.6 Opus, Gemini 3.1 Pro) using a standardized English-language prompt requiring TOP-1/TOP-2/TOP-3 diagnoses and a confidence score (1-5). Beyond diagnostic accuracy, refusal rate, format compliance, and a visual grounding index (VGI) were measured. VGI was based on a 10-case subset re-evaluated with falsified metadata to test whether models relied on image features or metadata. Binary diagnostic accuracy (malignant vs. benign) was assessed using TOP-1 classification. Moreover, sensitivity, specificity, PPV, NPV, and balanced accuracy were calculated. Inter-model agreement was tested using McNemar's test and Cochran's Q.

Results
Claude 4.6 Opus achieved the highest sensitivity (0.93; 95% CI: 0.79-0.98), while Gemini 3.1 Pro showed superior specificity (0.77; 95% CI: 0.59-0.88). TOP-1 exact class accuracy was 53.3% for ChatGPT-5.4, 66.7% for Claude 4.6 Opus, and 65.0% for Gemini 3.1 Pro. TOP-3 exact class accuracy was 91.7% for ChatGPT-5.4, 88.3% for Claude 4.6 Opus, and 90% for Gemini 3.1 Pro. Balanced accuracy remained consistent across all models and ranged from 0.7-0.73, with no statistically significant differences in performance (Cochran's Q = 0.273, p = 0.87). The diagnostic performance of all LLMs is presented in the Table 1. Across all models, only one refusal was recorded (Gemini 3.1 Pro), whereas task refusal was entirely absent among the remaining models. The visual grounding test revealed that all models altered their TOP-1 diagnosis when clinical metadata was falsified (VGI 67-100%).

Parameter	ChatGPT-5.4	95% CI	Claude 4.6 Opus	95% CI	Gemini 3.1 Pro	95% CI
Sensitivity	**0.833**	0.664-0.927	**0.933**	0.787-0.982	**0.7**	0.521-0.833
Specificity	**0.567**	0.392-0.726	**0.5**	0.332-0.668	**0.767**	0.591-0.882
PPV	**0.658**	0.499-0.788	**0.651**	0.502-0.776	**0.75**	0.566-0.873
NPV	**0.773**	0.566-0.899	**0.882**	0.657-0.967	**0.719**	0.546-0.844
Balanced accuracy	**0.7**	0.575-0.801	**0.717**	0.592-0.815	**0.733**	0.61-0.829

CI – confidence interval; PPV – positive predictive value; NPV – negative predictive value

Table 1. The diagnostic performance of all analyzed large language models LLMs.

Conclusions

This study shows that LLMs may be technically feasible and promising tool for dermoscopic images classification with minimal or no task refusal. However, diagnostic accuracy was only moderate, and the high VGI scores suggest that models' reasoning is significantly linked with textual metadata rather than visual evidence alone. Despite the risk of data contamination within the HAM10000 dataset, presented results serve as the base for prospective validation on large datasets.

EA DV CONGRESS
VIENNA
30 SEP - 3 OCT 2026

Abstract N°: 1446

PROVOKE AI: Dynamic AI-generated Clinical Questions and Description Improve Dermatological Diagnostic Accuracy – A proof of concept Study

Hang Nguyen*[1], Yoon Kyoung Kim[2], Quang Do[3], Hoang Le[3], Grevelink Joannes[4], Folkert Blok[5]

[1] Belle.ai, Toulouse, France
[2] Faculty of Medicine, Imperial College London, London, United Kingdom
[3] Belle.ai, Hanoi, Viet Nam
[4] People's Health Clinic, Park City, Utah, United States
[5] Department of Dermatology, Amsterdam University Medical Center, Amsterdam, Netherlands

Introduction

Accurate dermatological diagnosis begins with systematic lesion description and iterative clinical inquiry. However, many current automated systems rely on static, one-size-fits-all questionnaires which disrupt clinician workflow and overwhelm patients with irrelevant questions.

A proof-of-concept system was developed integrating CNN lesion analysis with the PROVOKE framework—a Dutch mnemonic for systematic skin lesion description (Plaats = location, Rangschikking = arrangement, Omvang = size/extent, Vorm = shape, Omtrek = border, Kleur = color, Efflorescentie = primary lesion type).

The system generates a structured description, preliminary differential diagnosis, and three CNN-guided, context-specific questions. To test the clinical value of these outputs, Large Language Models (LLMs) were used as proxies for clinician reasoning.

Materials and Methods

Our study utilized a proof-of-concept (POC) PROVOKE AI system - convolutional neural networks (CNNs)to generate structured descriptions. The analysis was performed on a dataset of 417 unique lesion images from a standard Dutch textbook, "Dermatovenereologie voor de eerste lijn."

A two-phase validation study was then conducted using leading Large Language Models (LLMs): Gemini-2.5 Pro and ChatGPT-4o.

- **Phase 1 (Static Analysis):** For each case, the LLMs received only the AI-generated PROVOKE description and were prompted to generate a top-3 differential diagnosis.
- **Phase 2 (Context-Guided Analysis):** The original PROVOKE description was augmented with three PROVOKE AI-generated questions and their corresponding answers to simulate a clinical inquiry. The LLMs were then prompted again for a top-3 differential diagnosis.

Results

We evaluated the top-3 diagnostic accuracy of six different configurations across 417 dermatological image cases, using textbook-labeled ground truth as reference. The performance was stratified by disease prevalence ("All" vs.

“Common” cases) as in Table 1.

To compare our system with LLM performance, we first used Gemini 2.5 Pro to generate medical descriptions for each image and to provide three triage question–answer pairs. ChatGPT 4o was then asked to produce a top-3 diagnosis using only the descriptions and again using both the descriptions and the triage information. Accuracy was 53.1% overall without questions and 56.7% with them, showing minimal gain. These findings indicate that, in this setup, LLMs achieved only moderate performance, and the provided questions offered little benefit—underscoring the importance of carefully designing effective, context-relevant triage questions.

Table 1: Evaluation of the POC PROVOKE system and LLM, focusing on its performance and the quality of generated descriptions and question–answer pairs, as assessed through LLM-based evaluation.

	Input	Without questions		With 3 questions - answers	
		Overall	Common diseases	Overall	Common diseases
PROVOKE AI	Image	86.8%	85.8%	89.0%	88.5
Chat GPT 4o	Description + QAs by PROVOKE AI	35.7%	39.4%	68.6%	70.0%
	Description +				

Conclusions

This proof-of-concept study demonstrates that PROVOKE AI, a CNN-based system for structured lesion description, achieves high diagnostic accuracy (>85% overall). Crucially, the system leverages this accuracy to generate dynamic, discriminating questions that substantially enhance downstream reasoning, enabling LLMs to reach top-3 accuracies above 80% for common diseases, even without image access. These results position CNN-guided questioning as a powerful paradigm for future AI in dermatology: combining robust image recognition with targeted clinical inquiry. Ongoing work will expand PROVOKE descriptors (100→300) and extend to multimodal inputs to further improve precision and generalizability.

EADV CONGRESS
VIENNA
30 SEP - 3 OCT 2026

Abstract N°: 1506

A Case of Lupus Panniculitis Confirmed by Re-evaluating the Subcutis: Importance of Adequate Biopsy Depth

Seungmin Park*[1], Jiwon Bang[1], Sae Hee Kim[1], Ji Won Lim[1], YiNa Yoon[1], JaeYoung Sung[1], ChangYong Kim[1], Da-Ae Yu[1], YangWon Lee[1], YongBeom Choe[1]

[1] Konkuk university school of medicine, Seoul, Korea, Rep. of South

Case Presentation

A 20-year-old female revisited our department in 2025 with depressed scars and induration involving the face, trunk, and bilateral buttocks. In 2021, she had been suspected of having connective tissue disease-associated panniculitis on the basis of clinicopathologic and serologic findings and was referred to the rheumatology department. Physical examination revealed firm, indurated plaques accompanied by lipoatrophic changes. The biopsy performed in 2021 did not show histopathologic features characteristic of lupus panniculitis. In 2025, a re-biopsy with adequate sampling depth was performed, and upon slide review by a dermatologist, inflammatory changes involving the subcutaneous fat layer, including lobular panniculitis and fat necrosis with hyaline necrosis and lipomembranous changes, were identified.

Conclusion

Lupus panniculitis is a rare subtype of chronic cutaneous lupus erythematosus characterized by inflammatory involvement of the subcutaneous adipose tissue, typically presenting as indurated nodules or plaques that may eventually progress to lipoatrophy and fibrosis. Because the disease often follows a chronic, relapsing course, diagnosis may be difficult owing to nonspecific early clinical features and histopathologic overlap with other inflammatory or sclerosing disorders. This case highlights the importance of obtaining an adequately deep tissue sample and carefully evaluating the subcutaneous fat layer in patients with suspected autoimmune-associated panniculitis.

Keywords: Lupus panniculitis; Lupus profundus; Cutaneous lupus erythematosus; Long-term follow-up

EA DV CONGRESS
VIENNA
30 SEP - 3 OCT 2026

Abstract N°: 1559

Ochre Fluorescence in Melanoma: A Dermoscopic Clue Under Ultraviolet-Induced Fluorescence Dermoscopy

Guillem Esteve-Boncompte*[1], Yomara Indira Morant Garcia[1], Felip Vilardell Villellas[2], Pawel Pietkiewicz[3, 4], Veronica Sanmartín[1], Rosa M Martí[1]

[1] Hospital Universitari Arnau de Vilanova, Lleida, Spain

[2] Department of Pathology, Hospital Universitari Arnau de Vilanova, Lleida, Spain

[3] Zwierzyniecka Medical Center, Poznań, Poland, Prisca Sapientia Institute, Zürich, Switzerland, Poznań, Poland

[4] Prisca Sapientia Institute, Zürich, Switzerland

Introduction

Ultraviolet-induced fluorescence dermoscopy (UVFD) is a noninvasive imaging technique that uses ultraviolet light, typically at 365 nm, to induce visible fluorescence from endogenous and exogenous cutaneous chromophores, providing information that complements conventional dermoscopy. Unlike standard dermoscopy, which relies on reflected visible light, UVFD enables the visualization of fluorescence-based signals and enhances superficial structures that may otherwise be inapparent. This modality shares its fundamental principle with Wood's lamp examination, while offering dermoscopic magnification and improved morphologic correlation. Recent studies have expanded the applications of UVFD across a broad spectrum of dermatologic conditions, including infectious, inflammatory, keratinization, and neoplastic disorders, where it may reveal diagnostically relevant fluorescence patterns and improve lesion assessment. In dermato-oncology, UVFD has demonstrated the ability to enhance keratin-related structures, improve border delineation, and provide additional diagnostic clues in cutaneous tumors. In melanocytic lesions, the absorption of ultraviolet light by melanin results in hypofluorescent areas, increasing lesion contrast and potentially aiding in margin definition. More recently, a characteristic "ochre fluorescence" has been described as a highly specific clue for melanoma, particularly in invasive forms, although its sensitivity remains limited. In this context, we present a case of melanoma exhibiting ochre fluorescence under UVFD, highlighting its potential diagnostic value and clinical implications.



Clinical image of an asymmetric, irregularly pigmented melanoma in situ on the back, arising within a dysplastic nevus.

Case Presentation

A 59-year-old patient presented with a 15 × 16 mm pigmented lesion on the back, with no clearly defined onset but progressive clinical concern. On dermoscopic examination, the lesion was asymmetric in color and structures and fulfilled criteria for a melanocytic lesion. It showed an atypical pigment network (thickened and not fading at the periphery), an eccentric pigmented blotch occupying approximately 30% of the lesion, and hypopigmented scar-like areas associated with blue-white structures, suggestive of regression. Ultraviolet-induced fluorescence dermoscopy (UVFD) revealed predominantly hypofluorescent areas corresponding to melanin absorption, along with focal ochre fluorescence. Notably, these areas spatially corresponded to the hypopigmented scar-like regions observed under polarized dermoscopy, consistent with areas of regression. The lesion was excised, and

histopathological examination confirmed a superficial spreading melanoma in situ arising on a dysplastic nevus (Clark level I), with associated regression changes. Surgical margins were free.

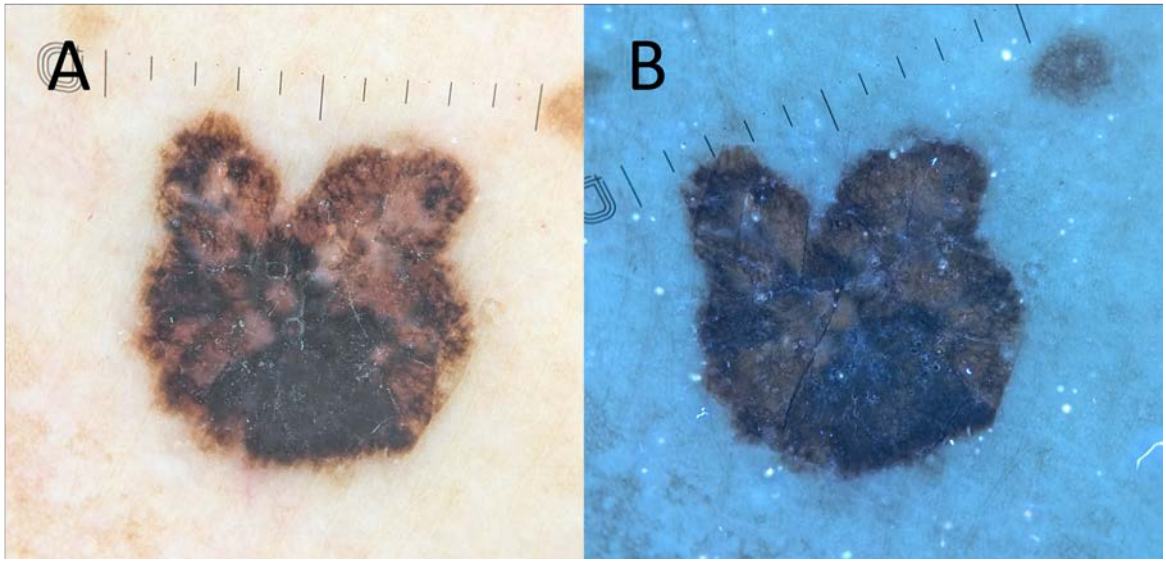

Polarized dermoscopy and UVFD of melanoma in situ. (A) Polarized dermoscopy showing asymmetry in color and structure, an atypical pigment network, an eccentric pigmented blotch, and hypopigmented scar-like areas with blue-white structures. (B) Ultraviolet-induced fluorescence dermoscopy (UVFD) highlighting focal ochre fluorescence corresponding to the regression-like hypopigmented areas. Images acquired with DermLite DL5 (3Gen, San Juan Capistrano, CA, USA).

Conclusion

This case highlights the potential value of ultraviolet-induced fluorescence dermoscopy (UVFD) as a complementary tool in the evaluation of melanocytic lesions. Recent multicenter data suggest that UVFD can improve visualization of selected dermoscopic structures and enhance lesion border definition, while also revealing distinctive fluorescence patterns not visible under conventional dermoscopy. Ochre fluorescence is a highly specific but low-sensitivity clue for melanoma, reported in 23% of melanomas versus 3% of nonmelanomas, with 97% specificity and higher frequency in invasive than in situ melanoma (40% vs 6%). In our case, ochre fluorescence corresponded to dermoscopic regression areas in a superficial spreading melanoma in situ arising on a dysplastic nevus, supporting its possible role as an additional warning sign. However, UVFD should not replace clinical assessment, conventional dermoscopy, or histopathology. Further prospective studies are required to clarify the reproducibility, clinicopathologic correlation, and diagnostic significance of ochre fluorescence in melanoma.

EADV CONGRESS
VIENNA
30 SEP - 3 OCT 2026

Abstract N°: 1623

Neurothekeoma presenting with satellite papules. Clinico-dermoscopic and High-Frequency Ultrasound Correlation.

Rebeca Martin Velasco*[1], Caridad Elena Morales Munera[1], Esther Roe[1], anna mozos[1], Ashfaq Marghoob[2], ORIOL YELAMOS PENA[1]

[1] Hospital De La Santa Creu I Sant Pau, Barcelona, Spain

[2] Memorial Sloan Kettering Skin Cancer Center, Hauppauge, United States

Introduction

Subcutaneous papules and nodules pose a diagnostic challenge, as visual inspection and dermoscopy are of limited value. With the increasing bedside availability of noninvasive techniques such as High-Frequency Ultrasound (HFUS), characterization of clinically non-specific lesions has improved, helping guide diagnosis and management.

We report a case of neurothekeoma with an atypical presentation with satellite papules, in which HFUS contributed to lesion characterization beyond clinical and dermoscopic assessment.

Case Presentation

A 33-year-old woman presented with a two-year history of a firm nodule surrounded by two smaller papules on the dorsum of the foot (Fig. 1A). Dermoscopy showed a homogeneous pink background with whitish areas, arborizing and linear vessels, without ulceration (Fig. 1C,D). As the lesion was clinically and dermoscopically nonspecific, a deeper dermal process was suspected and HFUS was performed, revealing 2 hypoechoic nodules involving the dermis and hypodermis. Within the lesion, hyperechoic linear structures parallel to the skin surface were observed, together with perpendicular hypoechoic linear structures at the deeper border (Fig. 1E). Color Doppler showed moderate vascular flow at the periphery and within the nodule (Fig. 1 F). The lesion's firm consistency, non-specific dermoscopic findings with irregular vascular pattern, infiltrative border on HFUS, and positive intralesional Doppler signal raised suspicion for dermatofibrosarcoma protuberans or other malignant dermal neoplasms. An excisional biopsy was performed. Histopathology demonstrated an S100-negative, multilobulated myxoid dermal proliferation of spindle and epithelioid cells (Fig. 1B), consistent with neurothekeoma. Margins were clear with no recurrence after 1 year of follow-up.

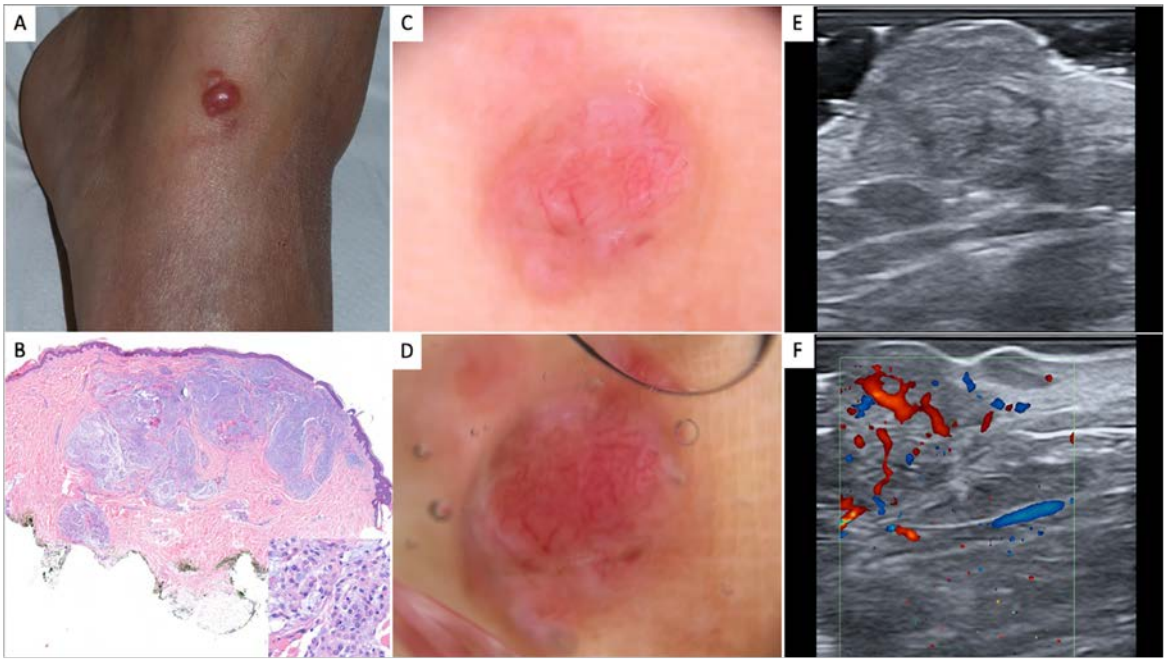

Fig. 1. (A) Clinical presentation of a pink-reddish nodule on the dorsum of the foot, surrounded by two adjacent smaller papules. Non-contact polarized (C) and contact non-polarized dermoscopy (D) displaying a homogeneous pink background with whitish areas, alongside prominent arborizing and linear vessels without ulceration. (E) High-frequency ultrasound (B-mode) demonstrating a well-defined, slightly hypoechoic dermal nodule and a smaller adjacent nodule, featuring intralesional transverse hyperechoic linear structures and hypoechoic projections perpendicular to the skin surface at the deeper border. (F) Color Doppler showing a moderate peri and intra-lesional vascular flow. (B) Histopathology demonstrating a well-circumscribed, multilobulated myxoid dermal proliferation (low magnification). The corner inset provides a detailed view of spindle and epithelioid cells at higher magnification.

Conclusion

HFUS is a non-invasive, accessible bedside imaging modality. Compared to conventional ultrasound it provides higher-resolution but lower-penetration imaging, enabling visualization from the epidermis to the superficial hypodermis, up to 10mm in depth with 22Mhz probes. This makes it particularly suitable for the evaluation of subcutaneous lesions (1).

Neurothekeoma is an infrequent benign dermal tumor of fibrohistiocytic origin. Retrospective evaluation of over 300 neurothekeomas revealed that it most frequently presents as a solitary red-pink papule or nodule on head or neck of young women (2,3). Lower extremities are an infrequent localization, and presentation with adjacent satellite papules has not been previously reported in the literature.

Several dermoscopic reports of neurothekeoma have described linear/arborizing vessels and white areas on a pink-red background (4). However, these findings are non-specific, as dermoscopy cannot visualize structures beyond the papillary dermis (5), making dermal lesions appropriate for HFUS assessment. To date, only two reports of HFUS in neurothekeoma have been described. As in our case HFUS revealed hypoechoic nodules, although doppler flow was less prominent and no hyper or hypoechoic linear structures were visible (6,7). These structures may reflect the tumor’s lobulated histopathology, although larger series are needed to confirm these findings and their relation to histopathology.

Clinical examination and dermoscopy may be non-specific in dermal or subcutaneous lesions, limiting diagnostic utility. HFUS can provide useful information on lesion depth, internal architecture, borders, and vascularity, contributing to the differential diagnosis and biopsy decision-making. While HFUS does not replace histopathological confirmation, recognizing these architectural patterns may help in the diagnosis of subcutaneous tumors.

EADV Congress 2026, VIENNA
30 SEPTEMBER - 03 OCTOBER 2026
POWERED BY M-ANAGE.COM

EADV CONGRESS
VIENNA
30 SEP - 3 OCT 2026

Abstract N°: 1631

A Case of Prostate Cancer with Extensive Systemic Metastasis Presenting as Multiple Scalp Nodules

Siji Chen*[1], Hao Cheng[1]

[1] Sir Run Run Shaw Hospital, Hangzhou, China

Introduction

The skin is often regarded as a "window" to visceral malignancies. In some instances, cutaneous metastases can serve as the initial clinical manifestation of an underlying internal disease. This report presents a case where advanced prostate cancer was initially identified through the onset of metastatic scalp lesions.

Case Presentation

A 65-year-old male patient presented with a chief complaint of "multiple red masses on the scalp for over 2 months." The lesions initially presented as firm papules and subsequently rapidly increased in number and size, with some becoming soft in texture, accompanied by no pain or pruritus. The patient had a history of a spontaneous fracture of the left femoral neck six months prior and lacked a history of regular medical examinations.

A biopsy of the scalp mass revealed an essentially normal epidermis. Within the dermis, atypical tumor cells were observed infiltrating in nest-like masses with a disorganized cellular arrangement, interspersed with fibrous connective tissue. Immunohistochemistry (IHC) results showed: PSA (+), NKX3.1 (+), AR (+), and CK-pan (+), while markers including CK7 (-), CK20 (-), TRPS1 (-), P40 (-), and S-100 (-) were all negative. The Ki-67 proliferation index was approximately 30%. Laboratory tests indicated a serum PSA level > 1241 ng/mL. A subsequent prostate needle biopsy confirmed prostatic acinar adenocarcinoma. PET-CT findings indicated a malignant prostate tumor with extensive systemic bone metastases, alongside multiple brain, cutaneous, and subcutaneous metastases.

Conclusion

Through the presentation of metastatic scalp nodules as the primary clinical sign, specific skin IHC markers (such as PSA and NKX3.1) were utilized to rapidly identify the primary tumor site, ultimately leading to a definitive diagnosis of advanced prostate cancer. This case emphasizes that in clinical practice, physicians should maintain a high index of suspicion for potential visceral tumor metastasis when encountering sudden-onset skin nodules with textural changes in middle-aged and elderly men. Early differentiation and diagnosis should be achieved by integrating characteristic IHC techniques.

EA DV CONGRESS
VIENNA
30 SEP - 3 OCT 2026

Abstract N°: 1657

Diagnostic performance of human-artificial intelligence (AI) collaboration in teledermoscopy: a retrospective validation study of a novel 8-class AI tool

Carolina Nätterdahl[1], Isabelle Krakowski[2], Kari Nielsen[3], Teo Helkkula[1], Nikki Adler[4], Johan Kappelin[5], Cristina Vico-Alonso[4], Cecilia Sand[1], Karim Saleh[1], Albert Duvetorp[6], Katharine Hopkins[7], Kevin Yang[1], Hugh Roberts[8], Sinja Kristiansen[7], Alex Chamberlain[8], Irina Baranovskaya[7], Tine Vestergaard[9], Magdalena Claesson[10], Bertil Persson[1], Victoria Mar[4], Jan Lapins[2], Åsa Ingvar*[1]

[1] Department of Dermatology and Venereology, Skåne University Hospital, Lund, Sweden, Dermatology and Venereology, Lund University Skin Cancer Research Group (LUSCaR), Department of Clinical Sciences Lund, Lund University, Lund, Sweden

[2] Dermatology and Venereology Division, Department of Medicine Solna and Huddinge, Karolinska Institutet, Karolinska University Hospital, Stockholm, Sweden,, Stockholm, Sweden

[3] Department of Dermatology and Venereology, Helsingborg Hospital, Department of Clinical Sciences Lund, Lund University, and Department of Dermatology, Skåne University Hospital, Lund, Sweden, Dermatology and Venereology, Lund University Skin Cancer Research Group (LUSCaR), Helsingborg, Sweden

[4] School of Public Health and Preventive Medicine, Monash University, Melbourne, Victoria, Australia, Victorian Melanoma Service, Alfred Hospital, Melbourne, Australia

[5] Department of Dermatology, Landskrona Hospital, Landskrona, Sweden, Dermatology and Venereology, Lund University Skin Cancer Research Group (LUSCaR), Department of Clinical Sciences Lund, Lund University, Landskrona, Sweden

[6] LEO Foundation Skin Immunology Research Center, Department of Immunology and Microbiology, University of Copenhagen, Denmark, Dermatology and Venereology, Department of Clinical Sciences Lund, Lund University, Copenhagen, Denmark

[7] Department of Dermatology and Venereology, Skåne University Hospital, Dermatology and Venereology, Lund University Skin Cancer Research Group (LUSCaR), Department of Clinical Sciences Lund, Lund University, Malmö, Sweden

[8] Victorian Melanoma Service, Alfred Hospital, School of Translational Medicine, Monash University, Melbourne, Australia

[9] Department of Dermatology and Allergy Centre, Odense University Hospital, Odense, Denmark

[10] Department of Dermatology and Venereology, Sahlgrenska University Hospital, Department of Dermatology and Venereology, Institute of Clinical Sciences, Sahlgrenska Academy, University of Gothenburg, Gothenburg, Sweden

Introduction

Artificial intelligence (AI) is emerging as a key tool for improving skin cancer diagnostics, yet the impact of human-AI collaboration on diagnostic accuracy needs to be further evaluated. This study examines the combined diagnostic performance of dermatologists and a novel 8-class AI tool for skin lesion assessments.

Materials and Methods

This retrospective study analyzed 1,597 teledermoscopic referrals from routine clinical care in Sweden. Twenty-one dermatologists assessed each case first without and subsequently with the AI tool built on vision transformers and fully connected neural networks. The primary outcome was change in accuracy for benign-malignant classification. Secondary outcomes included class-specific accuracy and changes in management recommendations. Ground

truth was established using histopathology, face-to-face consultations, or teledermoscopic consensus.

Results

Baseline sensitivity and specificity for benign-malignant classification were 80% and 90%, increasing to 81% (p = 0.43) and 91% (p = 0.05) after AI integration. Class-specific analyses showed significant improvements in specificity for nevi, seborrheic keratoses, and vascular lesions, and significant improvements in sensitivity for actinic keratoses and dermatofibromas. In case of non-agreement between dermatologists and AI, dermatologists changed their primary diagnosis in 41% of cases where the AI prediction was correct but overturned their own correct diagnosis when the AI was incorrect in 15% of cases. While overall management specificity did not significantly improve, AI assistance enabled correct management of 7 melanomas that were initially missed.

Table 1. Sensitivity and specificity for dermatologists before and after the artificial intelligence (AI) tool

Categorization	*Sensitivity before AI % (CI 95%)*	*Sensitivity after AI % (CI 95%)*	*p-value*	*Specificity before AI % (CI 95%)*	*Specificity after AI % (CI 95%)*	*p-value*
Malignant/benign	80·1 (76·5-83·3)	80·8 (77·3-84·0)	0·43	90·0 (88·0-91·7)	91·0 (89·1-92·7)	0·05
*≤8 years of experience**	85·4 (78·8-90·5)	86·6 (80·3-91·5)	0·45	86·0 (82·0-89·5)	87·5 (83·5-90·7)	0·58
*>8 years of experience^*	78·0 (73·7-82·0)	78·5 (74·2-82·4)	0·34	92·0 (89·7-93·9)	92·8 (90·6-94·7)	0·34
MM/non-MM	81·6 (75·1-87·0)	83·2 (76·9-88·4)	0·51	96·1 (95·0-97·1)	96·8 (95·8-97·7)	0·05
*≤8 years of experience**	91·5 (79·6-97·6)	95·7 (85·5-99·5)	0·42	94·8 (92·4-96·6)	95·9 (93·6-97·5)	0·61
*>8 years of experience^*	78·0 (70·0-84·8)	78·8 (70·8-85·4)	0·36	96·8 (95·4-97·8)	97·3 (96·0-98·2)	0·36
BCC/non-BCC	74·9 (68·5-80·6)	78·7 (72·5-84·0)	0·10	95·8 (94·6-96·8)	95·6 (94·4-96·6)	0·65
SCC /non-SCC	53·2 (45·4-60·9)	51·5 (43·7-59·2)	0·61	96·8 (95·7-97·6)	97·3 (96·4-98·1)	0·06
Nevus/non-nevus	79·5 (73·5-84·7)	82·3 (76·6-87·2)	0·21	95·5 (94·3-96·5)	96·6 (95·5-97·5)	0·001
SK/non-SK	80·3 (74·3-85·4)	82·6 (76·9-87·5)	0·27	93·7 (92·3-94·9)	94·9 (93·6-96·0)	0·01
AK/non-AK	57·9 (50·8-64·8)	66·8 (59·9-73·3)	<0·001	95·8 (94·7-96·8)	95·3 (94·0-96·3)	0·10
DF/non-DF	81·3 (74·9-86·6)	85·6 (79·7-90·3)	0·04	99·1 (98·4-99·5)	98·9 (98·3-99·4)	0·50
Vascular/non-vascular	84·6 (78·8-89·4)	85·6 (79·9-90·2)	0·69	98·6 (97·9-99·2)	99·2 (98·6-99·6)	0·02

MM = malignant melanoma; BCC = basal cell carcinoma; SCC = squamous cell carcinoma; SK = seborrheic keratosis; AK = actinic keratosis; DF = dermatofibroma. *Assessors with ≤8 years of dermoscopic experience, n = 7 ^ Assessors with >8 years of dermoscopic experience, n = 14

Conclusions

Access to an 8-class AI tool added value to teledermoscopic assessments by dermatologists. Although overall gains in accuracy were modest, potentially reflecting the already high baseline performance of experienced assessors, all significant changes represented improvements with no indications of performance deterioration. These findings highlight the potential of human-AI collaboration and support integrating AI assistance into teledermoscopy workflows, with further evaluation in real-world clinical environments warranted.

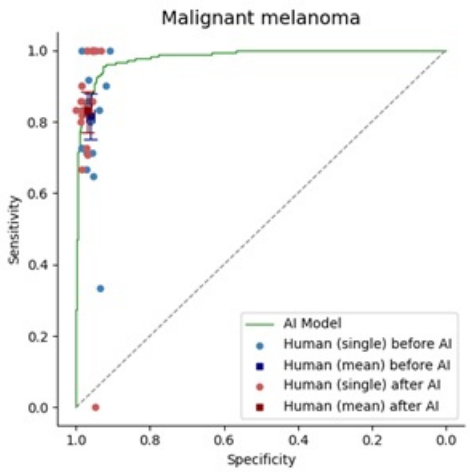

Figure 1. One-versus-rest receiver operating characteristic (ROC) curves for melanoma showing performance of individual human assessor and mean of human assessors before and after use of

aritificial intelligence tool and AI.

EADV CONGRESS
VIENNA
30 SEP - 3 OCT 2026

Abstract N°: 1678

Rapid Bedside Diagnosis of Disseminated Histoplasmosis in Advanced HIV Using Tzanck Smear: A Case Report

Kirk Llew Quijote*[1], Emmerson Gale Vista[1]

[1] Research Institute for Tropical Medicine, Muntinlupa City, Philippines

Introduction

Disseminated opportunistic infections remain a leading cause of morbidity and mortality among people living with HIV (PLHIV), particularly in regions where tuberculosis and fungal infections overlap. Histoplasmosis, an AIDS-defining illness, may present with nonspecific systemic features and cutaneous lesions that closely mimic differential diagnoses such as disseminated herpes simplex virus (HSV) infection, molluscum contagiosum, and monkeypox (Mpox). In severely immunocompromised patients, skin findings often serve as the first clue to systemic infection. While definitive diagnosis relies on culture and histopathology, these require time. Rapid bedside tests such as potassium hydroxide (KOH) mount and Tzanck smear (Giemsa stain) can provide immediate insights and significantly influence management decisions in settings where empiric therapy is necessary but uncertain.

Case Presentation

We report the case of a 34-year-old Filipino male newly diagnosed with advanced HIV (CD4 count: 24 cells/μL) who presented with diffuse erythematous and umbilicated papules, plaques, and pustules involving the skin and oral mucosa. Eleven weeks earlier, he had been diagnosed with HIV during hospitalization for fever, weight loss, and chronic cough, and was started on anti-tuberculosis therapy, antiretrovirals, and prophylactic antimicrobials.

On admission, his cutaneous lesions had worsened despite antiviral therapy. Differential diagnoses included (1) disseminated HSV infection, (2) disseminated deep fungal infection, and (3) disseminated Mpox. Each condition required a distinct treatment approach, and the choice of antimicrobial was initially uncertain. While skin and blood cultures were sent, results were expected to take days. To provide rapid direction, a tissue KOH mount and Tzanck smear (Giemsa stain) were performed at bedside. Both revealed intra- and extracellular yeast cells, strongly suggestive of a disseminated fungal infection.

This pivotal finding led to the immediate initiation of empiric antifungal therapy with amphotericin B deoxycholate, even before histopathology and culture confirmed the diagnosis. Subsequent biopsy revealed yeast-like organisms within macrophages highlighted by PAS and GMS stains, consistent with *Histoplasma capsulatum*. Skin tissue cultures yielded white cottony molds on macroscopic examination and thick-walled, tuberculate macroconidia under microscopy, confirming *Histplasma capsulatum*. Blood cultures from two separate sites also yielded *Staphylococcus epidermidis*, confirming Gram-positive bacteremia. Despite initiation of amphotericin B and vancomycin, the patient developed disseminated intravascular coagulation and septic shock, ultimately succumbing to multi-organ failure.

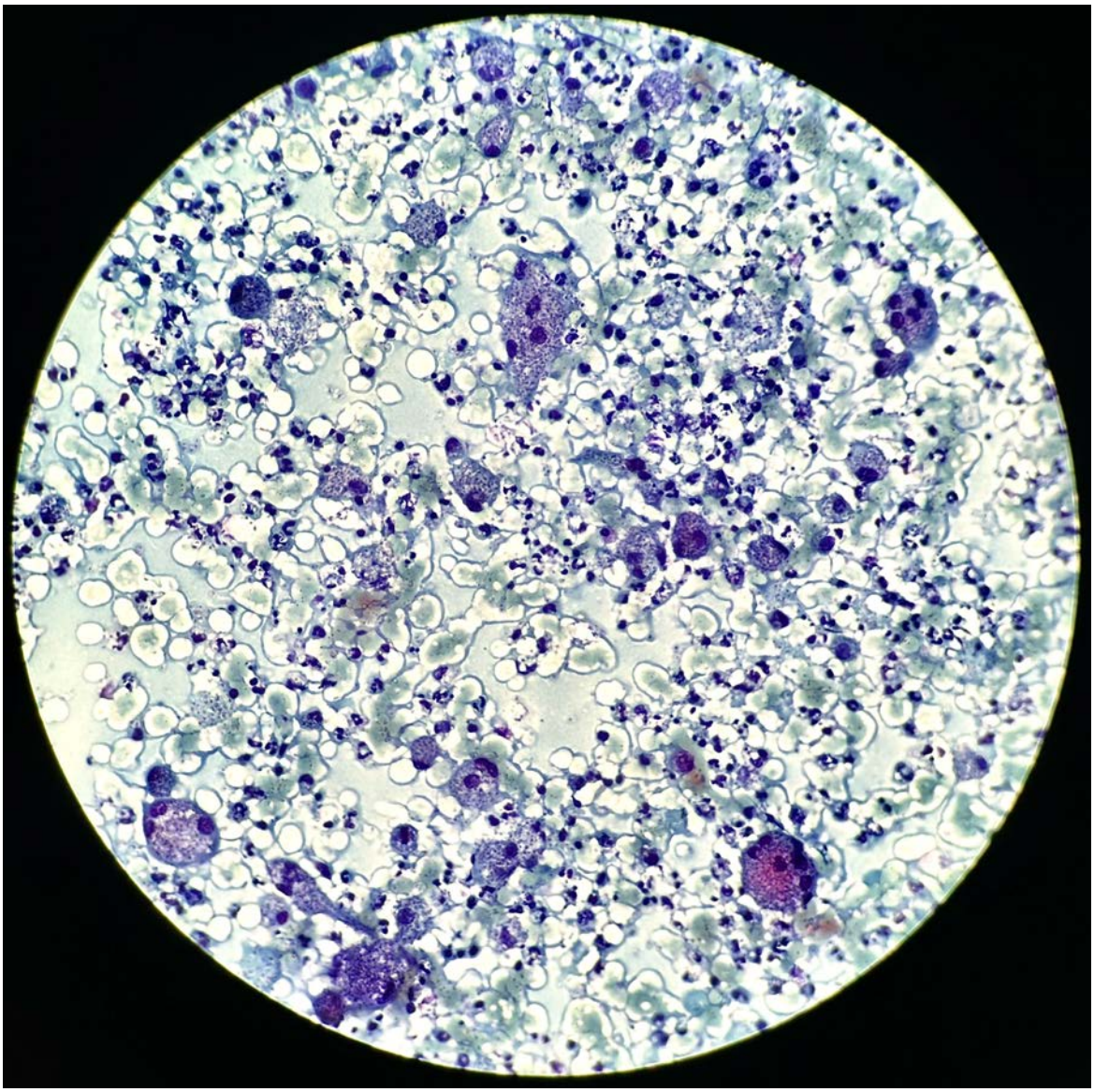

Tzanck smear findings of intra- and extracellular yeast cells (Giemsa stain, 10x)

Conclusion

This case illustrates the diagnostic challenge of obscure cutaneous eruptions in advanced HIV, where viral, fungal, and poxviral etiologies overlap. The Tzanck smear, traditionally employed for herpesvirus infection diagnosis, demonstrated its broader utility by providing rapid visualization of fungal elements. Its bedside availability allowed for timely initiation of antifungal therapy before culture or histopathology results were available. In regions where histoplasmosis remains under-recognized and antigen testing is unavailable, rapid smear techniques serve as critical diagnostic tools. Dermatologists, by recognizing subtle cutaneous clues and employing such methods, bridge the gap between uncertain differentials and decisive management.

The Tzanck smear played a pivotal role in expediting the diagnosis of disseminated histoplasmosis in this patient with advanced HIV, guiding early antifungal initiation despite diagnostic uncertainty. This case highlights the enduring value of simple, rapid dermatologic diagnostic tools in resource-limited and high-burden settings, where timely intervention may determine survival.

EADV CONGRESS
VIENNA
30 SEP - 3 OCT 2026

Abstract N°: 1712

Developing a Long-Tail Dermatologic Disease Diagnosis Model Across Skin Tones Using Generative Synthetic Data

Yuanjing Gao*[1], Juncheng Wang[2]

[1] Peking Union Medical College Hospital, Beijing, China

[2] Department of Dermatology, Affiliated Provincial Hospital, Fuzhou University, Fuzhou, China

Introduction

Artificial intelligence–based diagnosis of skin diseases is challenged by both long-tail class distribution and phenotype variation across skin tones. Public dermatology datasets contain relatively limited samples of rare diseases and darker skin types, which restricts model generalizability across diverse populations. This study aimed to develop a cross-skin-tone diagnostic model for long-tail dermatologic diseases by integrating generative synthetic data with multi-source real-world data.

Materials and Methods

Fitzpatrick17k and DDI were integrated, and disease labels were harmonized for distribution analysis and model development. A ConvNeXt classifier was used as the baseline model. To address the underrepresentation of darker skin tones, AI-based image generation was applied to perform cross-skin-tone synthesis for Fitzpatrick skin types IV–VI, adding approximately 100 images for diseases lacking darker-skin representation, followed by targeted augmentation strategies such as rotation and translation. In addition, 2,000 images from a self-constructed dataset of Asian patients were incorporated for supplementary training. Model performance was evaluated on both public datasets and the self-constructed dataset, including disease classification and skin-tone classification.

Results

The merged Fitzpatrick17k-DDI dataset showed a marked long-tail distribution, with 31.6% of disease categories represented by only 1–10 images. The baseline ConvNeXt model performed well on common benign skin conditions, whereas its performance was lower for rare diseases, complex inflammatory disorders, and some malignant subtypes. After incorporating darker-skin synthetic augmentation and targeted enhancement, skin-tone classification performance improved, with skin accuracy reaching approximately 88%–97% across different Fitzpatrick subgroups in Fitzpatrick17k, while disease classification accuracy ranged from 59.12% to 72.52%. After adding the self-constructed Asian dataset, the model achieved an accuracy of 72.59% on that dataset. The framework also supported single-image disease prediction, skin-tone classification, and literature-assisted generation of diagnostic reports.

Conclusions

The integration of generative synthetic data, targeted augmentation, and multi-source real-world data can effectively improve the performance of cross-skin-tone long-tail dermatologic disease diagnosis, particularly for underrepresented skin-tone populations. This strategy provides a practical pathway toward developing fairer and

more generalizable artificial intelligence models for dermatologic diagnosis.

EA DV CONGRESS
VIENNA
30 SEP - 3 OCT 2026

Abstract N°: 1926

Real-Time LC-OCT Monitoring of Hypertrophic Actinic Keratosis Clearance Following Cryotherapy, Laser, or 5-Fluorouracil Therapy

Giulio Bortone*[1], Vincenzo Coppolelli[2], Luca Gargano[2, 2], Mehdi Boostani[3], Steven Paul Nisticò[2], Giovanni Pellacani[2], Carmen Cantisani[2]

[1] UOC of Dermatology, Department of medical and cardiovascular science, La Sapienza Medical School of Rome, Italy,, Rome, Italy
[2] UOC of Dermatology Department of internal and cardiovascular science. University Sapienza of Rome, Rome, Italy
[3] department of dermatology Rosewell Park Comprehensive Cancer CENTER, BUFFALO, NEW YORK, United States

Introduction

Assessment of treatment response in hypertrophic actinic keratoses(hAKs), defined as Olsen grade 2 to 3/KIN 2 to 3/PRO II to III lesions, relies predominantly on clinical inspection and dermoscopy.However, macroscopic clearance does not reliably correspond to biological resolution: histopathological studies have documented persistence of keratinocyte atypia in a substantial proportion of clinically cleared lesions, with recurrence rates reaching 85% at one year in unselected cohorts. Line-field confocal optical coherence tomography (LC-OCT) enables longitudinal non-invasive monitoring at cellular resolution of the structural changes induced by treatment, providing access to biological response parameters well beyond what is assessable by dermoscopy alone.To evaluate whether LC-OCT-derived imaging parameters allow identification of the most appropriate treatment modality according to lesion grade and biological behavior at follow-up. A secondary aim is to characterize the LC-OCT features of hAK lesions for the three modalities examined - ablative CO2 laser, cryotherapy with liquid nitrogen, and topical 0.5% 5-fluorouracil combined with 10% salicylic acid - and to propose non-invasive criteria for LC-OCT-defined complete response, partial response and subclinical disease persistence.

Materials and Methods

Retrospective analysis of a LC-OCT imaging database of hAK lesions classified as KIN 2 to 3 / PRO II to III, acquired as part of routine clinical practice. A total of 150 hypertrophic actinic keratoses were included and allocated to three treatment groups of 50 lesions each: ablative CO2 laser, cryotherapy with liquid nitrogen, and topical 0.5% 5-fluorouracil combined with 10% salicylic acid, with treatment allocation based on individualized clinical assessment of lesion grade, thickness and anatomical site.

Case Presentation

Results

Cryotherapy produces within 72 hours a characteristic hypo reflective sub-epidermal space,corresponding to the cryo-induced blister.At four weeks, reduction of hyperkeratosis, regression of keratinocytic atypia and progressive normalization of the DEJ are observed, alongside post-inflammatory hyperpigmentation and residual dermal inflammatory infiltrate. CO2 laser results in immediate ablation of the epidermis and superficial dermis, with exposure of the papillary dermis and early hyperreflective granulation tissue on LC-OCT vertical sections.Re-epithelialization proceeds from perilesional intact skin and follicular keratinocytes, while thermal coagulation of the photodamaged superficial dermis initiates a wound healing response.Within twelve months, dermal collagen remodeling is documentable by LC-OCT as progressive reorganization of collagen fibers within the superficial

dermis, with features consistent with nucleogenesis. Topical 0.5% 5-fluorouracil plus 10% salicylic acid produces within eight weeks the appearance of central intraepidermal fluid and active perivascular inflammatory infiltrate. In KIN 3/PRO III hAKs, hyperkeratosis frequently persists at eight weeks with incomplete DEJ normalization.LC-OCT-defined complete biological response is characterized by the convergence of documented absence of keratinocyte atypia, DEJ UI below 15% corresponding to PRO I, regular stratum corneum and normalization of the vascular pattern.

Conclusion

This retrospective analysis of routinely acquired LC-OCT imaging data,suggests that LC-OCT enables a biologically grounded assessment of treatment response in hAKs.LC-OCT identified subclinical disease persistence not visible on clinical examination in a clinically relevant proportion of lesions, informing retreatment decisions and contributing to the design of a sequential multimodal approach.The adoption of standardized LC-OCT-derived response criteria appears promising for the definition of more robust biological endpoints in clinical trials on actinic keratosis and for improving the individualized management of field cancerization.

EA DV CONGRESS
VIENNA
30 SEP - 3 OCT 2026

Abstract N°: 2037

Microneedle-Based Interstitial Fluid Sampling Enables Early Detection of Herpes Zoster

Fang-Ying Wang*[1]

[1] Department of Dermatology, Chang Gung Memorial Hospital, Linkou Medical Center, College of Medicine, Chang Gung University, Taoyuan, Taiwan

Introduction
Early diagnosis of herpes zoster (HZ) remains a major clinical challenge during the prevesicular stage, when characteristic vesicles are absent and cutaneous lesions frequently mimic other inflammatory or infectious dermatoses. Although varicella–zoster virus (VZV) replication is already active within the epidermis at this stage, current diagnostic approaches rely on vesicle fluid or invasive tissue sampling, limiting timely confirmation and delaying antiviral treatment. We hypothesized that epidermal interstitial fluid (ISF), which reflects the local virologic microenvironment, could serve as an accessible diagnostic reservoir if sampled using a minimally invasive approach.

Materials and Methods
A hydrogel-forming alginate microneedle (MN) platform was developed for minimally invasive sampling of epidermal ISF. MN patches with controlled calcium crosslinking were fabricated and systematically optimized to balance mechanical strength and fluid absorptivity. Device performance was evaluated through mechanical testing, penetration assessment, swelling and release studies, and biocompatibility analyses in vitro and in vivo. A prospective pilot study was conducted in adults presenting with erythematous plaques clinically suspicious for early-stage HZ, along with control participants with clinically similar conditions. MN-derived ISF samples were analyzed using real-time polymerase chain reaction (PCR) for VZV DNA detection and a lateral flow–based rapid antigen assay to evaluate point-of-care applicability.

Results
The optimized MN patches demonstrated reliable epidermal penetration without structural failure, high fluid absorptivity, and favorable biocompatibility with minimal cytotoxicity and no detectable tissue irritation. In the clinical cohort (n = 8), MN-mediated sampling enabled detection of VZV DNA in all patients with suspected early-stage HZ prior to vesicle formation, with complete concordance with subsequent clinical diagnosis. No false-positive results were observed among control participants. This approach achieved 100% sensitivity and 100% specificity in this pilot cohort. Notably, VZV was detectable at low cycle threshold values, indicating active viral presence within the epidermal microenvironment during the prevesicular phase. In addition, MN-derived ISF samples were compatible with rapid antigen testing, enabling visual detection of viral signals and supporting the feasibility of early point-of-care diagnosis.

Conclusions
Microneedle-mediated ISF sampling provides a minimally invasive, well-tolerated, and clinically translatable strategy for early virologic confirmation of HZ prior to vesicle formation. By addressing the key limitation of sample accessibility in early disease, this approach has the potential to shift diagnostic timing earlier in the disease course, enabling prompt antiviral therapy and improved clinical outcomes. Beyond HZ, this platform may represent a broadly applicable diagnostic paradigm for cutaneous diseases in which critical biomarkers are localized within the skin.

EADV CONGRESS
VIENNA
30 SEP - 3 OCT 2026

Abstract N°: 2065

Pigmented Demodicosis Mimicking Melasma: Multimodal Diagnostic Correlation in a Treatment-Refractory Case

Ludmila Porfirio*[1], Monica Carolina Quezada Pardo[1], Luiz Henrique dos Santos[1], Luz karime Zuñiga[1], Luciana Araujo[1]

[1] IMS Dermatologia, Rio de Janeiro, Brazil

Introduction

Pigmented demodicosis is an uncommon and probably underrecognized presentation of *Demodex* infestation in which facial hyperpigmentation predominates over the classic papulopustular eruption. Because of its atypical appearance, it may mimic melasma, lichen planus pigmentosus and other acquired facial dyschromias, leading to delayed diagnosis and ineffective treatment.

Case Presentation

A 43-year-old woman with Fitzpatrick skin phototype IV and severe asthma treated with mepolizumab presented with a two-year history of diffuse hair shedding. Dermatologic examination revealed telogen effluvium and incidental brownish hyperpigmented macules involving the temporal regions and chin. The patient reported a previous diagnosis of melasma and multiple unsuccessful treatments.

Clinical examination showed subtle erythema and mildly rough skin texture associated with the hyperpigmentation. Dermoscopy demonstrated numerous follicular white protrusions, follicular plugs containing amorphous material, and perifollicular annular pigmentation, raising suspicion for demodicosis. Direct microscopic examination confirmed the presence of Demodex mites.

Punch biopsy revealed basal layer hyperpigmentation, superficial perivascular lymphohistiocytic infiltrate with melanophages, and dilation of a vellus follicular ostium containing Demodex organisms, supporting the diagnosis of pigmented demodicosis.

Treatment with oral ivermectin combined with topical ivermectin resulted in progressive improvement and complete resolution of the facial hyperpigmentation, with no recurrence during six months of follow-up.

Conclusion

Pigmented demodicosis should be considered in the differential diagnosis of persistent or treatment-refractory facial hyperpigmentation. Dermoscopy may provide important diagnostic clues through follicular white protrusions, follicular plugs, and perifollicular annular pigmentation. Early recognition of this entity is clinically relevant because targeted anti-demodectic therapy may lead to complete resolution and help avoid unnecessary treatment for other pigmentary disorders.

POWERED BY M-ANAGE.COM

EA DV CONGRESS
VIENNA
30 SEP - 3 OCT 2026

Abstract N°: 2072

Perfomance of an Artificial Intelligence Tool for the Triage of Inflammatory Dermatoses in Darker Skin Phototypes: A Brazilian Pliot Study

Isabella Arivabene Pancieri*[1], Pietra Diniz Pereira[2], Julia Laluce Cardoso[3], Diogo Pazzini Bomfim[4], Raul Cartagena Rossi[5]

[1] Centro Universitário do Espírito Santo (UNESC), Colatina, Brazil
[2] Universidade de Mogi das Cruzes (UMC), Mogi das Cruzes, Brazil
[3] Instituto Lauro de Souza Lima (ILSL), Bauru, Brazil
[4] Faculdade de Medicina de Marília (FAMEMA), Marília, Brazil
[5] Universidade de Taubaté (UNITAU), Taubaté, Brazil

Introduction

Artificial intelligence (AI) diagnostic tools are increasingly used in dermatology, particularly for triage of common dermatoses in primary care and teledermatology. However, most algorithms are trained predominantly on images of lighter skin phototypes, which may reduce accuracy when applied to populations with darker skin. This limitation raises concerns about algorithmic bias, diagnostic inequity, and reduced effectiveness in regions such as Latin America, where skin tone diversity is high. Despite the rapid expansion of AI, evidence evaluating performance in darker phototypes remains limited. This study aimed to assess the diagnostic accuracy and feasibility of a commercially available AI-based classifier for identifying inflammatory dermatoses in individuals with Fitzpatrick phototypes IV–VI in a Brazilian outpatient setting.

Materials and Methods

We conducted a cross-sectional pilot study including consecutive adult patients seen at a specialized dermatology clinic between January and March 2026. Eligible participants had a confirmed diagnosis established by board-certified dermatologists of atopic dermatitis, psoriasis, seborrheic dermatitis, lichen planus, or pityriasis rosea. Standardized clinical images were captured using smartphone cameras under uniform ambient lighting and uploaded to VisualDx, an AI dermatology platform that uses machine learning pattern recognition to generate probability ranked differential diagnoses. For each case, the top three suggestions were analyzed. Diagnostic accuracy was determined by comparing AI outputs with the dermatologist’s diagnosis (gold standard): top-1 accuracy reflected cases in which the first ranked prediction matched the reference diagnosis, and top-3 accuracy those in which the correct diagnosis appeared among the first three suggestions. Sensitivity and specificity for each disease category were calculated using standard formulas, sensitivity = true positives / (true positives + false negatives) and specificity = true negatives / (true negatives + false positives) using a one-vs-all binarization approach for each condition. A subgroup analysis comparing phototype IV versus V–VI was performed to explore potential performance differences across skin tones.

Results

A total of 112 patients were included (mean age 38.6 ± 12.4 years; 68% female). The distribution of inflammatory dermatoses was: atopic dermatitis (n=28), psoriasis (n=23), seborrheic dermatitis

(n=31), lichen planus (n=17), and pityriasis rosea (n=13). Most participants (74%) had phototypes V–VI. Overall top-1 accuracy was 61.6%, while top-3 accuracy reached 82.1%. Psoriasis demonstrated the highest top-1 accuracy (78.3%), followed by seborrheic dermatitis (67.7%) and atopic dermatitis (60.7%). Performance was lower for lichen planus (42.8%) and pityriasis rosea (46.1%). The AI tool underestimated diagnoses in conditions where pigmentary alteration or violaceous tones predominated, particularly in phototypes V–VI. Top-1 accuracy for darker tones was 56.3% compared with 70.4% for phototype IV. Mean processing time was <5 seconds per image, supporting feasibility in busy outpatient or teledermatology workflows.

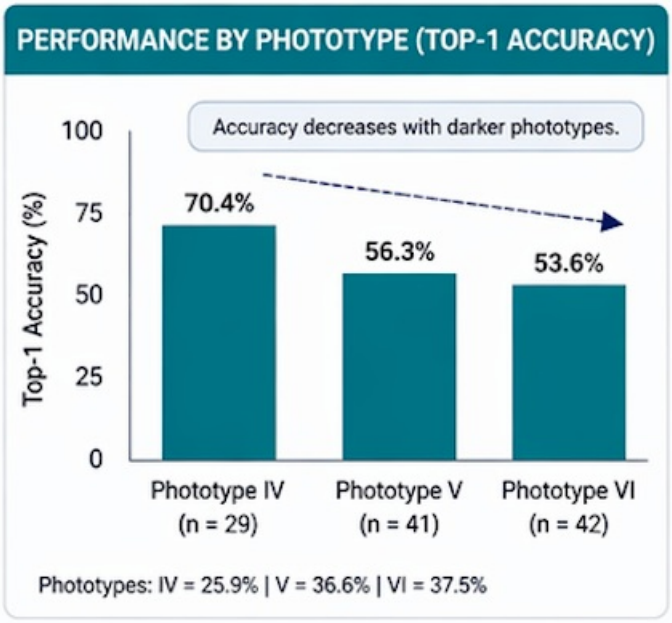

Figure 1. Performance of the AI classifier across skin phototypes (Top-1 accuracy). Top-1 diagnostic accuracy progressively decreased with darker skin phototypes, ranging from 70.4% in phototype IV to 53.6% in phototype VI. This gradient highlights a systematic decline in algorithmic performance associated with increasing pigmentation, suggesting underrepresentation of higher phototypes in training datasets. Sample distribution: phototype IV (n=29; 25.9%), phototype V (n=41; 36.6%), phototype VI (n=42; 37.5%).

Conclusions

This pilot study suggests that AI-based triage is feasible and moderately accurate for common inflammatory dermatoses in darker skin phototypes. However, performance inconsistencies especially in pigment-altering conditions underscore the need for broader and more diverse image datasets to reduce algorithmic bias and improve diagnostic equity. The lower accuracy in phototypes V–VI highlights gaps in current training models and reinforces the importance of incorporating regional images from Latin America and other underrepresented populations to enhance the reliability of AI-assisted dermatology. Further studies with larger cohorts, multimodal inputs, and algorithm refinement are warranted.

EA CONGRESS
VIENNA
30 SEP - 3 OCT 2026

Abstract N°: 2278

Line-Field Confocal Optical Coherence Tomography as a Noninvasive Tool for Diagnosis and Therapeutic Monitoring in Extramammary Paget Disease

Francesca Svara*[1], Marco Virone[1], Lucia Finistauri Guacci[1], Andrea Ascione[2], Vito Gomes[3], Margherita Testa[3], Claudio Conforti[4, 5], Giovanni Pellacani[1], Flavia Persechino[1], Luca Ambrosio[1, 5]

[1] Dermatology Unit, Department of Medical and Cardiovascular Sciences, "Sapienza" University of Rome, Rome, Italy

[2] Department of Experimental Medicine, Sapienza University of Rome., Rome, Italy

[3] Unit of Histopathology, Istituto Dermopatico dell'Immacolata IDI-IRCCS, Rome, Italy

[4] Link University of Rome, Department of Life Science, Health and Health Professions, Rome, Italy

[5] IDI-IRCCS, Dermatological Research Hospital, Rome, Italy

Introduction

Extramammary Paget disease (EMPD) is a rare intraepithelial adenocarcinoma arising in apocrine gland–bearing skin and often presenting with nonspecific clinical features that mimic inflammatory dermatoses, frequently resulting in delayed diagnosis. Histopathology remains the diagnostic gold standard, and surgery is considered the first-line treatment. However, in selected patients, conservative approaches such as topical imiquimod may be considered as an alternative therapeutic option. In this setting, close monitoring of treatment response and early detection of recurrence are essential, traditionally relying on serial biopsies. Non-invasive imaging techniques may therefore represent a valuable adjunct, potentially reducing the need for repeated invasive procedures while supporting both diagnosis and longitudinal follow-up.

Case Presentation

We report two cases of primary cutaneous EMPD in elderly male patients. The first patient presented with a long-standing pruritic erythematous plaque involving the inguinal region, previously treated as fungal infection without improvement. Clinical and dermoscopic examination showed a well-demarcated erythematous plaque with erosions and vascular structures. Baseline LC-OCT revealed epidermal disorganization, acanthosis, and large atypical intraepidermal cells with Paget-like morphology, associated with disruption of the honeycomb pattern and a blurred dermoepidermal junction (Fig.1a) Histopathology confirmed EMPD (Fig.1b). Topical imiquimod 5% cream was initiated twice weekly, with monthly clinical and LC-OCT follow-up. At 12 weeks, marked clinical improvement with reduction of erythema and erosions was observed. LC-OCT demonstrated restoration of epidermal architecture, reappearance of a regular honeycomb pattern, and absence of atypical cells. Two biopsies were performed, both confirming complete histological response (Fig 1c).

The second patient presented with a one-year history of an erythematous lesion of the genital area, initially misdiagnosed as inflammatory balanitis. Clinical and dermoscopic findings were suggestive of EMPD. Baseline LC-OCT showed epidermal architectural disorganization with atypical Paget cells and disruption of the honeycomb pattern, later confirmed by histopathology (Fig.1d,e). Topical imiquimod 5% cream was initiated three times weekly. After 8 weeks of treatment, near-complete clinical resolution was observed. Follow-up LC-OCT demonstrated normalization of epidermal architecture and disappearance of atypical cells, consistent with therapeutic response (Fig.1f).

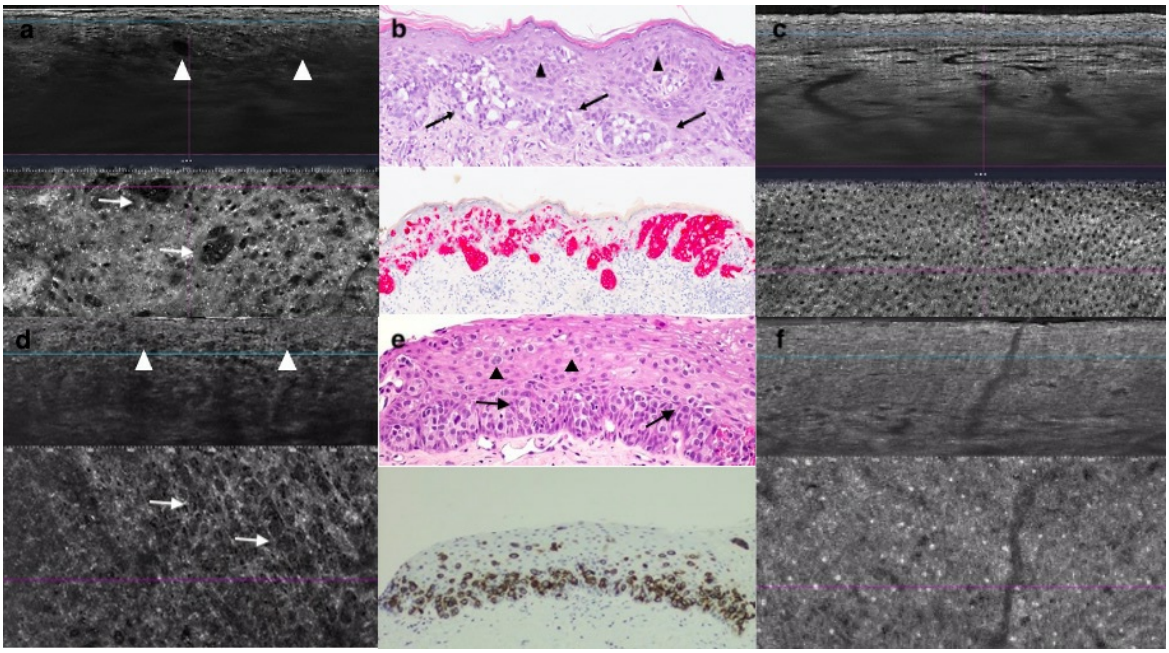

Figure1: At baseline, LC-OCT vertical sections in both cases showed epidermal disorganization with acanthosis, focal blurring of the dermoepidermal junction, and large atypical Paget cells, either isolated or arranged in gland-like or nest-like aggregates (white arrowheads). Horizontal sections demonstrated loss of the regular honeycomb pattern with solitary or clustered Paget cells within the suprabasal layers (white arrows) (a,d). Histopathology revealed intraepidermal proliferation of atypical cells, partly arranged in nests with glandular alignment along the basal layer (black arrows) and partly distributed singly or in small clusters within the upper epidermal layers (black arrowheads). These cells appeared slightly larger than keratinocytes, with greyish cytoplasm and occasional vacuolization (H&E, 20×). CK7 immunohistochemistry highlighted their distribution throughout the epidermis (10×) (b,e). After 12 and 8 weeks of treatment, respectively, LC-OCT sections showed reduced acanthosis, restoration of a regular honeycomb pattern, a well-defined dermoepidermal junction and absence of atypical cells in both basal and suprabasal layers (c,f).

Conclusion

EMPD remains a diagnostic challenge due to its nonspecific clinical presentation and overlap with benign dermatoses. LC-OCT is an emerging non-invasive imaging modality that provides high-resolution vertical and horizontal visualization of the epidermis, enabling identification of key features such as architectural disarray and atypical intraepidermal cells. In our cases, LC-OCT findings correlated with histopathology at baseline and closely paralleled clinical evolution during treatment. Importantly, in the first case, LC-OCT findings were corroborated by two histological assessments at week 8, reinforcing the reliability of this technique in evaluating treatment response. LC-OCT may represent a valuable non-invasive adjunct in the management of EMPD, supporting both diagnosis and real-time monitoring of disease progression and treatment response. Its integration into clinical practice could help reduce the need for repeated biopsies and optimize follow-up strategies.

EA DV CONGRESS
VIENNA
30 SEP - 3 OCT 2026

Abstract N°: 2302

Diagnostic performance of artificial intelligence compared to dermatologists in detecting basal cell carcinoma in dermoscopic images: a systematic review and meta-analysis

Linda Bruckner*[1], Christian Posch[1, 2]

[1] Sigmund Freud University, Vienna, Austria
[2] Hietzing Hospital, Vienna, Austria

Introduction
Artificial intelligence (AI)-based algorithms have shown promising performance in skin cancer detection and are increasingly integrated into dermatological diagnostics. However, evidence regarding their diagnostic accuracy for basal cell carcinoma (BCC) in dermoscopic images remains limited. This meta-analysis aimed to compare the diagnostic performance of AI-based algorithms and dermatologists in detecting BCC.

Materials and Methods
A comprehensive literature search was conducted in PubMed/MEDLINE, ScienceDirect, The Lancet between January 2015 and September 2025, using keywords such as “basal cell carcinoma”, “non-melanoma skin cancer”, “artificial intelligence” and “deep learning”. Only diagnostic test accuracy studies published in English were included. Eligible studies directly compared the diagnostic test accuracy of AI-based algorithms with dermatologists using dermoscopic images. The reference standard was histopathological confirmation or expert consensus. Studies without direct comparison, without dermoscopic images, or using alternative reference standards were excluded. Extracted Data included study characteristics (study design, population, AI-based algorithm, reference standard) and diagnostic accuracy outcomes. The primary outcomes were pooled sensitivity and specificity, with SROC analysis used to assess overall diagnostic accuracy. Risk of bias was assessed using the QUADAS-2 tool.

Results
Six studies met the inclusion criteria. Pooled sensitivity and specificity were 88% (95% CI: 81–92%) and 96% (95% CI: 87–99%) for AI-based algorithms, and 85% (95% CI: 77–90%) and 97% (95% CI: 91–99%) for dermatologists. SROC curves for AI-based algorithms were positioned closer to the upper left corner compared to dermatologists, indicating higher overall diagnostic performance. In most studies, risk of bias was assessed as unclear due to inadequate reporting of recruitment methods.

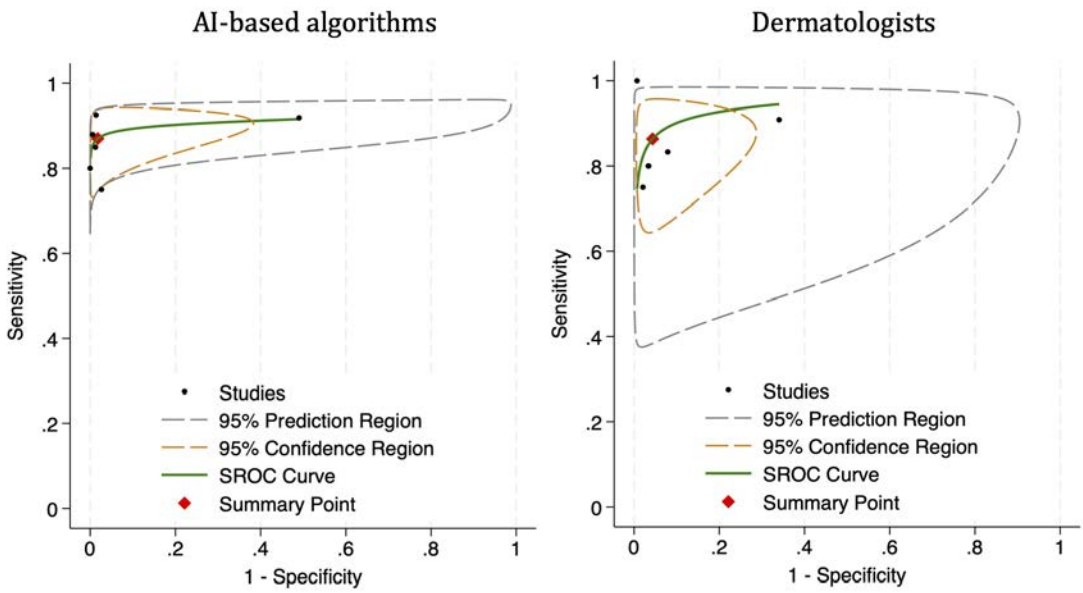

Figure 1: SROC curves comparing AI-based algorithms and dermatologists for basal cell carcinoma detection

Conclusions

In this meta-analysis, AI-based algorithms demonstrated comparable diagnostic performance to dermatologists in detecting BCC in dermoscopic images. SROC analysis suggested slightly higher diagnostic accuracy for AI-based algorithms, however the differences were modest. These findings suggest a potential role for AI-based algorithms as a supportive tool in clinical decision-making for BCC detection. This analysis is limited by the small number of included studies and the absence of formal statistical testing for differences between groups. Further prospective studies are required to validate these findings in real-world clinical settings.

EA DV CONGRESS
VIENNA
30 SEP - 3 OCT 2026

Abstract N°: 2367

Thermal Imaging as a Tool for Assessing Treatment Response in Morphea: A Case Report

Jason Britton*[1], Rachel Montgomery[1]

[1] Leeds Teaching Hospitals NHS Trust, Leeds, United Kingdom

Introduction

Although thermal Imaging/thermography has been used in the assessment of Morphoea [1], this imaging modality has not previously been used to assess the response of this condition to Phototherapy. We present a case of morphoea where thermal imaging has been helpful in monitoring disease activity and response to treatment.

Determining and monitoring disease activity can be challenging. Current available validated scoring tools have limitations. Thermal Imaging is not routinely used. Blood flow and skin temperature are important factors when assessing disease activity

Materials and Methods

The patient is a 47-year-old woman with an eleven-year history of biopsy proven morphoea localised to the left arm above her anti-cubital fossa. This had been treated with topical clobetasol propionate with no benefit. At the last clinical assessment, she had developed a further adjacent patch unresponsive to topical treatment in the form of clobetasol propionate and protopic 0.1% ointment and was referred for Ultraviolet 1 (UVA1) phototherapy (340nm – 400nm).

Localised treatment was delivered to the affected areas 3 times per week using a Sellamed 3000 unit (Sellamed, Germany). The initial dose was 70% of her UVA1 MED escalated by 20% increments at each visit, adjusted according to erythema response as required, to a maximum of 60 J/cm2. She received a total of 30 exposures.

The patient had thermal imaging prior to, at the mid-point and at end of treatment using a FLIR SC305 camera (Teledyne, FLIR). Images were acquired of the lesion and an area of normal skin and imported into Thermacam Researcher 2.10 (Teledyne FLIR) software. Using the graphical user interface tools in the software be-spoke regions of interest were drawn around the lesions identified in the images and an adjacent area of normal skin. A reduction in the difference in temperature of the lesion and normal skin as measured by thermography probably indicates a positive response to UVA1 phototherapy.

Results

The patient reported softening of the patches of morphoea with no evidence of any inflammation. Thermography results from the regions of interest drawn over the images of the lesion and adjacent normal skin are shown below in table 1. The maximum temperature difference between the lesion and unaffected skin is 1.7°C prior the start of treatment reducing 1.1°C at the midpoint and 0.4°C at the end of phototherapy.

	Average Temperature (°C)			
Visit	Lesion 1	Lesion 2	Normal Skin	Max. Difference
Prior	30.2	29.8	28.5	1.7
Min-point	31.8	31.3	30.7	1.1
End	31.4	31.4	31	0.4

Table 1: Region of interest results acquired from the thermal images.

Conclusions
Conclusion

Determining and monitoring disease activity in morphoea can be challenging. Current available validated scoring tools are subjective and have significant limitations**.** Skin blood flow and temperature are important factors indicating disease activity. The reduction in temperature detected by thermography mirrors the clinical response and patient reported treatment outcome. This suggests thermal imaging may be a helpful tool for assessing disease activity and response to UVA1 phototherapy. This suggests thermal imaging may a helpful tool for assessing disease activity and response to phototherapy.

References

[1] Detecting and quantifying activity/inflammation in localized scleroderma with thermal imaging Skin Research and Technology 2019 Mar;25(2):118-123. doi: 10.1111/srt.12619.

EA DV CONGRESS
VIENNA
30 SEP - 3 OCT 2026

Abstract N°: 2529

Multimodal non-invasive imaging supports surveillance and management of pigmented lesions in Noonan syndrome withmultiple lentigines

Marco Di Filippo*[1], Anna Pogorzelska-Antkowiak[2], Luca Gargano[1], Antonio Di Guardo[1], Giulio Bortone[1], Antonella Tammaro[3], Giovanni Pellacani[1], Steven Paul Nisticò[1], Carmen Cantisani[1]

[1] UOC of Dermatology Department of internal and cardiovascular science. University Sapienza of Rome, Rome, Italy

[2] EsteDerm Private Dermatology Clinic, Tychy, Poland, Tychy, Poland

[3] Dermatology Unit, Health Science Department, Magna Graecia University, Catanzaro, Italy

Introduction

In patients presenting with marked generalized lentiginosis, further diagnostic evaluation may be warranted to exclude underlying syndromic conditions. Noonan syndrome with multiple lentigines (NSML), formerly known as LEOPARD syndrome, is a rare autosomal dominant RASopathy mainly caused by mutations in the PTPN11 gene. Patients with NSML frequently present with extensive lentiginosis and numerous melanocytic lesions, thereby potentially limiting the specificity of clinical and dermoscopic evaluation. Although dysregulation of the RAS/MAPK signaling pathway has raised interest in a possible increased risk of melanoma in NSML, available evidence remains limited. Data regarding the role of non-invasive imaging techniques in the management and surveillance of pigmented lesions in NSML are currently scarce. We report the use of integrated non-invasive imaging for longitudinal surveillance and lesion-specific assessment in a patient with genetically confirmed NSML and an extensive burden of pigmented lesions.

Case Presentation

We report the case of a 40-year-old man referred for dermatologic evaluation of numerous pigmented lesions in the context of recurrent gastrointestinal bleeding. Multidisciplinary investigations eventually led to genetic testing and diagnosis of NSML associated with a missense PTPN11 variant (c.1492C>T; p.Arg498Trp). The patient subsequently underwent structured dermatologic follow-up including clinical examination, serial total body photography (TBP), digital dermoscopy, and reflectance confocal microscopy (RCM). Additional melanocytic lesions had been previously excised during follow-up, all showing benign histopathologic findings. Clinical examination revealed marked generalized lentiginosis, mainly involving the trunk, associated with numerous melanocytic lesions. Serial TBP was used to monitor the overall stability over time.

Among multiple lesions, a clinically and dermoscopically equivocal melanocytic lesion located on the trunk was selected for further evaluation. Dermoscopy of this lesion demonstrated a predominantly reticular pattern with mild structural asymmetry, focal pigment network thickening, and moderate chromatic heterogeneity. Although not overtly suggestive of malignancy, these features raised diagnostic uncertainty in the context of a complex syndromic phenotype. Subsequent RCM examination demonstrated preserved epidermal architecture with a regular honeycomb pattern and well-defined dermal papillae, without evidence of melanoma-specific criteria, including architectural disarray or pagetoid atypical cells. The overall confocal pattern was consistent with a benign melanocytic lesion, thereby increasing diagnostic confidence and supporting a conservative management approach. Based on integrated clinical, dermoscopic, TBP,

and confocal findings, surgical excision was safely deferred and a structured dermoscopic follow-up was scheduled.

Conclusion

The evaluation of pigmented lesions in NSML is particularly challenging because of the extensive burden of lentigines and melanocytic lesions, which can reduce the diagnostic accuracy of conventional clinical and dermoscopic assessment. This case highlights the added value of multimodal non-invasive imaging in both longitudinal surveillance and lesion-specific management in patients with complex syndromic phenotypes. In particular, serial TBP contributed to overall lesion stability assessment, while RCM provided decisive additional information, increasing diagnostic confidence and directly guiding management by safely avoiding surgical excision of a clinically equivocal lesion. Further studies are needed to better define the role of non-invasive imaging strategies in the management of patients with NSML and numerous pigmented lesions.

EADV CONGRESS
VIENNA
30 SEP - 3 OCT 2026

Abstract N°: 2554

Line-field confocal optical coherence tomography for in vivo characterization of fibrofolliculoma in Birt–Hogg–Dubé syndrome: a clinical case

Giulia Azzella*[1], Diletta Cordelli[1], Andrea Ascione[2], Giovanni Pellacani[1], Steven Paul Nisticò[1], Camilla Chello[1]

[1] Dermatology Unit, Department of Medical and Cardiovascular Sciences, Sapienza University of Rome, Rome, Italy

[2] Unit of Pathological Anatomy, Department of Radiological, Oncological and Anatomopathological Sciences, Sapienza University of Rome, Rome, Italy

Introduction

Birt–Hogg–Dubé syndrome is a rare autosomal dominant disorder caused by pathogenic variants in FLCN, characterized by a combination of skin, lung, and kidney findings. In dermatology, the most typical lesions of the syndrome are fibrofolliculomas and trichodiscomas, now considered part of the same morphologic spectrum.

These cutaneous lesions are important because they may represent the first sign of the syndrome. Their recognition is therefore relevant not only for the skin findings themselves, but also because Birt–Hogg–Dubé syndrome is associated with pulmonary cysts, spontaneous pneumothorax, and renal tumors.

Line-field confocal optical coherence tomography (LC-OCT) provides real-time vertical and horizontal imaging of the epidermis and superficial dermis at near-cellular resolution. Its ability to visualize follicular and perifollicular architecture in vivo makes it a potentially useful tool for the evaluation of fibrofolliculomas.

Case Presentation

A 43-year-old woman with genetically confirmed Birt–Hogg–Dubé syndrome was referred for evaluation of multiple facial papules clinically suspected to be fibrofolliculomas. One representative lesion was selected for LC-OCT examination prior to biopsy.

On LC-OCT, the lesion appeared as a superficial, well-defined folliculocentric papule centered on the infundibular unit, with a regular, symmetrical architecture. The most notable finding was the presence of thin epithelial projections extending from the infundibular component into the surrounding stroma, within a hyper-reflective perifollicular fibrous background.

Based on these findings, the lesion was selected for histopathologic examination. Histopathology confirmed the diagnosis, showing a folliculocentric fibroepithelial proliferation with an infundibular component and thin epithelial strands extending into a perifollicular fibrous stroma.

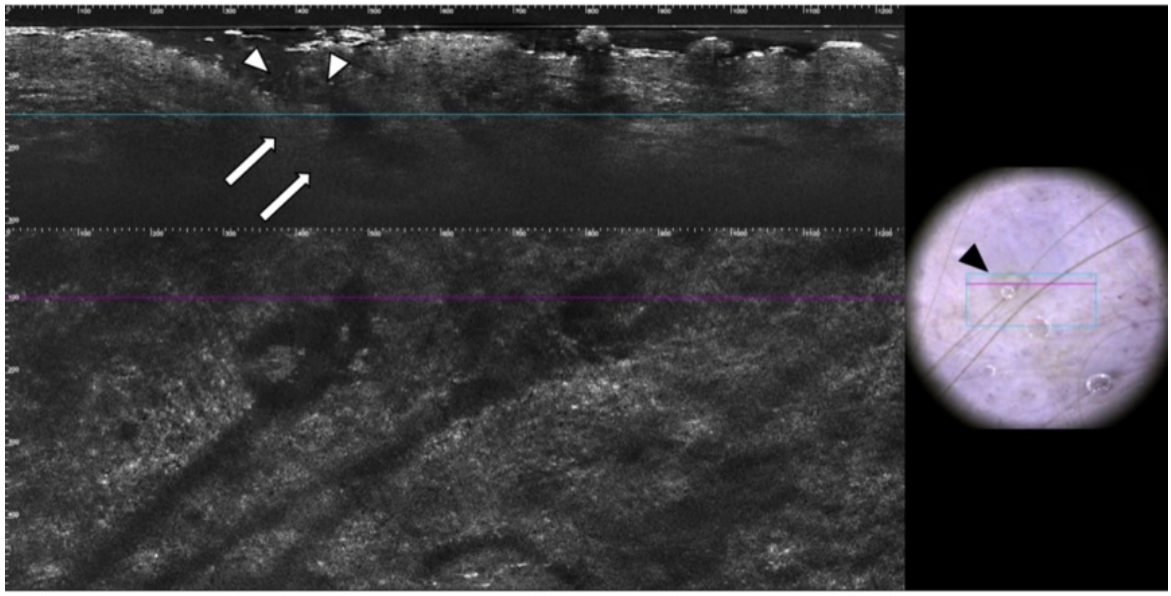

LC-OCT image showing a superficial folliculocentric lesion centered on the infundibular unit (arrowheads), with thin epithelial projections extending into a hyper-reflective perifollicular stroma (arrows). The inset shows the corresponding dermoscopic view of the lesion.

Conclusion

LC-OCT contributed to the non-invasive characterization of a representative papule as morphologically compatible with fibrofolliculoma, refining lesion selection before histopathologic confirmation rather than replacing biopsy.

Recognition of fibrofollicular features remains clinically relevant in Birt–Hogg–Dubé syndrome, as it may raise suspicion of the disease and prompt appropriate genetic and systemic evaluation.

Fibrofolliculoma should be distinguished from other small facial papules, including angiofibroma, fibrous papule, trichodiscoma, perifollicular fibroma, trichoepithelioma, and basal cell carcinoma, which may show overlapping clinical features but differ in their underlying architecture, making LC-OCT potentially useful in their non-invasive differentiation.

While available non-invasive descriptions of fibrofolliculoma mainly derive from reflectance confocal microscopy, to our knowledge LC-OCT features of fibrofolliculoma have not been previously described in the literature. LC-OCT may provide additional value through combined vertical and horizontal imaging at near-cellular resolution, allowing a more complete in vivo assessment of follicular and perifollicular architecture.

EA DV CONGRESS
VIENNA
30 SEP - 3 OCT 2026

Abstract N°: 2593

Diagnostic Accuracy of Novel Optical Imaging Techniques for Melanoma Detection: A Systematic Review and Meta-Analysis

Noémi Varga*[1, 2], Lili Gulyás[2], Fanni Meznerics[2], Katarina Barkovskij-Jakobsen[2], Bence Szabó[3], Péter Hegyi[3], András Bánvölgyi[2], Márta Medvecz[2], Norbert Kiss[2]

[1] University of Debrecen Medical School, Department of Dermatology, Debrecen, Hungary

[2] Semmelweis University, Department of Dermatology, Venereology and Dermatooncology, Budapest, Hungary

[3] Semmelweis University, Centre for Translational Medicine, Budapest, Hungary

Introduction

The incidence of melanoma is increasing worldwide, requiring early detection to improve survival rates. Although dermoscopy is the standard non-invasive tool for diagnosing melanoma, it relies on experience and skill. Advances in optical imaging technologies and artificial intelligence have the potential to improve diagnostic accuracy. Our objective was to compare the diagnostic accuracy of novel non-invasive optical imaging techniques for melanoma detection.

Materials and Methods

A systematic literature search was conducted in three databases (Medline, Embase, and CENTRAL) on November 15, 2023. Inclusion criteria focused on studies comparing the accuracy of optical imaging methods against histopathology. Outcomes consisted of measures of diagnostic accuracy. Random-effects meta-analyses were performed for each method with 95% confidence intervals to summarize all relevant effect sizes.

Results

Of the 16,239 records, 141 articles met the inclusion criteria, of which 138 articles were eligible for the meta-analysis. Reflectance confocal microscopy (RCM) and dermoscopy combined with artificial intelligence (DSC + AI) had the highest sensitivity (0.93), with DSC + AI showing higher specificity (0.77 [0.70–0.83]) than RCM (0.749 [0.7475–0.7504]). Multispectral imaging combined with AI also showed high sensitivity (0.92 [0.82–0.97]) and relatively high specificity (0.80 [0.67–0.89]). Standalone dermoscopy exhibited balanced sensitivity (0.87 [0.84–0.90]) and specificity (0.82 [0.78–0.86]).

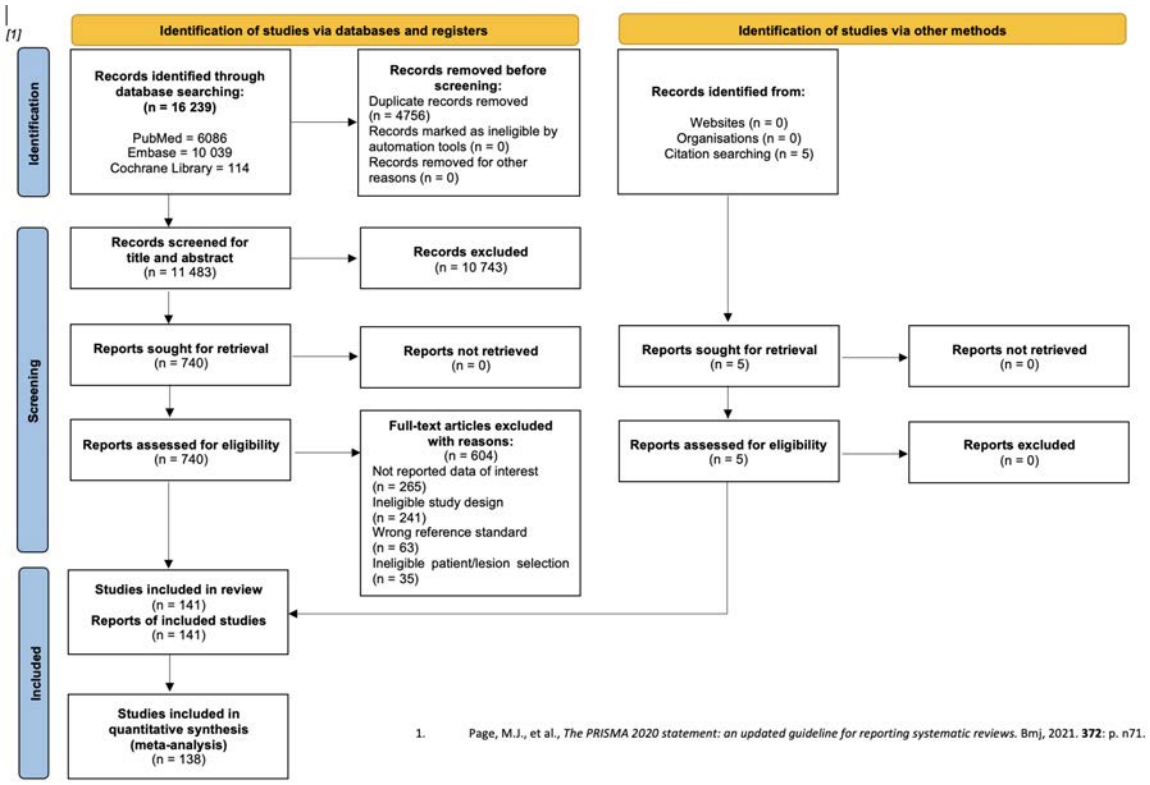

Preferred Reporting in Systematic Reviews and Meta-analyses (PRISMA) flowchart showing the selection process

Conclusions

In melanoma diagnosis, both RCM and DSC + AI can serve as second-step optical evaluation methods for suspicious lesions following initial screening with DSC. By maintaining a strong emphasis on multimodal imaging, healthcare providers could improve early detection and patient outcomes for melanoma.

EA DV CONGRESS
VIENNA
30 SEP - 3 OCT 2026

Abstract N°: 2646

Prognostic value of corneometry in assessing the course of rosacea and correlation with the intensity of erythema.

Khrystyna Nykolaichuk*[1]

[1] Ivano-Frankivsk National Medical University, Ivano-Frankivsk, Ukraine

Introduction

Rosacea is a chronic dermatosis characterized by a complex interaction among vascular disorders, neurogenic inflammation, and epidermal barrier dysfunction. One of the key indicators of the state of the stratum corneum is the level of its hydration. Violation of the skin's moisture-retaining properties not only intensifies the patient's subjective sensations (burning, tightness, tingling, and itching) but also triggers exacerbation of the inflammatory process.

Despite extensive study of the clinical forms of rosacea, the search for objective biophysical markers that would allow predicting the further development of the disease and assessing the effectiveness of therapy remains a priority in dermatology. Corneometry, a non-invasive method for assessing skin electrical conductivity, enables the quantitative determination of epidermal hydration in real time.

Objective: to assess the skin condition of patients with rosacea, considering the severity of centrofacial erythema and skin hydration, to develop prognostic criteria for the course of the disease, and to optimize treatment.

Materials and Methods

During 2024-2026, we examined 89 patients aged 28-68 years with rosacea (53 with erythematotelangiectatic and 36 with papulopustular phenotypes). The duration of dermatosis ranged from 0 to 17 years.

For the assessment of the skin condition, we used:

1. The CEA scale (Clinician Erythema Assessment) – to determine the intensity of erythema.
2. The corneometry using the BT-Analyzer at standardized facial points of cheeks under controlled environmental conditions for the evaluation of the stratum corneum hydration state.
3. Non-contact (polarized) dermoscopy by the Heine Delta 30 dermatoscope to find out the specific patterns.
4. Statistical analysis of the obtained data using Spearman's correlation and multivariate ordinal logistic regression analyses.

Results

In 35,96% of participants (32 patients), we observed grade 2 erythema, and in 55,05% (49 patients), grade 3. Corneometry values indicated significant xerosis in all patients with rosacea. Critically low skin moisture - less than 30 % (Me=14%, $[Q_1\text{-}Q_3]$=12-17 %) corresponded to dermatoscopic findings of skin dehydration in 70.79 %of participants (diffuse white scales that obscure the underlying vascular structures, blurred looped vessels, exaggerated skin furrows, and fine lines). Correlation analysis revealed a moderate negative association ($r = -0.548$; $p = 0.001$) between the degree of erythema and skin hydration level. The more severe the erythema, the lower the hydration level. The regression model showed that a 1% increase in skin moisture level reduces the risk

of severe erythema by 47%.

Conclusions

In patients with rosacea, reduced stratum corneum hydration indicates transepidermal water loss, leading to systemic impairment of the skin barrier and the release of pro-inflammatory cytokines, which, in turn, support vasodilation and enhance erythema. We found a correlation between the degree of dehydration and the severity of erythema: the lower the corneometry score, the more intense the facial redness. Therefore, it emphasizes the need to restore the skin barrier as a priority therapeutic strategy in the management of rosacea.

Regarding corneometry in rosacea, it is not just a method for measuring moisture. It is a predictive analysis tool that allows assessment of the epidermal barrier before clinical symptoms become critical, determining the exacerbation risk in the early stages. In addition, its results can be used to assess treatment efficacy. The lack of dynamics to increase the level of moisture against the background of rosacea therapy is a harbinger of rapid relapse or resistance to treatment.

EA DV CONGRESS
VIENNA
30 SEP - 3 OCT 2026

Abstract N°: 2794

Interobserver agreement on significant morphological change during short-term teledermoscopic monitoring of atypical melanocytic lesions

Sofia Berglund*[1], Sam Polesie[1], Bengü Nisa Akay[2], Jonathan Bowling[3], Alex Chamberlain[4], Johan Dahlén Gyllencreutz[5], Aimilios Lallas[6], Ashfaq Marghoob[7], Cristian Navarrete-Dechent[8], Kari Nielsen[9], Linda Tognetti[10], John Paoli[1]

[1] Institute of Clinical Sciences, Sahlgrenska Academy, University of Gothenburg, Gothenburg, Sweden
[2] Ankara University, Medicine Faculty, Department of Dermatology, Ankara, Türkiye
[3] Private Practice, Oxford, United Kingdom
[4] Glenferrien Dermatology, Melbourne, Australia
[5] Department of Dermatology, Region Västra Götaland, Frölunda Specialist Hospital, Department of Dermatology and Venereology, Institute of Clinical Sciences, Sahlgrenska Academy, University of Gothenburg, Gothenburg, Sweden
[6] First Department of Dermatology, School of Medicine, Faculty of Healh Sciences, Aristotle University, Thessaloniki, Greece
[7] Memorial Sloan Kettering Cancer Center, New York, United States
[8] Pontificia Universidad Catolica de Chile, Santiago, Chile
[9] Dept of Clinical Sciences, Lund, Division of Dermatology. Medical Faculty, Lund University, Lund, Sweden
[10] Dermatology Unit, Department of Medical, Surgical and Neurological Sciences, University of Siena, Siena, Italy

Introduction

Atypical melanocytic lesions (AMLs) with low suspicion of malignancy on low-risk patients can be short-term monitored to distinguish melanomas from nevi without excising an excessive number of benign lesions. Significant morphological change during short-term monitoring should result in excision and histopathological examination to rule out melanoma. The main objective of this study was to investigate the interobserver agreement of short-term monitoring of AMLs since ‘significant change’ is a subjective assessment. The overarching aim was to identify areas for methodological improvement in short-term monitoring.

Materials and Methods

Nine readers from eight countries participated in this interobserver study containing assessments of 269 retrospectively collected AML image pairs that had undergone prior teledermoscopic short-term monitoring of approximately four months. The cases included 18 histopathologically confirmed melanomas: 16 *in situ* and 2 thin invasive (Breslow 0.3 mm and 0.7 mm, respectively). For all image pairs, readers were asked to evaluate the presence of significant morphological change and the need of excision and to specify (if applicable) what changes had occurred. Other possible management decisions were ‘unchanged and no need for further follow-up visits but continuous self-examination’ or ‘subtle or uncertain change and suggested additional long-term monitoring’. The readers were also instructed to rate the level of certainty in their assessments.

Results

Across readers, the number of AMLs assessed as changed and requiring excision ranged from 39 (14.5%) to 83

(30.9%) with a mean of 62 lesions (23.0%). The interobserver agreement amongst readers was fair (κ=0.23, 95% CI 0.21-0.24) with a Gwets AC coefficient of 0.33 (95% CI 0.29-0.37). Significant change and excision was recommended in 78.4% of the assessments of the 18 melanomas while long-term monitoring was recommended in 8.0%. No significant change or need for long-term monitoring was chosen in 13.6% of the assessed melanomas. The thin invasive melanoma with a Breslow thickness of 0.7 was assessed as in need of excision by all nine readers, while the other one with a Breslow thickness of 0.3 was assessed as changed by seven of the nine readers and as unchanged by two readers. Overall, the most commonly specified reasons for excision were: high suspicion of melanoma in the first image (n=142), new or changed dots and globules (n=109), new or changed atypical network (n=102), regression (n=52), and gray/blue color (22). Overall, 68% of the assessments were performed with a very high or high level of certainty.

Conclusions

The assessment of significant change during short-term monitoring of AMLs varies even among experienced dermatologists. Nevertheless, previously verified melanomas were most often identified, and many unnecessary excisions of nevi would theoretically have been avoided. To enhance the methods reliability, consensus assessment by two physicians may be an alternative. Also, it is important that the selection of lesions is optimized since the method itself is not a second opinion assessment of the baseline image. Additional meta data of the patients perceived history of change or lack of it could also facilitate the assessments. In conclusion, continued systematic analysis of short-term monitoring of AMLs is necessary to increase the external validity and thereby mitigate inevitable subjectivity that comes with visual assessments of dermoscopic images even among expert dermatologists.

EADV CONGRESS
VIENNA
30 SEP - 3 OCT 2026

Abstract N°: 2797

Implementation of a dual care model supported by artificial intelligence to reduce waiting lists in dermatology

Giuseppe Razzani*[1], Maria Elena Sanchez-Largo[2], Taig Mac Carthy[1], Alfonso Medela[3], Gerardo Fernandez[1], Andy Aguilar[1], Antonio Martorell[1, 4], Ignacio Hernandez[3], María Ribagorda[1]

[1] Clinical Endpoint Innovation - Legit.Health, Bilbao, Spain

[2] Hospital Universitario De Torrejón, Torrejón de Ardoz, Spain

[3] Medical Data Science - Legit.Health, Bilbao, Spain

[4] Manises Hospital, Manises, Spain

Introduction

The progressive increase in healthcare demand, combined with limited clinical capacity, represents a major structural challenge for healthcare systems, leading to prolonged waiting lists in dermatology. A monthly deficit of 183 consultations (2,196 annually) and a 64% increase in new patient visits highlighted the limitations of a traditional face-to-face care model.

Materials and Methods

A digital transformation strategy based on a dual care model integrating digital and in-person care was implemented, supported by artificial intelligence (AI). The model included AI-assisted digital triage, structured teledermatology, and remote follow-up of selected patients. This approach enabled improved case prioritization and optimization of referral pathways. Clinical activity and resource utilization were analyzed before and after implementation.

Results

Following implementation, digital triage improved alignment between healthcare demand and available clinical capacity. The number of new patient visits doubled compared to the exclusively face-to-face model. This was associated with improved resource utilization and a reduction in system bottlenecks, without evidence of compromised quality of care. The model enabled more efficient allocation of in-person consultations to higher-priority cases.

Conclusions

AI-supported hybrid care models allow better alignment between healthcare demand and clinical capacity in dermatology. Their implementation can reduce waiting lists while optimizing resource utilization. These findings support digital transformation as a key strategy to enhance efficiency and sustainability in dermatology services.

EA DV CONGRESS
VIENNA
30 SEP - 3 OCT 2026

Abstract N°: 2802

From innovation to clinical practice: Real-World deployment of AI-assisted digital triage in Public Healthcare

María Ribagorda*[1], Taig Mac Carthy[1], Alfonso Medela[2], Gerardo Fernandez[1], Andy Aguilar[1], Antonio Martorell[3], Ignacio Hernandez[2], Giuseppe Razzani[1]

[1] Clinical Endpoint Innovation - Legit.Health, Bilbao, Spain

[2] Medical Data Science - Legit.Health, Bilbao, Spain

[3] Manises Hospital, Manises, Spain

Introduction

Increasing demand for dermatology services has led to prolonged waiting times, overloaded referral pathways, and growing pressure on healthcare systems. In this context, digital transformation strategies supported by artificial intelligence (AI) have emerged as promising tools to optimize care delivery and improve patient prioritization. Beyond enhancing workflow efficiency and resource allocation, AI-assisted triage systems may also facilitate the earlier identification of clinically significant and potentially malignant conditions, enabling more timely intervention and improving overall quality of care.

Materials and Methods

A digital transformation strategy based on a dual care model integrating digital and in-person dermatology was implemented in a regional public healthcare system. The model combined AI-assisted triage in primary care, structured teledermatology, and remote follow-up of selected patients. The AI system stratified cases according to clinical urgency and recommended the most appropriate management pathway, including follow-up in primary care or referral to specialist dermatology services

Clinical activity and resource utilization were evaluated over a 12-month period before and after implementation. Outcomes included referral appropriateness, prioritization of urgent cases, waiting times, and dermatologist agreement with AI in a representative sample. Additionally, patients identified through the waiting list during the implementation phase were systematically reviewed to evaluate the detection of clinically significant and potentially malignant lesions.

Results

Implementation of the model was associated with improved referral quality and more appropriate use of specialist consultations. Prioritization of high-urgency cases was significantly enhanced, facilitating earlier access to specialized dermatological assessment and more timely clinical intervention. Waiting times for urgent patients decreased, reflecting more efficient resource allocation. Dermatologist agreement with AI-supported triage was high, particularly in common inflammatory conditions and benign lesions.

Importantly, the system enabled identification of patients with clinically significant conditions, including suspected malignant lesions, among those awaiting assessment, allowing earlier prioritization and specialist evaluation.

Conclusions

Implementation of an AI-supported digital care model improves efficiency and prioritization in dermatology within a public healthcare setting. Beyond optimizing referral pathways, this approach may facilitate the earlier detection of clinically significant and malignant conditions among patients on waiting lists, thereby improving both healthcare system efficiency and patient safety.

EADV CONGRESS
VIENNA
30 SEP - 3 OCT 2026

Abstract N°: 2804

A deep-learning standardized system for acquisition and automated quality assessment of dermatological images

Taig Mac Carthy*[1], Paola Pasquali[2], Ignacio Hernandez[3], Alfonso Medela[3], Gerardo Fernandez[1], Antonio Martorell[4], Andy Aguilar[1], Giuseppe Razzani[1], María Ribagorda[1], Agustín Oyhamburú[1]

[1] Clinical Endpoint Innovation - Legit.Health, Bilbao, Spain

[2] Pius Hospital De Valls, Valls, Spain

[3] Medical Data Science - Legit.Health, Bilbao, Spain

[4] Manises Hospital, Manises, Spain

Introduction

Image quality remains a major and unresolved challenge in teledermatology. Recent applications of artificial intelligence (AI) for automated image quality assessment (IQA) in dermatology are limited by small datasets and by methodological approaches that do not follow International Telecommunications Union (ITU) guidelines.

Materials and Methods

We developed and validated a convolutional neural network (EfficientNet-V2-M) using three dermatology datasets labeled according to ITU guidelines: DIQA-Artificial (1,900 clinical and dermoscopic images), PAD-UFES-20 (2,298 close-up lesion images), and Diverse Dermatology Images (DDI, 656 images with heterogeneous quality and skin tones, additionally cropped to match PAD-UFES-20).

Images were annotated by 15 non-expert raters and 3 dermatologists, assigning a quality score from 1 (poor) to 5 (excellent). The mean score of non-experts was used for model training, while dermatologist annotations were reserved for independent evaluation.

To ensure generalization, additional non-dermatological IQA datasets (KonIQ-10k, GFIQA-21k, SPAQ, BIQ2021, LIVE-ItW, and KADID-10k) were included. All datasets were split into training, validation, and test sets to prevent data leakage, with 5-fold cross-validation applied. Model performance was assessed using the Pearson Linear Correlation Coefficient (PLCC).

Results

The model demonstrated strong correlation between predicted and reference quality scores across datasets. Consistent performance was observed in both dermatological and non-dermatological benchmarks, with high PLCC values across all evaluated datasets (Table 1).

Table 1.

Test set	Anotator	PLCC
Kadid-10k	Non expert	0.929 ± 0.012
GFIQA-20k	Non expert	0.957 ± 0.002
KonIQ-10k	Non expert	0.937 ± 0.004
SPAQ	Non expert	0.912 ± 0.003
LIVE-ItW	Non expert	0.813 ± 0.011
DIQA-Artificial	**Dermatologists**	**0.739 ± 0.016**
DIQA-Artificial	Non expert	0.886 ± 0.011
PAD-UFES-20	**Dermatologists**	**0.662 ± 0.025**
PAD-UFES-20	Non expert	0.813 ± 0.008
DDI (cropped)	**Dermatologists**	**0.853 ± 0.020**
DDI (cropped)	Non expert	0.632 ± 0.034
DDI (original)	**Dermatologists**	**0.623 ± 0.057**
DDI (original)	Non expert	0.681 ± 0.051

Dermatological datasets showed moderate to high agreement with expert annotations, including PAD-UFES-20 and DDI. Performance was higher in controlled datasets such as KonIQ-10k and GFIQA-21k, while more heterogeneous datasets such as LIVE-ItW showed comparatively lower but robust correlation.

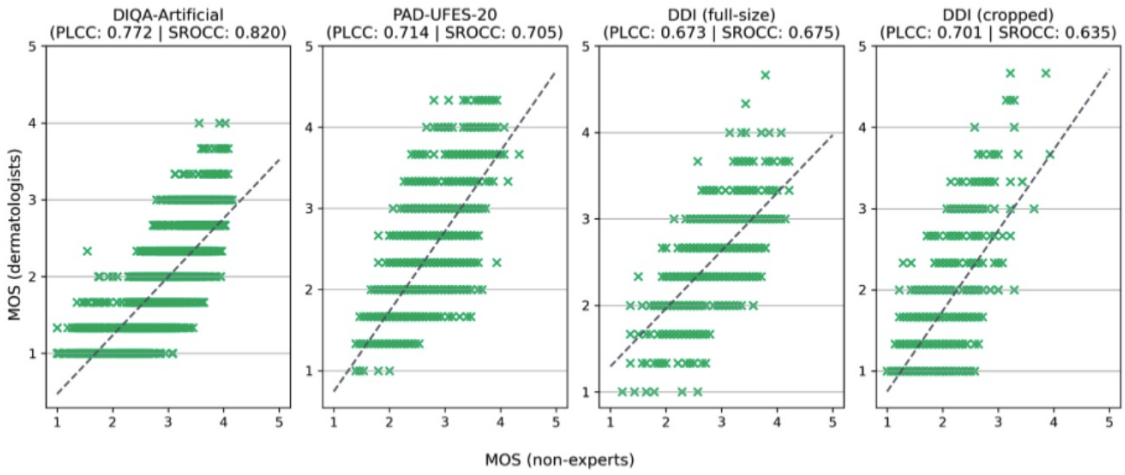

Figure 1. Representative outputs of the deep-learning image quality assessment system, illustrating model performance across dermatological datasets annotated according to ITU guidelines.

Conclusions

Deep learning-based image quality assessment models can reliably estimate dermatological image quality and generalize across heterogeneous datasets. These findings support the development of automated quality control tools that can improve data reliability in teledermatology and reduce dependence on manual expert labeling.

EADV CONGRESS
VIENNA
30 SEP - 3 OCT 2026

Abstract N°: 2952

Mycology Is Not Optional: Emerging Resistant Fungi and the Future of Dermatology Practice

Maryna Zhuravlova*[1]

[1] Luhansk state medical university, Rivne, Ukraine

Introduction

Clinical mycology has often been treated as a routine ancillary component of dermatology, limited to potassium hydroxide microscopy and empirical antifungal therapy. However, this approach is increasingly insufficient. Emerging and resistant fungal pathogens, including resistant dermatophytes, atypical tinea presentations, non-*albicans Candida* species, and multidrug-resistant fungi, are changing the diagnostic and therapeutic landscape. Inappropriate empirical antifungal use, corticosteroid-antifungal combinations, delayed species identification, and limited access to susceptibility testing may contribute to treatment failure, chronicity, transmission, and resistance selection.

Materials and Methods

A literature-informed and working experience based clinical framework was developed to address common outpatient scenarios in dermatology: chronic or recurrent dermatophytosis, tinea capitis, onychomycosis, inflammatory or steroid-modified tinea, suspected resistant dermatophyte infection, and yeast or mould infection in immunocompromised or healthcare-exposed patients. The framework emphasizes diagnostic decision-making before systemic or repeated empirical antifungal therapy. The presentation will be supported by multiple illustrative cases from real-world outpatient dermatology practice, highlighting common diagnostic pitfalls, delayed recognition, treatment failure, steroid-modified fungal infections, and suspected resistant or emerging pathogens. Practical outpatient mycology procedures will be demonstrated using video materials, including appropriate sampling from skin, hair, scalp, and nails (with some innovative techniques), preparation and interpretation of direct microscopy, and indications for fungal culture, histopathology with fungal stains, molecular identification, and antifungal susceptibility testing. Current and emerging antifungal treatment options will also be discussed with attention to rational prescribing, safety monitoring, resistance concerns, and real-world availability in clinical practice.

Results

The proposed outpatient mycology-stewardship model includes seven practical steps: 1) identify red flags for fungal disease, including chronicity, recurrence, treatment failure, atypical morphology, alopecia, nail involvement, immunosuppression, travel history, household clustering, and previous corticosteroid exposure; 2) obtain appropriate samples before treatment whenever possible; 3) use accessible office-based tools such as potassium hydroxide microscopy, dermoscopy/trichoscopy, Wood’s lamp examination when relevant, nail clipping, and histopathology with fungal stains; 4) request fungal culture and species-level identification for scalp infection, nail disease, recalcitrant dermatophytosis, inflammatory tinea, and suspected emerging pathogens; 5) escalate to molecular identification, mass spectrometry, or antifungal susceptibility testing through reference laboratories when treatment fails or resistance is suspected; 6) avoid empirical corticosteroid-antifungal combinations and unnecessary repeated antifungal courses without diagnostic confirmation; and 7) educate patients regarding adherence, duration of therapy, transmission, fomites, household contacts, and the need for follow-up documentation of clinical and, when indicated, mycological cure.

Conclusions

Mycology should be repositioned from a neglected supportive test to a core dermatology stewardship discipline. In the era of emerging resistant fungi, rational antifungal treatment begins before prescribing: with suspicion, correct sampling, microscopy, culture, species identification, and selective use of molecular and susceptibility methods. Outpatient mycology stewardship can reduce misdiagnosis, inappropriate therapy, resistance selection, and delayed recognition of emerging pathogens.

EADV CONGRESS
VIENNA
30 SEP - 3 OCT 2026

Abstract N°: 2954

Breast sarcoidosis: When should it be considered?

Majd Alrube*[1], Saliha Takheroubt[1], Lemya Mezdour[1], Asma Haciane[1], Issam TABLIT[1], Samira Zobiri[1]

[1] Mustapha University Hospital Center, Algiers, Algeria

Introduction

Sarcoidosis is a systemic granulomatous inflammatory disease of unknown etiology, affecting both sexes with a predominance in young women. It is characterized by non-caseating epithelioid granulomas and commonly involves the lungs, eyes, liver, and spleen. Breast involvement is extremely rare. We report the association of erythema nodosum with breast sarcoidosis, highlighting that erythema nodosum may reveal this rare extra-thoracic manifestation.

Case Presentation

We report the case of a 34-year-old woman presenting with painful lower-limb lesions associated with fever and difficulty walking for two months. Clinical examination revealed inflammatory painful hypodermic nodules on both lower limbs, consistent with erythema nodosum.

Questioning revealed a seven-month history of chronic right-sided mastitis. The patient initially developed a painful inflammatory swelling of the right breast that was red, warm, and indurated, later progressing to fistulization with purulent and bloody discharge followed by superficial ulceration. Multiple courses of antibiotics failed to improve symptoms. Systemic corticosteroids led to partial improvement, but treatment was discontinued because of persistent pain, discharge, and poor tolerance with acneiform eruption.

Breast examination showed a rounded erythematous-violaceous atrophic plaque in the upper outer quadrant of the right breast, corresponding to a previous ulceration scar, associated with clustered punctiform fistulous openings covered with yellowish and sometimes hemorrhagic crusts. Two deep painful indurations of the underlying mammary gland were palpated. The contralateral breast and lymph node areas were normal.

Laboratory tests, including complete blood count, liver and renal function tests, hormonal profile, and angiotensin-converting enzyme levels, were normal. Chest radiography was normal, the tuberculin skin test was anergic, and infectious investigations, particularly for tuberculosis, were negative. Multiple breast ultrasounds showed non-specific findings. Breast biopsies revealed granulomatous mastitis with non-caseating epithelioid and giant-cell granulomas.

Given the association of erythema nodosum with chronic granulomatous mastitis, sarcoidosis was suspected. Additional investigations including high-resolution chest CT scan, minor salivary gland biopsy, phosphocalcic assessment, and ophthalmological examination showed no systemic involvement. The diagnosis of isolated breast sarcoidosis associated with erythema nodosum was retained.

The patient was treated with colchicine followed by systemic corticosteroids combined with azathioprine, leading to progressive improvement without new fistulization.

Chronic inflammatory mastitis raises important differential diagnoses, particularly inflammatory breast cancer and infectious mastitis such as tuberculosis. In our patient, malignancy was excluded histologically, while negative infectious investigations and absence of caseous necrosis argued against tuberculosis. Sarcoidosis is a systemic granulomatous disease characterized by non-caseating epithelioid giant-cell granulomas. It mainly affects young women and usually involves the lungs, lymph nodes, skin, and eyes. Breast involvement is extremely rare and may mimic inflammatory breast cancer, making histology essential for diagnosis.

Despite the absence of systemic involvement, the diagnosis of isolated breast sarcoidosis was retained based on concordant clinical and histological findings. Treatment mainly relies on systemic corticosteroids, sometimes requiring immunosuppressive agents.

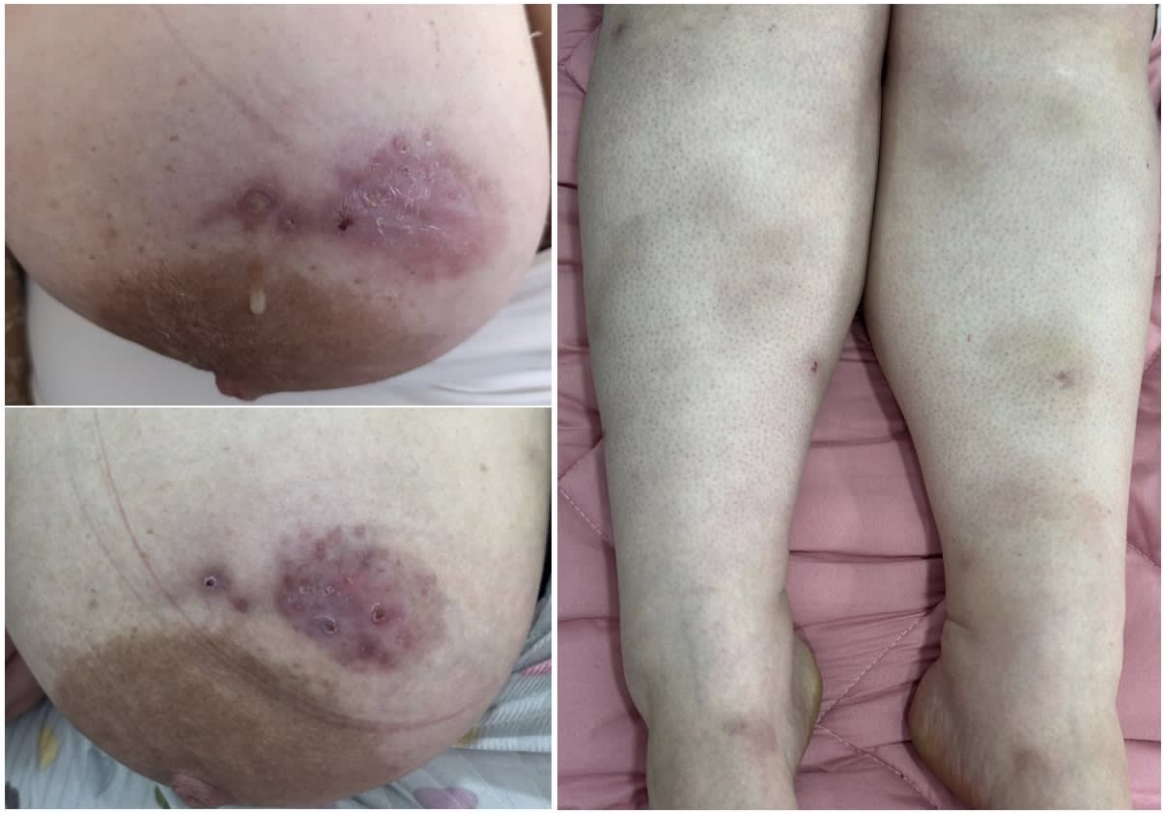

Conclusion

Isolated breast sarcoidosis is a rare manifestation that may mimic malignant or infectious breast disease. Diagnosis relies on clinical and histological findings after exclusion of other granulomatous causes, particularly tuberculosis and neoplasia.
Our case highlights the importance of considering this entity in chronic granulomatous mastitis associated with erythema nodosum, even without systemic involvement.

EA DV CONGRESS
VIENNA
30 SEP - 3 OCT 2026

Abstract N°: 3036

Generative AI-Augmented Deep Learning for Distinguishing Nail Unit Melanoma from Nail Melanonychia: A Multicenter Study with Human-AI Collaboration Analysis

Jemin Kim*[1], Jihee Boo[1], Jihee Kim[1], Jongwook Oh[2], Hamin Kim[3], Byung Ho Oh[2], Mi Ryung Roh[4]

[1] Department of Dermatology and Cutaneous Biology Research Institute, Yongin Severance Hospital, Yonsei University College of Medicine, Gyeonggi-do, Korea, Rep. of South

[2] Department of Dermatology and Cutaneous Biology Research Institute, Severance Hospital, Yonsei University College of Medicine, Seoul, Korea, Rep. of South

[3] Department of Pediatrics, Severance Hospital, Institute for Innovation in Digital Healthcare, Yonsei University College of Medicine, Seoul, Korea, Rep. of South

[4] Department of Dermatology and Cutaneous Biology Research Institute, Gangnam Severance Hospital, Yonsei University College of Medicine, Seoul, Korea, Rep. of South

Introduction

Nail unit melanoma (NUM) is frequently misdiagnosed as benign nail melanonychia (NM) on clinical photographs, leading to delayed biopsy and advanced-stage presentation. Development of image-based deep learning models is constrained by NUM rarity and class imbalance. We developed a deep learning classifier augmented with generative synthetic images, evaluated its generalizability across independent external datasets, and assessed its impact on dermatologists' diagnostic accuracy and biopsy decision-making.

Materials and Methods

This multicenter retrospective study assembled 1,323 clinical images (NUM n=406; NM n=917) from four tertiary referral institutions and 74 published reports, split into a training set (n=1,171) and an internal test set (n=152). Two independent external test datasets (A, n=94; B, n=96) with no patient overlap and either temporal or geographic separation were used for validation. Synthetic images were generated with StyleGAN2 with adaptive discriminator augmentation (StyleGAN2-ADA) and a denoising diffusion probabilistic model (DDPM), producing 4,000 images per architecture (GAN4000, DIFF4000). Four backbones (ResNet18, EfficientNet-b0, Vision Transformer, Swin Transformer) were trained under three conditions: original data only, original+GAN4000, and original+DIFF4000. Performance was assessed with accuracy, sensitivity, specificity, and ROC-AUC, with bootstrap-derived 95% CIs. Thirty-nine board-certified dermatologists—stratified into surgical dermatologists with ≥10 years' experience (S≥10yr, n=11), surgical dermatologists with <10 years' experience (S<10yr, n=12), and medical dermatologists (M, n=16)—completed a three-part reader study: classification of the internal test set without AI (Part I) and with AI predictions (Part II), and selection of a biopsy stage from generative sequential NM-to-NUM images (Part III).

Results

EfficientNet-b0 with GAN4000 achieved the best performance on the internal test set, with accuracy 0.928 (95% CI, 0.888–0.967), ROC-AUC 0.973 (0.944–0.992), sensitivity 0.895, and specificity 0.961; performance was maintained or improved on both external datasets, and decision curve analysis showed superior net benefit across clinically plausible thresholds. Synthetic images were rated of acceptable clinical realism across six qualitative domains (Likert means 3.25–3.42), with no significant difference between specialists and residents. Among the 39 readers, classification accuracy increased from 0.647 (0.629–0.664) without AI to 0.736 (0.720–0.752) with AI (P<0.001). The largest gain was observed in medical dermatologists (+0.123, P<0.001), followed by S<10yr (+0.094, P<0.001), whereas S≥10yr showed only a marginal change (+0.035, P=0.10). Trust in AI did not differ across subgroups

(P=0.652), but Attitude (clinical engagement) was significantly higher in S≥10yr than in M (P=0.012). In Part III, S≥10yr selected biopsy at later morphologic stages—more closely resembling NUM—than the other subgroups (Kruskal-Wallis P=0.017). Misclassified NUM cases were more frequently in situ (95.8% vs. 53.1%, P<0.001) and lacked ulceration/nodule (P=0.01) and nail plate destruction (P=0.04). Grad-CAM analysis showed model attention concentrated on ulceration, nodule, and nail plate destruction in true-positive predictions.

Conclusions

A deep learning classifier augmented with generative synthetic images accurately differentiated NUM from NM across internal and external datasets and significantly improved dermatologists' diagnostic accuracy, with the greatest benefit observed in less surgically engaged readers. Generative sequential images additionally revealed differences in biopsy thresholds across experience subgroups, suggesting a potential educational role. Generative AI-augmented deep learning, with explainability and human-AI collaboration analysis, may support earlier biopsy decisions and reduce diagnostic delays in nail unit melanoma.

EADV CONGRESS
VIENNA
30 SEP - 3 OCT 2026

Abstract N°: 3099

From text to diagnosis: Retrospective real-world concordance of text-based AI in Swiss teledermatology

Naomi Mueller*[1, 2], Elisabeth Goessinger[1, 2, 3], Philippe Gottfrois[1], Alexander Navarini[1, 2], Christian Greis[4]

[1] Department of Dermatology, University Hospital Basel, Basel, Switzerland
[2] Faculty of Medicine, University of Basel, Basel, Switzerland
[3] ViDIR Group, Department of Dermatology, Medical University of Vienna, Vienna, Austria
[4] Department of Dermatology, University Hospital Zurich, Zurich, Switzerland

Introduction
Teledermatology has become an established component of dermatological care, enabling patients to obtain specialist assessment remotely through digital platforms. At the same time, there is growing interest in using artificial intelligence (AI), especially large language models (LLMs), to assist with diagnostic decision-making in dermatology. Current research on LLMs in teledermatology predominantly concentrates on cloud-based LLMs using image-driven and multimodal strategies. However, beyond the predominant focus on visual data, the potential clinical value of patient-reported textual information for diagnosis may be underrecognized. Simultaneously, the increasing reliance on cloud-based AI systems has intensified concerns surrounding the protection of sensitive medical data. Compared with cloud-based systems, locally-hosted LLMs offer advantages by enabling patient information to remain within local infrastructures while also supporting data sovereignty, model traceability and reproducibility. This study investigated whether patient-reported textual information without accompanying clinical images provides enough diagnostic information for a locally-deployed LLM to generate accurate differential diagnoses in a teledermatology setting. Furthermore, the study explored the feasibility of a locally-hosted LLM as a privacy-preserving alternative to cloud-based systems.

Materials and Methods
This retrospective study included 1322 patients from a real-world Swiss teledermatology cohort treated by teledermatologists at a university hospital between May 2019 and November 2024. Patients provided a free-text description of their skin complaint, together with structured clinical metadata. The structured information contained details of symptom characteristics, duration, any previous similar conditions, treatment history, and demographic information such as age, sex, pregnancy status, and allergies. The locally-hosted LLM IBM Granite was used to analyse patient-reported information to generate three differential diagnoses, ranked by probability. These predictions were compared with teledermatologist-established reference diagnoses. Diagnostic performance was classified as top-1 concordance when the first-ranked diagnosis matched the reference diagnosis, top-3 concordance when the correct diagnosis appeared among the three generated suggestions, and discordance when no diagnostic match was observed. In addition, the relationship between free-text length and diagnostic concordance was statistically analysed using rank-based concordance groups. Reproducibility was assessed by processing identical patient input three times under unchanged conditions and comparing agreement across repeated analyses.

Results
Using text-based patient input alone, IBM Granite achieved top-1 concordance in 20.3% of cases (n=268), while a correct diagnosis appeared within the three generated suggestions in 40.1% of cases (n=530). Patient free-text descriptions had a median length of 335 characters (IQR 204.0–589.8). The median of the free-text description improved with higher concordance rank. A statistically significant positive correlation was observed between text length and rank-based concordance (Spearman ρ=0.078, p=0.004). Furthermore, free-text length differed

significantly across concordance groups (H(2)=8.377, p=0.016). Post-hoc analysis demonstrated a significant difference between cases with concordance at rank 1 and discordant cases (p=0.045). In terms of reproducibility, the highest level was seen for the first-ranked diagnosis, with complete agreement across repeated analyses in 93.3% of cases.

Main category of diagnosis	n	Top 1 (n, %)	Top 3 (n, %)	Discordance (n, %)
Inflammatory skin diseases	310	135 (43.5%)	195 (62.9%)	115 (37.1%)
Benign neoplasms of the skin	302	13 (4.3%)	59 (19.5%)	243 (80.5%)
Infectious skin diseases	279	33 (11.8%)	96 (34.4%)	183 (65.6%)
Acneiform and follicular disorders	175	40 (22.9%)	102 (58.3%)	73 (41.7%)
Other diagnoses	164	25 (15.2%)	44 (26.8%)	120 (73.2%)
Pre-cancerous lesions and skin cancer	39	8 (20.5%)	16 (41.0%)	23 (59.0%)
Skin appendage	34	13 (38.2%)	15 (44.1%)	19 (55.9%)
Pigmentary disorders	13	1 (7.7%)	3 (23.1%)	10 (76.9%)
Wound and artefacts	6	0 (0.0%)	0 (0.0%)	6 (100.0%)

n = number

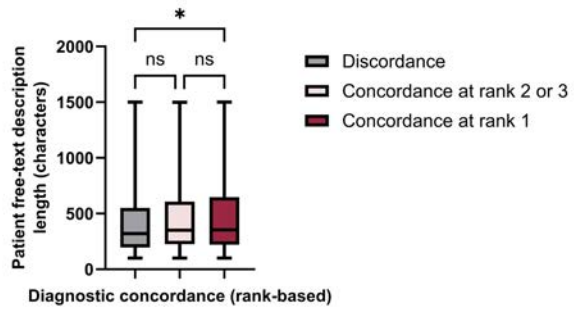

Table 1. Diagnostic concordance between LLM-generated and teledermatologist diagnoses. Figure 1. Length of patient free-text descriptions stratified by diagnostic concordance rank. Median and range are displayed. Discordance (n = 792), concordance at ranks 2 or 3 (n = 262), and concordance at rank 1 (n = 268). Kruskal–Wallis test with Dunn's post hoc multiple-comparison analysis: *: $p < 0.05$; ns = not significant ($p > 0.05$).

Conclusions

These results suggest that patient-written information can provide diagnostically relevant content even without clinical images. Locally-deployed LLMs may therefore offer a useful framework for privacy-oriented AI support in teledermatology.

EA DV CONGRESS
VIENNA
30 SEP - 3 OCT 2026

Abstract N°: 3287

LC-OCT in mucous membrane pemphigoid: a tool for diagnosis and treatment monitoring

Urszula Fałkowska*[1], Lidia Rudnicka[1], Małgorzata Olszewska[1]

[1] Department of Dermatology, Medical University of Warsaw, Warsaw, Poland., Warszawa, Poland

Introduction
Desquamative gingivitis is a clinical condition characterized by erythema, blisters, and erosions within the gingiva. It may be a manifestation of oral lichen planus or autoimmune bullous diseases, such as pemphigus vulgaris and mucous membrane pemphigoid (MMP) [1,2,3]. MMP remains diagnostically challenging, particularly in cases with isolated mucosal involvement. Differential diagnosis requires histopathological and direct immunofluorescence studies. Noninvasive imaging techniques such as line-field confocal optical coherence tomography (LC-OCT) enable real-time, high-resolution visualization of mucosal structures. Here, we present LC- OCT features of MMP and its usefulness in monitoring treatment response.

Case Presentation
An 87-year-old woman presented with a 6-month history of desquamative gingivitis. Previous treatment with topical corticosteroids had been ineffective. Clinical examination revealed gingival erythema and erosions involving both the maxillary and mandibular gingiva. LC-OCT imaging demonstrated multilocular subepithelial blistering, appearing as dark hyporeflective areas between the epithelium and the underlying lamina propria. The blisters showed a grayish signal consistent with fluid content. The stratified epithelial architecture and epithelial thickness were preserved. Areas of full-thickness epithelial loss consistent with erosions were also observed. Hyperreflective white dots corresponding to inflammatory cells were observed within the lamina propria and inside the subepithelial blister cavity. The basement membrane zone appeared indistinct, with blurred demarcation between the epithelium and lamina propria.

Direct immunofluorescence confirmed the diagnosis of mucous membrane pemphigoid. Systemic treatment with methotrexate at a dose of 10 mg administered subcutaneously once weekly was initiated, combined with topical fluocinolone acetonide. At 3-month follow-up, clinical examination showed persistent gingival erythema involving the maxillary and mandibular gingiva, with a significant reduction in pain. LC-OCT imaging demonstrated resolution of subepithelial blistering. The stratified epithelial architecture was continuous, with no areas of epithelial loss. A band of vacuolization was visible along the junction between the stratified squamous epithelium and the lamina propria. Parakeratosis was present within the epithelium. Inflammatory infiltrate persisted.

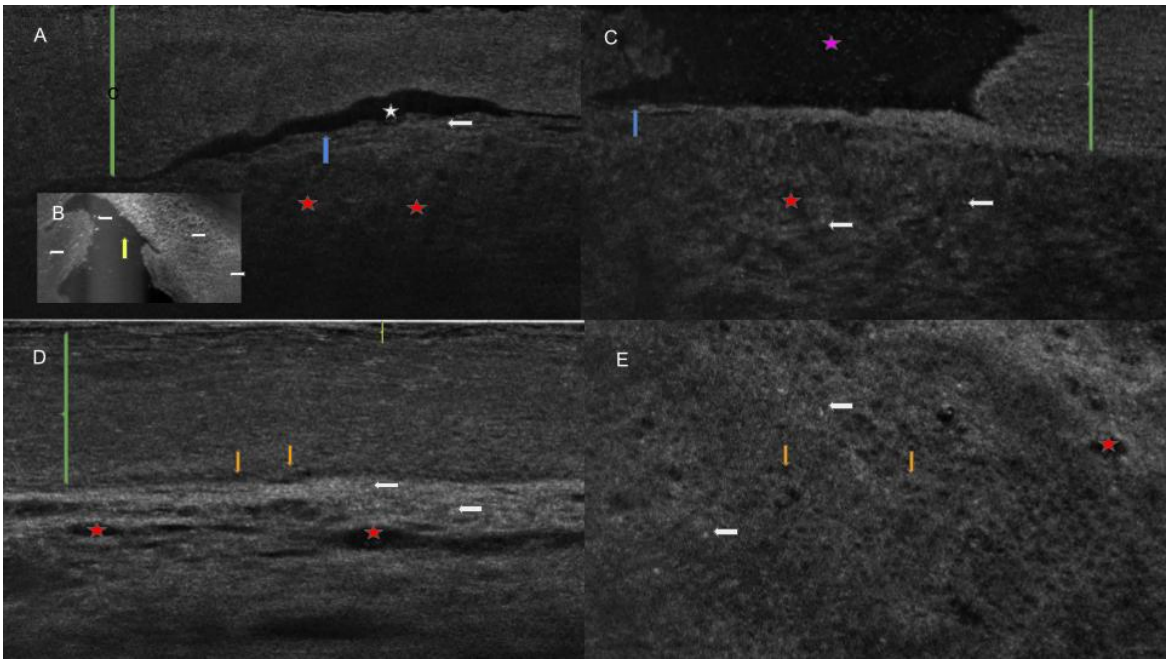

Figure 1. LC-OCT imaging of mucous membrane pemphigoid at baseline (A–C) and after 3 months of methotrexate treatment (D, E). (A, C, D) Vertical views; (B, E) horizontal views. White star: multilocular subepithelial blister; yellow arrow: fluid content; blue arrow: indistinct basement membrane zone; white arrows: inflammatory cells; green curly bracket: preserved epithelial thickness; orange arrows: vasculation between the stratified squamous epithelium and the lamina propria; red stars: vascular structures; yellow curly bracket: parakeratosis; pink star: erosion.

Conclusion

In this case, LC-OCT enabled noninvasive visualization of subepithelial blistering and its resolution during methotrexate treatment, correlating with clinical improvement. Despite the absence of erosions at follow-up, LC-OCT revealed persistent microscopic features, including vacuolization and inflammatory infiltrate, suggesting ongoing disease activity. These findings highlight the potential role of LC-OCT in monitoring treatment response and supporting individualized therapeutic decisions in mucous membrane pemphigoid.

EADV CONGRESS
VIENNA
30 SEP - 3 OCT 2026

Abstract N°: 3297

Eruptive Disseminated Spitz Nevi: Multimodal Imaging and Long-Term Follow-Up with Dermoscopy and Confocal Microscopy

Leonardo Balestra*[1], Patrick Silvetti[1], Laura Mazzoni[2], Serena Magi[2], Maria Beatrice De Felici Del Giudice[3], Valeria Boccaletti[4], Ignazio Stanganelli[2]

[1] School of Dermatology, University of Parma, Parma, Italy
[2] Skin Cancer Unit, Istituto Romagnolo per lo Studio dei Tumori "Dino Amadori" IRCCS IRST, Meldola, Italy
[3] Dermatology Unit, Azienda Ospedaliero-Universitaria di Parma, Parma, Italy
[4] Dermatology Unit, Azienda Ospedaliero-Universitaria di Brescia, Brescia, Italy

Introduction

Eruptive Disseminated Spitz Nevi (EDSN) is a rare clinical variant of Spitz nevus, a benign melanocytic lesion classically divided into three forms: solitary, agminated, and disseminated; the latter may present as either eruptive or non-eruptive. EDSN is an exceptional condition, with approximately 27 cases reported in the literature, and predominantly affects adolescents and young adults. Onset typically involves the trunk and proximal portions of the limbs, with subsequent spread to much of the body surface, while the palms, soles, mucosae, and scalp are generally spared, although rare exceptions have been described.

Case Presentation

A 12-year-old patient with a first-degree family history of melanoma presented with hundreds of asymptomatic pigmented lesions distributed over most of the body surface. The first lesions had appeared approximately four years earlier, initially as a limited number of lesions on the trunk and face; however, in the six months preceding the dermatological evaluation, a sudden and rapid spread to the entire body surface had been observed. Dermoscopic examination showed, in most lesions, a typical melanocytic pattern characterized by gray-black central pigmentation and symmetric peripheral radial streaks. Within this diffuse clinical picture, two lesions on the back — one in the interscapular region and one in the lumbar region — stood out because of clinical and dermoscopic atypia and were therefore selected for further evaluation by reflectance confocal microscopy.

Confocal images showed a typical honeycomb pattern, associated, however, with focal cytological atypia, including irregularly shaped and sized cells arranged in scattered dense nests, architectural disarray, single mononucleated cells within the nests, and dendritic and pagetoid cells.

Both lesions were surgically excised and submitted for histological examination. Histology showed, in both lesions, a symmetrical and well-circumscribed proliferation of hyperpigmented spindle-shaped melanocytes, arranged mainly in irregular fascicles at the dermoepidermal junction and within the papillary dermis. The overall findings were therefore compatible with Spitz nevi, confirming the diagnosis of EDSN. Over the following 11 years, the patient was monitored through serial clinical and videodermoscopic follow-up. The total number of melanocytic nevi progressively increased, consistent with the patient’s age and the nevogenic dynamics of adolescence. However, despite the persistence of a numerically impressive clinical picture, no further excision of suspicious lesions was required, except for a single atypical lesion on the back, which subsequently proved histologically to be a compound nevus with inflammation.

The current dermoscopic appearance is profoundly different from that observed at onset. The lesions now

predominantly show typical melanocytic patterns, with junctional nevi displaying a regular reticular pattern and compound nevi showing a globular pattern. In some areas, peripheral globules arranged in a “crown-like” distribution persist, a finding compatible with the patient’s age and physiological nevus maturation. No lesions with clearly spitzoid morphology or structures suggestive of significant atypia are currently observed.

Conclusion

This case of EDSN with 11 years of follow-up confirms the central value of non-invasive diagnostics in the management of multiple spitzoid lesions in pediatric age. The combination of serial digital dermoscopy and reflectance confocal microscopy made it possible to selectively identify lesions requiring excision, avoiding a high number of unnecessary surgical procedures while maintaining a high level of diagnostic safety. Long-term follow-up also documents the progressive transition from an initially heterogeneous and potentially alarming presentation toward benign dermoscopic phenotypes, supporting a conservative approach based on lesion stability, targeted selection of suspicious cases, and prolonged monitoring.

EA DV CONGRESS
VIENNA
30 SEP - 3 OCT 2026

Abstract N°: 3544

The "Mid-Substance Tear" Concept For Fibrotic Hypodermal Bands: A Systematic Review Applying Musculoskeletal Tendon Injury Models To The Remodeling Of Hidradenitis Suppurativa Tunnels

Zeel Lightwala*[1], Randa Abdelhamid[1], Krish Lightwala[1]

[1] Belarusian state medical university, Minsk, Belarus

Introduction
Hidradenitis suppurativa (HS) is a chronic inflammatory skin disease that creates painful, tunneling fibrotic bands deep in the skin (hypodermis). Once these tunnels become fibrous, they rarely reverse with standard anti-inflammatory or antibiotic treatments. No open-source, biomechanics-based tool exists to predict which tunnels will eventually break down and heal on their own versus those that will persist or worsen. Interestingly, HS tunnels look and behave much like injured tendons. For the first time, the "mid-substance tear" model from orthopedic tendon injury was applied to HS to see if tendon healing mechanics could predict long-term tunnel behavior.

Materials and Methods
A systematic review was conducted following PRISMA guidelines (PROSPERO CRD42024583102). PubMed, Embase, Web of Science, and Scopus were searched from 2000 to 2025. Studies were included if they described HS tunnel morphology on ultrasound, MRI, or histology with at least 12 months of follow-up, or if they applied any biomechanical modeling to fibrotic dermal bands. Out of 1,876 screened records, 52 studies met the criteria – covering 3,847 patients and 9,214 individual tunnels. Three biomechanical features were extracted: tunnel wall tensile strength (measured by elastography), intraluminal fibrosis density (on histology), and the peritunnel inflammation gradient (by MRI). Using Python, scikit-learn, and XGBoost with nested cross-validation, a predictor of tunnel "rupture/remodeling" (complete resolution) versus persistence was trained on 70% of tunnels (n=6,450) and validated on the remaining 30% (n=2,764). The ground truth was 18-month ultrasound resolution or surgical confirmation.

Results
The mid-substance tear model predicted tunnel resolution at 18 months with a ROC AUC of 0.89 (95% CI, 0.86–0.92), accuracy of 87%, precision of 0.85, and recall of 0.88. In contrast, traditional clinical scoring systems (Hurley stage, IHS4) managed only an AUC of 0.61 (95% CI, 0.56–0.66). The strongest predictors of spontaneous remodeling were: a loss of tensile strength greater than 60% compared to normal adjacent skin (odds ratio 5.8, $p<0.001$), the presence of central necrosis within the tunnel wall on histology (OR 4.2, $p=0.002$), and a peritunnel immune environment dominated by CD163+ M2 macrophages (OR 3.7, $p=0.004$). Tunnels that met all three "mid-substance tear" criteria showed a 74% remodeling rate within 18 months without any surgery, compared to only 12% in tunnels with intact tensile strength. In a real-world prospective test of 412 tunnels followed for 12 months, the model reclassified 31% of Hurley stage II patients: 18% as "high remodeling potential" (surgery was safely avoided, and tunnels remained stable or resolved), and 13% as "low remodeling, high persistence" (these patients underwent early tunnel excision, which achieved an 89% cure rate). Over 24 months of follow-up, recurrence in persistently classified tunnels was 41% with medical therapy alone versus only 9% with early excision guided by the model.

Conclusions

The mid-substance tear concept from tendon injury medicine applies directly to the fibrotic hypodermal bands of hidradenitis suppurativa. This biomechanical framework can predict which tunnels will heal on their own and which will persist. Patients identified as having high remodeling potential can safely avoid surgery, while those with low remodeling benefit from early tunnel excision. The full search strategy, extracted data, and prediction code are publicly available for independent validation and clinical integration.

EA DV CONGRESS
VIENNA
30 SEP - 3 OCT 2026

Abstract N°: 3587

The ABC of Dermatologic Ultrasound: A Histopathology-Oriented Approach to Sonographic Analysis of Elementary Lesions and Basic Pathological Processes

Artur Bezugly*[1], Pavel Belkov[1], Nikita Bezugly[1]

[1] Laboratory of Noninvasive Skin Diagnostics ANTA-Med, Moscow, Russian Federation

Introduction

High-frequency ultrasound (HFUS; 18–33 MHz) and ultra-high-frequency ultrasound (UHFUS; 50–75 MHz) provide near-histological resolution of the skin and show strong correlation with histopathology. However, a systematic, clinically intuitive method to translate the dermatologist's elementary-lesion understanding into ultrasound interpretation is still lacking. We aimed to develop a sonographic framework that directly mirrors the histopathological processes underlying primary and secondary skin lesions.

Materials and Methods

We retrospectively analyzed HFUS/UHFUS images (18, 22, 33, 50, and 75 MHz) of a large series of histopathologicaly verified dermatological lesions collected over more than 20 years. All scans were performed according to a standardized protocol. For each primary (macule, papule, plaque, nodule, vesicle, bulla, pustule, wheal) and secondary (scale, crust, erosion, ulcer, scar, atrophy, lichenification) elementary lesion, characteristic sonographic features—epidermal and dermal thickness and echogenicity, internal lesion structure feature, layer involvement, margin definition, and vascularity—were defined. In parallel, we identified ultrasound patterns for the fundamental pathological processes: serous/infiltrative inflammation, purulent inflammation, proliferative inflammation, fibrosis/sclerosis, atrophy, and necrosis.

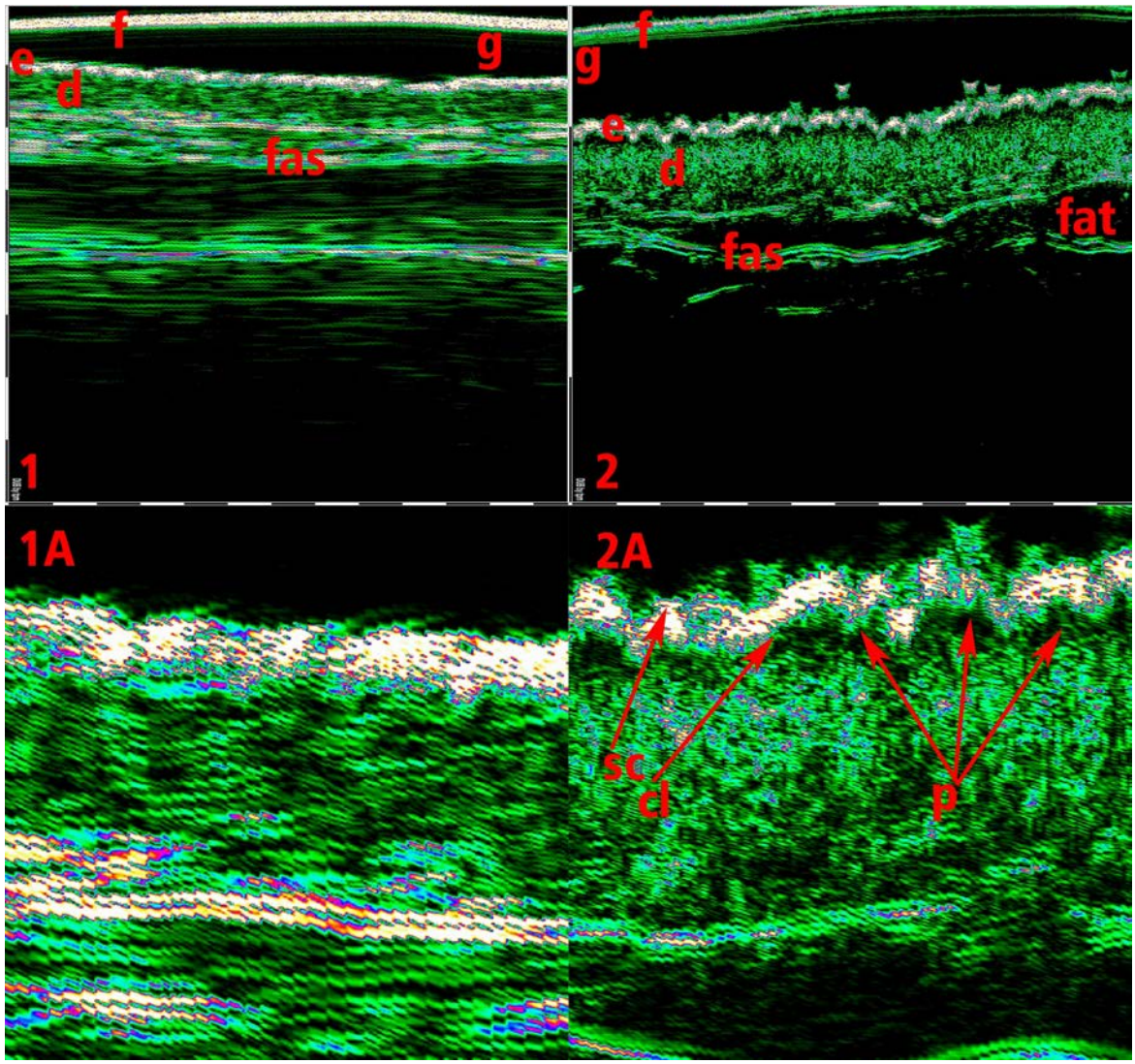

Intact skin 1 - scan 22 MHz, 1A - scan 22 MHz in ZOOM mode, 2 - scan 75 MHz, 2A - scan 75 MHz in ZOOM mode,f-foil on the ultrasound probe tip, g-ultrasound gel, e-epidermis, d-dermis, fas-fascia, fat-subcutaneous fat, sc - stratum corneum, cl - cellular epidermal layers, p - dermal papillaes.

Results

Each pathological process exhibited a distinct sonographic signature.

- **Serous inflammation** was characterized by anechoic intraepidermal or subepidermal fluid collections; the level of the split (intra- vs. subepidermal) directly mirrored the histologic cleavage plane, reliably differentiating pemphigus vulgaris from bullous pemphigoid and Duhring dermatitis.
- **Infiltrative inflammation** accompanied increasing of papillary and reticular dermis thickness and diffuse echogenicity decrease, infiltrates structure hypoechoic or hypo-anechoic, margins ill-defined (urticaria, psoriatic plaques) or clear (psoriatic papules), in systemic dermatoses (psoriasis, atopic dermatitis) Subepidermal Low-Echogenic Band (SLEB) registered in the affected area and in some cases on visually unchanged skin, vascularity increased in Color and Power Doppler mode, an increase in vessels with slow blood flow is determined, mainly along the edges of the infiltrate. Infiltrative inflammation patterns features allow differentiate psoriasis, lichen planus, morphea and other dermatoses.
- **Purulent inflammation** presented as heterogeneous hypo-anechoic cavities in the epidermis, dermis or subcutaneous fat, with a posterior acoustic enhancement and peripheral hypervascularity, distinguishing dermal and subdermal abscesses, deep purulent folliculitis.
- **Proliferative inflammation** showed solid hypoechoic dermal thickening with irregular epidermal hyperplasia and acanthotic projections, deep dermal vessels dilatation, and signs of fibrosis in deep dermis, allowing separation of lichenified chronic dermatitis and lichen planus from purely exudative processes.

- **Fibrosis/sclerosis** appeared as hyperechoic dermal and subdermal bands with posterior acoustic shadowing and sharp dermal-subcutaneous borders, enabling staging of morphea (active hypoechoic vs. sclerotic hyperechoic), specific patterns allows differentiation of keloids and hypertrophic scar types.
- **Atrophy** was identified by measurable thinning of the epidermis, dermis, and/or subcutis, often with a condensed hyperechoic appearance.
- **Necrosis** manifested as a homogeneous anechoic area with complete loss of normal layered architecture, sometimes containing echogenic debris.

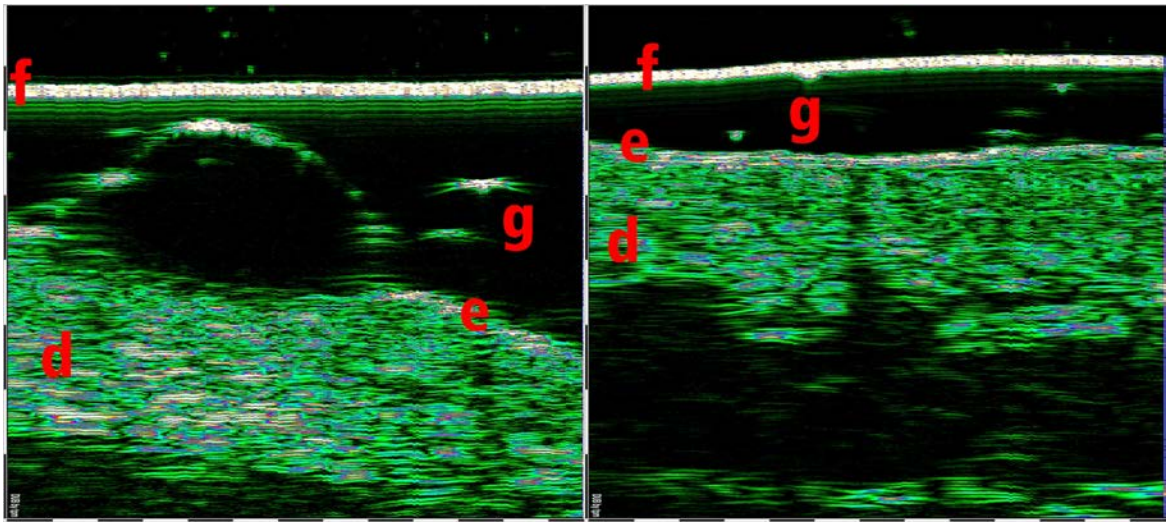

Serous Inflammation, Dermatitis herpetiformis. Left bullous lesion, right contralateral visually healthy skin, f - foil on the ultrasound probe tip, g - ultrasound gel, e - epidermis, d - dermis.

Conclusions

Interpreting HFUS/UHFUS images through the lens of elementary lesion morphology and basic histopathological processes provides a systematic, clinically intuitive diagnostic framework. This “dermatological” approach makes the underlying tissue pathology visible, enhances differential diagnosis, and can be seamlessly integrated into daily dermatologic practice.

EADV CONGRESS
VIENNA
30 SEP - 3 OCT 2026

Abstract N°: 3681

Schulman's fasciitis: an atypical presentation of a rare disease

Kichou Asma*[1], Taibi Lynda[1], Imene Mahiou[1], Samira Zobiri[1]

[1] Mustapha, Algiers, Algeria

Introduction

Schulman's fasciitis, also known as EosinophilicFasciitis, is a rare inflammatory disease characterized by collagenous thickening of the fascia associated withperipheral hypereosinophilia.
Its clinical presentation is variable and may mimic othermore common conditions, such as Scleroderma, makingthe diagnosis difficult and often delayed.
Few cases have been reported in the literature, whichlimits knowledge of its clinical manifestations and optimal management.
We report a case of Schulman's fasciitis to highlight the clinical and laboratory features of this rare disease

Case Presentation

A 45-year-old patient with a history of deafness and mutism since childhood presented with progressive skin induration. Physical examination revealed painfulthickening of the forearms, legs, and lateral aspects of the thighs, associated with swelling of the hands and diffuse hyperpigmentation of all four limbs.
The symptoms had begun six years earlier, initiallyinvolving the feet and legs, and subsequently extendingto the thighs and upper limbs within a few months.
Laboratory investigations showed polyclonal hypergammaglobulinemia. The eosinophil count waswithin normal limits, and the autoimmune panel wasnegative except for the presence of anti–smooth muscle antibodies at a significant titer.
Magnetic resonance imaging of the soft tissues demonstrated dermo-hypodermal infiltration withoutevidence of muscle involvement.
Histopathological examination of a skin biopsyconfirmed the diagnosis of Eosinophilic Fasciitis. It revealed dermal and hypodermal fibrosis extending to the fascia, associated with a lymphoplasmacyticinflammatory infiltrate involving the dermis, hypodermis, and fascia.
Treatment with methotrexate was initiated, with good tolerance and a favorable clinical response. After severalmonths of therapy, disease progression stabilized, with a reduction in hand edema and no further progression of cutaneous sclerosis.

Conclusion

This case highlights an atypical presentation of Schulman's fasciitis, characterized by the absence of peripheral eosinophilia, which resulted in a six-yeardiagnostic delay. It emphasizes the importance of considering this diagnosis whenever clinical, radiological, and histological criteria are met.
Early and appropriate management remains crucial to optimize clinical outcomes and prevent functionalsequelae, even in atypical presentations.

EADV CONGRESS
VIENNA
30 SEP - 3 OCT 2026

Abstract N°: 3975

Line-Field Confocal Optical Coherence Tomography Improves Diagnostic Accuracy and Reduces Inappropriate Management: A Multi-Reader Pre-Post Study

Maria Luísa Santos e Silva Caldeira Marques*[1, 2], Mary-Ann El Sharouni[1, 2, 3], Christoph Sinz[2], Emilie Cullum[1], Terence Wong[2], Rhonda Harvey[1], Bruna Marchi Nunes Gallo[1], Natalie Teh[2, 4], Tara Sholji[1], Sophie Hu[1, 5], Pascale Guitera[1, 2, 5]

[1] Sydney Melanoma Diagnostic Centre, Royal Prince Alfred Hospital, Sydney, Australia
[2] Melanoma Institute Australia, Sydney, Australia
[3] The Daffodil Centre, The University of Sydney, Sydney, Australia
[4] Faculty of Medicine, The University of New South Wales, Sydney, Australia
[5] Faculty of Medicine and Health, The University of Sydney, Sydney, Australia

Introduction
Current skin cancer diagnosis relies heavily on invasive biopsies, with over 15 benign lesions biopsied per confirmed malignancy. Line-field confocal optical coherence tomography (LC-OCT) enables non-invasive cellular-resolution imaging to 500 µm depth. While studies report high diagnostic accuracy for basal cell carcinoma (sensitivity 98%, specificity 80-90%), performance for melanocytic lesions and other cutaneous neoplasms remains challenging and operator-dependent. This study evaluated whether adding LC-OCT to dermoscopy following structured training improves diagnostic accuracy and reduces inappropriate management in suspicious skin lesions.

Materials and Methods
This prospective multi-reader multi-case study was conducted at a single tertiary skin cancer centre. One hundred consecutive diagnostically equivocal lesions suspicious for cutaneous malignancy, all requiring biopsy based on clinical and dermoscopic assessment, were included. Histopathology served as the reference standard. Eight readers participated. In the pre-training phase, readers independently evaluated all cases using dermoscopy alone, providing diagnosis and management recommendation (biopsy/excision, monitoring, routine follow-up, or non-surgical management). Readers were blinded to histopathology throughout the study.

Readers then completed structured LC-OCT training comprising: (1) online modules (8 hours total: 2 hours non-melanocytic lesions, 6 hours melanocytic lesions) covering LC-OCT imaging principles, morphological criteria, and guided case review; and (2) in-person training (10 hours). In the post-training phase, readers re-evaluated the same cases using LC-OCT combined with dermoscopy. Seven readers completed all 100 cases in both phases; one reader completed 44 cases, having contributed 56 cases to the study cohort.

Primary endpoint was diagnostic accuracy. Secondary endpoints included management appropriateness (classified as appropriate, acceptable, or inappropriate based on predefined criteria), and inter-reader agreement. Statistical analysis employed paired t-tests and mixed-effects regression models adjusting for clustering by lesions and readers.

Results
Diagnostic accuracy improved significantly when LC-OCT was added to dermoscopy, increasing from 36.9% (SD 8.6%) to 44.9% (SD 8.1%) (p=0.007). After adjusting for reader and lesion clustering, LC-OCT increased the odds

of correct diagnosis by 49% (adjusted OR 1.49, 95% CI 1.18-1.90, p<0.001).

Management recommendations changed significantly between modalities (p<0.001). The addition of LC-OCT reduced clearly inappropriate management decisions from 14.8% to 11.1% and increased acceptable management from 28.2% to 37.0%. In adjusted analysis, LC-OCT significantly improved the odds of avoiding inappropriate management (adjusted OR 1.55, 95% CI 1.08-2.21, p=0.016).

Inter-reader agreement was fair for both modalities. Fleiss' kappa for diagnostic accuracy remained 0.20 for both dermoscopy and LC-OCT. For management appropriateness, kappa improved modestly from 0.21 to 0.24 (p<0.001), indicating slight improvement in reader consensus.

Conclusions

Adding LC-OCT to dermoscopy following structured training significantly improved diagnostic accuracy and reduced inappropriate management decisions in suspicious skin lesions. These findings support LC-OCT as a valuable adjunct to dermoscopy for optimizing diagnostic and management decisions in equivocal cases.

EADV CONGRESS
VIENNA
30 SEP - 3 OCT 2026

Abstract N°: 4040

Systematic Benchmark of H&E-to-Transcriptomics Prediction in Skin Tissue

Regina Shaikhutdinova*[1], Namrata Singh[1], Julia Staller[1], Martin Simon[1], Johannes Griss[1]

[1] Medical University of Vienna, Vienna, Austria

Introduction

H&E stained tissue sections are widely used in clinical pathology due to their ability to provide fast, reliable, and inexpensive assessment of tissue structure and cellular organization. Recent advances in machine learning have substantially expanded their utility, enabling representation learning, cross-modal alignment, and prediction of spatial omics directly from H&E images. Multiple studies have been published, demonstrating that such predictions are feasible for metabolomics, transcriptomics, and proteomics at the slide, spot, and single-cell levels. However, most existing models have been validated on non-skin tissues, and rigorous and objective evaluations are still missing. Here, we present a benchmark of models that predict transcriptomics at single-cell resolution for human skin samples.

Materials and Methods

We evaluated three recently published methods: SpatialEx, a hypergraph-based model compatible with multiple pathology foundation models; GHIST, a deep learning framework using a UNet3+ backbone trained from scratch on paired H&E and spatial transcriptomics data; and Pixel2Gene, which uses the HIPT pathology foundation model to extract histological features that are fed into a simple MLP. As controls, we included simple linear regression models trained on embeddings from multiple foundation models, resulting in 15 models evaluated in this study. We evaluated all models on in-house Xenium 5K panel data from acute myeloid leukemia and hidradenitis suppurativa skin tissue, as well as publicly available Xenium v1 panel data containing 480 genes from lichen planus skin tissue.

Results

Our results show that the predictive performance of published models was limited for the majority of genes and, surprisingly, comparable to that of a simple linear regression model trained on foundation model embeddings. In the Xenium 5K dataset, only 3 genes reached a Pearson correlation coefficient (PCC) above 0.6 using the best-performing model, whereas 17 genes reached this threshold in the Xenium v1 dataset. The best-predicted genes were predominantly keratinocyte and epithelial differentiation markers, including keratins and desmosomal proteins, as well as several smooth muscle- and stromal-associated markers, all of which are strongly associated with visible tissue morphology and well-defined histological structures. Fibroblast-associated genes were predicted with substantially lower PCC values, while prediction of immune-related genes largely failed across all evaluated approaches.

Conclusions

These findings indicate that current models perform poorly for the majority of genes in skin samples, while also demonstrating better performance on the Xenium v1 panel, likely due to the higher sensitivity of the v1 chemistry, as previously reported. Overall, our results highlight the current limitations of transcriptomic prediction models for human skin samples, despite their reported success in other tissue types.

POWERED BY M-ANAGE.COM

EADV CONGRESS
VIENNA
30 SEP - 3 OCT 2026

Abstract N°: 4050

Diagnostic accuracy of LC-OCT versus dermoscopy in detecting recurrence of basal cell carcinoma

Simone Soglia*[1], Benedetta Galli[1], Edoardo Festa[1], Cesare Ariasi[1], Piergiacomo Calzavara-Pinton[1], Marina Venturini[1]

[1] University of Brescia, ASST Spedali Civili of Brescia, Brescia, Italy

Introduction
Detection of basal cell carcinoma (BCC) recurrence within post-treatment scars is clinically challenging, as scar-related fibrosis and vascular remodelling may mimic tumor recurrence on dermoscopy. Line-field confocal optical coherence tomography (LC-OCT) may improve non-invasive assessment by enabling visualization of tumor-specific architectural features. The aim of this study was to compare the diagnostic performance of dermoscopy and LC-OCT for the detection of BCC recurrence on post-treatment scars in a real-world clinical setting.

Materials and Methods
This retrospective, single-center observational cohort study included patients evaluated for suspected BCC recurrence within post-treatment scars who underwent both dermoscopy and LC-OCT. Dermoscopy was assessed using two predefined thresholds: a lenient threshold, classifying both low- and high-confidence suspicious findings as positive, and a strict threshold, classifying only high-confidence findings as positive. LC-OCT examinations were classified as positive or negative according to tumor-associated criteria. Final recurrence status was determined by histopathology when available or by at least 12 months of follow-up.

Results
Seventy-six patients with 78 lesions were included. BCC recurrence was confirmed in 33 lesions (42.3%), while 45 lesions (57.7%) were classified as non-recurrent. Under the lenient threshold, dermoscopy showed 90.9% sensitivity, 33.3% specificity, 50.0% positive predictive value, 83.3% negative predictive value and 57.7% accuracy. Under the strict threshold, dermoscopy showed 57.6% sensitivity, 71.1% specificity, 59.4% positive predictive value, 69.6% negative predictive value and 65.4% accuracy. LC-OCT showed 100.0% sensitivity, 84.4% specificity, 82.5% positive predictive value, 100.0% negative predictive value and 91.0% accuracy. LC-OCT was positive in all confirmed recurrent BCCs.

Conclusions
LC-OCT showed higher diagnostic accuracy than dermoscopy for detecting BCC recurrence within post-treatment scars. These findings suggest that LC-OCT may represent a valuable second-level imaging tool in equivocal scars, helping to reduce both missed recurrences and unnecessary procedures.

EA DV CONGRESS
VIENNA
30 SEP - 3 OCT 2026

Abstract N°: 4103

The Rise of AI-Powered Teledermatology: Transforming Skin Disease Diagnosis, Monitoring, and Personalised Treatment Plans in Remote Settings

Alicia Kwan Su Huey*[1, 2], Ece Karabulut[2, 3], Karan Choudhary[2, 4], Mert Uzun[2, 5], Sanobar Shariff[2, 6], Olivier Uwishima[2]

[1] Manchester University NHS Foundation Trust, Greater Manchester, United Kingdom
[2] Department of Research and Education, Oli Health Magazine Organization, Kigali, Rwanda
[3] Vakfikebir State Hospital, Trabzon, Türkiye
[4] Medscan Diagnostics, Delhi, India
[5] Karadeniz Technical University, Trabzon, Türkiye
[6] Yerevan State Medical University after Mkhitar Heratsi, Yerevan, Armenia

Introduction
Teledermatology can reduce access barriers by enabling remote assessment of inflammatory and neoplastic skin disease. The rapid integration of artificial intelligence (AI) into teledermatology raises questions about diagnostic performance, workflow impact, equity, and safety. This review synthesises evidence on AI-supported teledermatology across diagnosis, prioritisation, and follow-up.

Materials and Methods
A targeted narrative literature review was conducted using major biomedical databases to identify studies on AI-supported teledermatology. Search terms included teledermatology, artificial intelligence, machine learning, deep learning, computer vision, triage, monitoring and remote follow-up. English-language studies were prioritised where they reported diagnostic performance, workflow integration, triage utility, monitoring applications or barriers to real-world implementation.

Results
Across evaluated systems, AI demonstrated **high sensitivity for melanoma/skin cancer detection**, while **specificity for benign/inflammatory conditions was more variable**, contributing to false positives and avoidable downstream review. In studies of common dermatoses, reported diagnostic performance included **~80% sensitivity with ~50% specificity** in some settings. For lesion classification, computer-vision approaches achieved **~85% sensitivity and ~90% specificity** in selected datasets, with stronger performance in larger, more typical lesions. Beyond diagnosis, AI-assisted history-taking and decision support improved data capture and may enhance asynchronous teledermatology; in comparative studies, an LLM-enabled workflow achieved **~84% top-diagnosis concordance** with clinical teleassessment in a case series. AI also supported monitoring and personalised management, including image-based severity scoring, for example in psoriasis, with **material improvement versus average clinical scoring** in one evaluation. Key implementation barriers include image-quality artefacts, demographic/disease under-representation in training datasets, privacy/cybersecurity risk, and lack of harmonised governance for clinician accountability and follow-up.

Conclusions

AI-enabled teledermatology is most promising as **clinician-supervised decision support** for triage and monitoring rather than autonomous diagnosis. Acceptance and safety will depend on representative datasets, standardised image capture, transparent performance reporting, and robust data governance integrated into real clinical pathways.

EADV CONGRESS
VIENNA
30 SEP - 3 OCT 2026

Abstract N°: 4185

Motivational Patterns and Determinants of Skin Cancer Screening Participation: A Prospectively Conducted Cross-Sectional Healthcare Services Research Study

Natalia Julia Janke*[1]

[1] Department of Dermatology, Klinik Hietzing, Sigmund Freud Privat University, Vienna, Austria

Introduction
Rising skin cancer incidence and limited dermatological resources pose increasing challenges for healthcare systems. While population-wide screening programs remain controversial, little is known about the motivational and structural determinants of real-world skin cancer screening utilization. This study investigated participation patterns in skin cancer screening and their association with preventive healthcare behavior and healthcare access factors.

Materials and Methods
In this prospectively conducted cross-sectional questionnaire study, 320 patients from two tertiary care hospitals were surveyed between February and March 2026 using a standardized questionnaire. Motivations for participation in skin cancer screening were grouped into three predefined categories: risk-oriented, externally prompted, and prevention-oriented. Associations with participation in routine health check-ups were analyzed using chi-square testing and multivariable logistic regression. Diagnostic pathways and structural healthcare access factors were additionally assessed.

Results
Overall, 65.1% of participants reported previous participation in skin cancer screening, while 47.6% attended routine health check-ups. Among 187 classifiable cases, 50.3% were categorized as risk-oriented, 18.7% as externally prompted, and 31.0% as prevention-oriented. A significant association was observed between motivational category and participation in routine health check-ups ($p < 0.001$). Participation in routine health check-ups was independently associated with a higher likelihood of prevention-oriented motivation (OR 6.13; 95% CI 2.62-14.33; $p < 0.001$). Furthermore, 44.1% of skin cancer diagnoses followed self- or externally detected skin changes. Out-of-pocket payment was significantly associated with shorter waiting times ($p < 0.001$).

Conclusions
Participation in skin cancer screening reflects distinct motivational patterns ranging from generalized preventive attitudes to reactive, risk-driven healthcare utilization. Beyond individual determinants, structural factors including access to information, waiting times, and financing models substantially influence screening behavior. These findings support the implementation of risk-adapted and patient-centered prevention strategies within dermatological care pathways.

EA DV CONGRESS
VIENNA
30 SEP - 3 OCT 2026

Abstract N°: 4204

Diagnostic Accuracy of AI in Dermatology for Skin of Colour: A Systematic Review and Meta-analysis

Samia Rahman*[1], Samiha Mohsen[2], Samantha Bestavros[3], Aakankshya Kharel[4], Ryan Geng[3], Kaitlyn Ramsay[5], Evan Chan[3], Sheila Wang[3]

[1] Rao Dermatology, University of Alberta, New York, United States
[2] University of Calgary, Calgary, Canada
[3] University of Toronto, Toronto, Canada
[4] University of Alberta, Edmonton, Canada
[5] University of British Columbia, Vancouver, Canada

Introduction

Artificial intelligence (AI) has demonstrated promise in dermatology, however, the representation of darker skin tones within training and validation datasets remains limited, raising concerns about potential diagnostic inequities.[1-2] Therefore, we conducted a systematic review and meta-analysis to evaluate the current state of AI performance in dermatology diagnosis for skin of colour (SOC).

Materials and Methods

MEDLINE and Embase were searched through May 6, 2025, for studies evaluating AI models in dermatology including SOC populations (Fitzpatrick IV–VI). Studies restricted to Fitzpatrick I–III or lacking AI methodology were excluded. Risk of bias (ROB) was assessed using QUADAS-2 and PROBAST.

Results

Fifty studies were included and the majority focused on non-malignant conditions,skin tone classification/dyschromia. There were relatively few studies addressing cutaneous oncology (CO), this is contrary to the broader AI dermatology literature which is dominated by CO.5 This divergence may risk overlooking CO in FST IV-VI patients, where timely and accurate diagnosis is critical.

Reporting of SOC representation varied: 19 studies had >50% SOC participants, 8 studies reported <50%, and 23 studies did not specify. Fewer than 10% of studies provided stratified accuracy metrics. ROB across severalkey domains, including patient selection and index test conduct, was frequently high or unclear.

A categorical analysis revealed heterogeneous data with inconsistent study designs and reporting practices (Figure 1). Many evaluated different groups of conditions simultaneously and reported broad metrics, combining SOC and non-SOC populations.

This variability in design and reporting prohibited meta-analyses beyond melanoma and BCC. For melanoma, the pooled sensitivity and specificity across all skin types were 0.68 (95% CI 0.61–0.75; I^2=0.01%) and 0.85 (95% CI 0.59-1.10; I^2=99.3%), respectively**.** Only one study further reported SOC-specific performance, with lower sensitivity (0.53) and specificity (0.47) compared to the pooled estimates.[3] For basal cell carcinoma (BCC), pooled sensitivity and specificity were 0.70 (95% CI 0.39–1.01; I^2=92.65%) and 0.80 (95% CI 0.43–1.18; I^2=95.16%), respectively**.**[4,5]

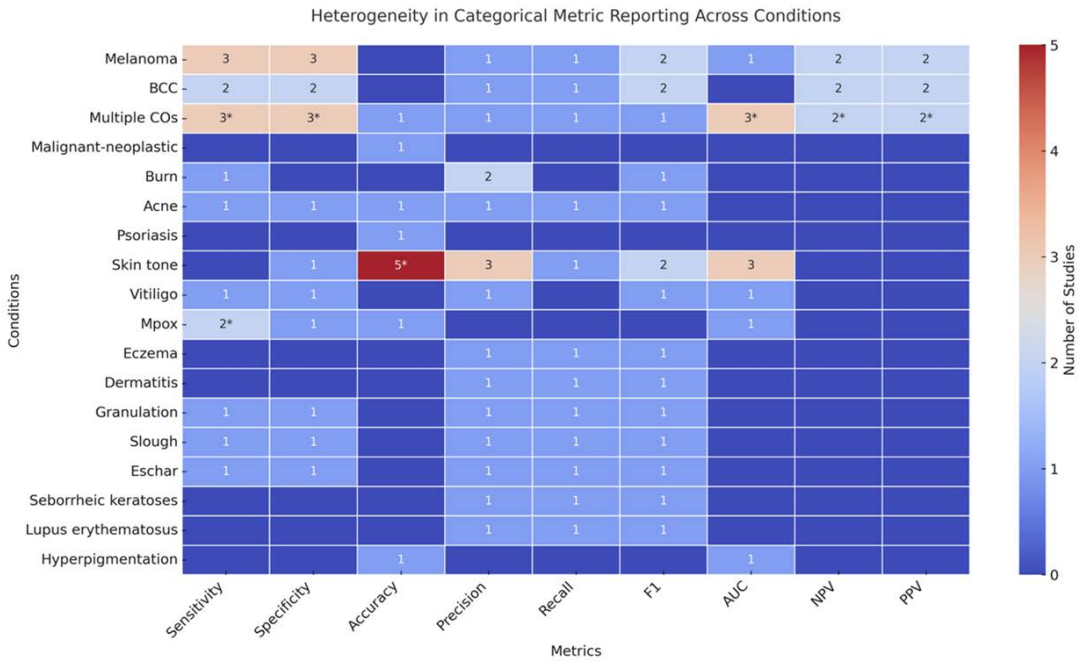

Figure 1: Heat map of categorical outcome reporting across dermatologic conditions. Each cell represents the number of studies reporting a given performance metric (e.g., sensitivity, specificity, accuracy, precision, recall, F1, AUC, PPV, NPV) for the corresponding condition. Warmer colours indicate a greater number of studies, highlighting the heterogeneity in reporting practices. Values marked with an asterisk (*) denote instances where differing subclassifications or combined conditions were reported, which precluded inclusion in the meta-analysis.

Conclusions

SOC-specific literature is more limited and inconsistently reported, compared to AI in dermatology diagnostics broadly, with findings indicating reduced diagnostic accuracy. Standardized reporting of dataset composition, stratum-specific diagnostic accuracy, and methodological rigor are needed to ensure equitable AI development in dermatology.

EADV CONGRESS
VIENNA
30 SEP - 3 OCT 2026

Abstract N°: 4256

Diagnostic Accuracy and Patient Experience Within a Secondary Care Teledermatology Service

Farzad Shams*[1], Zeeshaan-Ul Hasan[1], Padma Mohandas[1], Rebecca Chung[2], Gizem Gundogan[1], Salman Karsan[1], Adeline Roy[1], Catherine Harwood[1]

[1] Barts Health NHS Trust, London, United Kingdom
[2] Queen Mary University of London, London, United Kingdom

Introduction
Teledermatology is increasingly used to improve access to dermatology assessment and reduce waiting times for patients with suspected skin lesions. However, concerns remain regarding diagnostic accuracy, patient confidence in remote assessment pathways, and the cost-effectiveness of large-scale teledermatology services. This study evaluated diagnostic outcomes, biopsy patterns, patient satisfaction, and service efficiency within a secondary care teledermatology pathway.

Materials and Methods
A retrospective analysis was performed of 1,553 lesions from 1,163 patients referred through a secondary care teledermatology skin lesion pathway. Variables analysed included teledermatology assessment outcome, biopsy outcome, histopathological diagnosis, age, ethnicity, anatomical site, and Fitzpatrick skin type. Concordance between teledermatology assessment, face-to-face dermatology outcomes, and histopathological diagnosis was evaluated where available. Patient experience questionnaire data from 121 respondents was also reviewed.

Results
A total of 1,553 lesions were assessed via teledermatology, of which 361 lesions (23%) proceeded to biopsy. Of these, 172 lesions (63.7% of biopsied cases) underwent biopsy primarily because of suspected malignancy or diagnostic uncertainty, representing 11.1% of all lesions assessed through the pathway. Histopathological analysis confirmed 68 malignant lesions overall, with at least 5.2% of patients found to have one or more histologically confirmed malignancies.

Comparison between teledermatology assessment and subsequent face-to-face dermatology outcomes demonstrated concordance in 81.4% of cases, supporting the reliability of teledermatology as a secondary care triage pathway. Within the subgroup of lesions biopsied because of suspected malignancy or diagnostic uncertainty, teledermatology assessment demonstrated diagnostic accuracy of 78.5% for malignant versus non-malignant outcomes when compared with final histopathological diagnosis. This suggests teledermatology was able to appropriately stratify clinically suspicious lesions according to malignant potential and effectively identify lesions requiring further investigation or biopsy.

Patient satisfaction with the teledermatology pathway was high among the 121 questionnaire respondents. Overall, 92% of respondents reported being satisfied or very satisfied with the service, 91% stated they would recommend the pathway to family and friends, and 95% reported that the medical photographer made them feel at ease during image acquisition. Patients frequently described the service as efficient, professional, friendly, reassuring, and stress-free, with qualitative feedback highlighting rapid access to assessment, reduced waiting

times, and reassuring communication as key strengths.

Previous service evaluation within the same pathway demonstrated 37% lower per-patient costs for teledermatology compared with traditional face-to-face assessment (£16.16 vs £25.68 per patient). Estimated revenue per clinical session was also substantially higher for teledermatology (£3981.75 vs £1911.24).

Conclusions

Teledermatology appears to function effectively as a secondary care triage pathway for skin lesion assessment, demonstrating substantial concordance with subsequent face-to-face review, good diagnostic accuracy for clinically suspicious lesions, high patient satisfaction, and cost-effectiveness. These findings support the expanding role of teledermatology within secondary care dermatology services and may help inform future comparisons with AI-supported diagnostic pathways.

EA DV CONGRESS
VIENNA
30 SEP - 3 OCT 2026

Abstract N°: 4347

Comparing Conventional Late Fusion and Cross-Attention Architectures in Multimodal Melanoma Classification

Rocío Bueno-Molina*[1], Juan Carlos Hernández Rodríguez[1], Lourdes Durán López[2], Juan Pedro Domínguez Morales[2], Domingo Muñoz Espejo[3], Jose Juan Pereyra Rodriguez[1]

[1] Virgen del Rocío University Hospital, Sevilla, Spain

[2] Robotics and Technology of Computers Lab. University of Seville., Seville, Spain

[3] Independent Researcher, Seville, Spain

Introduction

Artificial intelligence (AI) models for melanoma diagnosis are predominantly based on dermoscopic image analysis alone. However, dermatologists integrate additional clinical context, such as patient age, sex, anatomical location, and lesion size, into diagnostic reasoning. Most previous multimodal approaches in dermatology have relied on late fusion strategies, where metadata are incorporated only at the final classification stage, potentially limiting the interaction between modalities. This study aimed to evaluate whether active multimodal integration using cross-attention mechanisms could improve the classification of melanoma in situ (MIS) versus invasive melanoma (MIV) compared with image-only and conventional late fusion approaches.

Materials and Methods

A retrospective multicentric study was performed using 2,363 dermoscopic images with histopathological confirmation of melanoma. Clinical metadata included sex, age, anatomical location, lesion diameter, and long-to-short axis ratio. Images were resized and preprocessed with Data Augmentation techniques. Two multimodal strategies were evaluated: a conventional late fusion model, in which metadata were concatenated with image features only at the final classification stage, and an attention-based multimodal model. In the latter, clinical metadata were processed through a dedicated multilayer perceptron (MLP) branch and actively integrated with dermoscopic image embeddings using gated fusion, residual connections, and multi-head cross-attention mechanisms. Performance was compared against an image-only baseline and previous late fusion approaches using accuracy, balanced accuracy, F1-score, Cohen's kappa, and area under the receiver operating characteristic curve (AUC). Statistical comparisons were performed using a one-sided Wilcoxon signed-rank test.

Results

The conventional late fusion model showed only limited gains over the image-only baseline. Compared with the image-only model, late fusion improved sensitivity from 0.51 to 0.52, specificity from 0.90 to 0.92, F1-score from 0.58 to 0.60, and AUC from 0.80 to 0.83, while accuracy remained unchanged at 0.78. Positive predictive value also increased from 0.69 to 0.77. However, these improvements did not reach statistical significance, suggesting that simply concatenating metadata at the final classification stage was insufficient to substantially improve model performance.

The multimodal cross-attention model outperformed the image-only approach across all major metrics. Mean AUC improved from 0.81 to 0.84, while balanced accuracy increased from 0.74 to 0.78. Improvements were also observed in F1-score (0.81 vs 0.84) and Cohen's kappa (0.45 vs 0.52). Statistical analysis demonstrated significant improvements in accuracy ($p = 0.031$), AUC ($p = 0.031$), F1-score ($p = 0.031$), and Cohen's kappa ($p = 0.031$). In contrast to conventional late fusion strategies evaluated in preliminary experiments, active cross-attention

integration enabled the model to dynamically relate metadata attributes to dermoscopic image features during training, improving discrimination between MIS and MIV.

Conclusions

Active multimodal integration using cross-attention mechanisms significantly improved melanoma invasion prediction compared with image-only and conventional late fusion approaches. These findings suggest that attention-based multimodal architectures may better emulate clinical diagnostic reasoning by contextualizing dermoscopic patterns with patient metadata. Such approaches could enhance clinically meaningful AI-assisted decision-making in melanoma management.

This work was funded by the MelaNO+ project (PI25/02067), funded by the Instituto de Salud Carlos III (ISCIII) and co-funded by the European Union.

EADV CONGRESS
VIENNA
30 SEP - 3 OCT 2026

Abstract N°: 4350

AI in dermatology

jasurbek yunusov*[1]

[1] Central Asian University, Republican dermatovenerological clinical hospital, Tashkent, Uzbekistan

Introduction

In the third quarter of the twentieth (XX) century, the invention of artificial intelligence was one of the greatest achievements of humanity, and until today AI has developed sufficiently to be used in many fields. For example, AI is used in car systems, education, art, and architecture. Moreover, in the last decade, AI has been used in medicine more and more. However, the scope of AI application is still narrow, and it is not widely used in dermatology in Uzbekistan. Nevertheless, AI can help dermatologists in decision-making, which can be very beneficial for patients.

Materials and Methods

A literature review was conducted using scientific databases such as PubMed, MDPI, and Google Scholar to collect relevant articles related to artificial intelligence in dermatology. Recent studies focusing on AI-based diagnostic tools and image analysis were included.

Results

Recent studies comparing convolutional neural networks (CNNs) with dermatologists in dermoscopic image classification show that AI can achieve comparable or superior performance. CNN models demonstrated higher diagnostic accuracy, with an AUC of up to 0.87 compared to 0.74–0.79 for dermatologists**,** along with improved specificity (up to 85% vs. 72.6%) and comparable sensitivity. These findings highlight the strong potential of AI to support clinicians in the detection and classification of melanoma and other pigmented skin lesions.
In another study a special app was developed by technical architects and tested on 900,000 ordinary people as an experiment to detect skin cancer early and showed a sensitivity of 95%. In another study, this indicator showed 91.33%.

Conclusions

AI-based diagnostic tools, particularly CNNs, show strong potential to assist dermatologists**.** At the same time, it is possible to increase the percentage of correct decision-making to above 90%, which may improve the quality of life of patients. Using AI can help patients identify and improve their condition early. It can also help doctors manage their time and focus more of their time and attention on patients with accurate diagnoses.

EA DV CONGRESS
VIENNA
30 SEP - 3 OCT 2026

Abstract N°: 4351

DermaScan AI: An AI-Powered Dermatology Image and Video Analysis System for Diagnostic Assistance,Educational Support, and Clinical Decision Enhancement Among Medical Students and Interns

Mohammad artaza*[1], Mohd Faizan Siddiqui[1], Roman Kalmatov[1]

[1] International Medical Faculty, Osh State University, Osh, Kyrgyzstan

Introduction

Dermatological diagnosis remains one of the most visually dependent domains in medicine, requiring advanced pattern recognition skills, extensive clinical exposure, and strong differential diagnostic reasoning. Despite increasing global prevalence of skin diseases, non-dermatologists including medical students, interns, and primary care clinicians continue to demonstrate low diagnostic accuracy in dermatological conditions due to limited training exposure and overlapping clinical presentations. Previous studies have shown that diagnostic accuracy among non-dermatologists ranges between 34–66% for common skin lesions, while family practitioners matched histopathological diagnoses in only 26% of neoplastic skin conditions compared to 75% among dermatologists. Pediatric dermatology studies additionally demonstrated misdiagnosis rates approaching 48%, with common conditions such as tinea capitis and molluscum contagiosum frequently overlooked. Conditions such as eczema, psoriasis, cellulitis, fungal infections, hidradenitis suppurativa, and early malignancies often present with similar morphological characteristics, leading to confusion among trainees and non-specialists. To address these gaps, we developed DermaScan AI, an AI-powered dermatology assistant capable of image-based skin pathology recognition, video-assisted dermatological analysis, preliminary medication recommendations, differential diagnostic assistance, educational pathology explanations, and clinical decision support for trainees.

Materials and Methods

A prototype-based observational and usability evaluation study was conducted to assess the effectiveness, educational value, and perceived clinical utility of DermaScan AI among medical students and clinical interns. The system integrated image upload analysis, video-based lesion examination, AI-assisted pathology prediction, medication guidance generation, differential diagnosis suggestions, and educational interpretation modules. The prototype was evaluated among 416 medical students and clinical interns involved in clinical rotations and early patient examination training. Participants evaluated the platform based on diagnostic usefulness, educational support, ease of use, confidence enhancement, clinical applicability, interpretation clarity, and utility in differentiating visually similar conditions.

Results

The evaluation demonstrated high perceived usefulness and educational applicability of DermaScan AI among medical trainees. Participants reported improved confidence in recognizing dermatological pathologies. The educational explanation feature was identified as highly beneficial for understanding disease morphology and differential diagnosis. The multimodal image and video analysis workflow improved interpretation of atypical and visually overlapping skin conditions. Medication guidance and pathology explanations enhanced clinical reasoning compared to conventional image-only diagnostic systems. Interns reported improved ability to differentiate inflammatory, infectious, and neoplastic lesions with similar visual presentations. Participants perceived the platform as both a dermatological learning assistant and a preliminary clinical decision-support system. The study

further identified that traditional dermatology education often lacks sufficient repetitive visual exposure necessary for diagnostic mastery, whereas AI-assisted augmentation may provide continuous accessible reinforcement.

Conclusions

DermaScan AI demonstrated promising potential as an innovative AI-assisted dermatology platform integrating diagnostic support, educational augmentation, medication guidance, and multimodal clinical interpretation. The prototype showed strong acceptance and perceived usefulness among medical students and clinical interns, suggesting potential applicability in dermatology education, preliminary clinical screening, early diagnostic support, and resource-limited healthcare environments.

EA DV CONGRESS
VIENNA
30 SEP - 3 OCT 2026

Abstract N°: 4406

Explainable AI- assisted Classification of Actinic keratosis and Malignant Skin Lesions using Deep Learning approach

Fellisha Marwein*[1], Yathish Balachander[1]

[1] Clinical Fellow NIHR Clinical Research Facility Royal Liverpool University Hospital, Liverpool, United Kingdom

Introduction
Artificial intelligence (AI) has significantly advanced dermatologic image analysis, particularly in skin cancer detection. However, most existing studies focus primarily on melanoma using black-box deep learning systems, while ultraviolet (UV)-associated premalignant lesions such as actinic keratosis (AK) remain underexplored. Early identification of AK is clinically important because of its potential progression to invasive cutaneous squamous cell carcinoma. Furthermore, limited studies have compared classical machine learning (ML) algorithms with explainable deep learning models using fully open-source dermatology datasets. Therefore, this study aimed to develop and compare Random Forest, Support Vector Machine, XGBoost, and EfficientNet convolutional neural network models with explainable AI techniques for multiclass classification of UV-associated premalignant and malignant skin lesions using the publicly available Hugging Face HAM10000 dataset.

Materials and Methods
A retrospective comparative artificial intelligence modelling study was conducted using the publicly available HAM10000 dermoscopic image dataset hosted on Hugging Face, comprising 700 annotated images across seven lesion classes, including actinic keratosis/intraepithelial carcinoma, melanoma, basal cell carcinoma, benign keratosis, dermatofibroma, melanocytic nevi, and vascular lesions. Images underwent standardized preprocessing, including resizing, normalization, and feature vector extraction. Three classical machine learning models Random Forest, Support Vector Machine, and Extreme Gradient Boosting were trained using flattened image-derived features. In parallel, an EfficientNet-B0 convolutional neural network employing transfer learning with pretrained ImageNet weights was developed for end-to-end image classification. Stratified 80:20 train–test splitting and cross-validation were implemented. Model performance was evaluated using accuracy, precision, recall, F1-score, confusion matrix analysis, and Grad-CAM explainable AI visualization for interpretability.

Results
EfficientNet-B0 demonstrated superior multiclass diagnostic performance, achieving accuracy of 70.0%, precision of 72.0%, recall of 70.0%, and F1-score of 71.0%, substantially outperforming classical ML models. Random Forest achieved the highest performance among conventional algorithms with accuracy of 49.3% and F1-score of 48.9%, followed by XGBoost (47.1%) and SVM (45.0%). Classification accuracy was highest for vascular lesions and melanocytic nevi, while actinic keratosis and basal cell carcinoma showed greater diagnostic overlap and misclassification. The deep learning model demonstrated enhanced capability in identifying complex spatial and morphological dermatologic features associated with UV-related lesions. Grad-CAM explainability maps localized diagnostically relevant lesion regions, improving interpretability and supporting clinical integration of transparent AI-assisted dermatologic screening and teledermatology workflows.

Conclusions

Deep learning using CNN's with Explainable AI (Efficient Net) significantly outperformed traditional machine learning approaches for multi-classification analysis of pre-malignant and malignant UV-exposure related skin lesions. The study provides evidence that transparent, artificial intelligence-based dermatologic diagnostics may be able to detect high risk lesions, including actinic keratoses, earlier than current methods; thereby allowing for reduced progression to invasive cancers. Furthermore, Grad CAM improve model transparency by highlighting areas of interest within each image that are most relevant to diagnosis; therefore enabling clinicians to understand why certain diagnoses were made based upon their input. The use of publically available Hugging Face datasets and open source code allows for replication of the study and support for scalable and affordable implementations in tele-dermatology applications and under-resourced screenings environments.

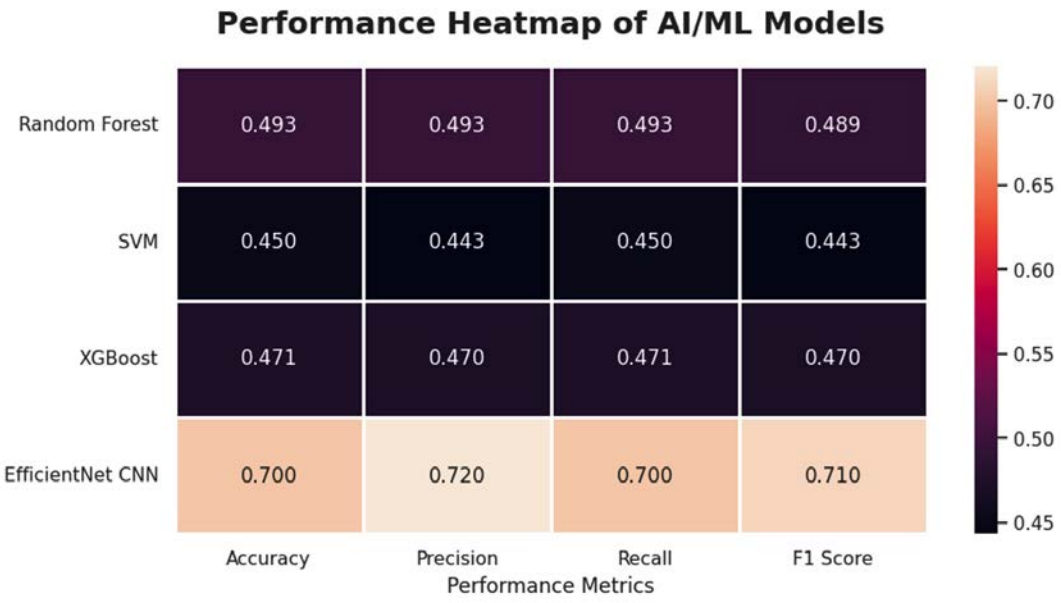

Figure 1 Title: Comparative Diagnostic Performance of Classical Machine Learning and Explainable Deep Learning Models